



Publicly Accessible Penn Dissertations


1-1-2014

Regulation of Adipocyte Transcription by PPARgamma Ligands

Sonia Step

University of Pennsylvania, soniastep@gmail.com

Follow this and additional works at: <http://repository.upenn.edu/edissertations>

 Part of the [Genetics Commons](#), and the [Molecular Biology Commons](#)

Recommended Citation

Step, Sonia, "Regulation of Adipocyte Transcription by PPARgamma Ligands" (2014). *Publicly Accessible Penn Dissertations*. 1456.
<http://repository.upenn.edu/edissertations/1456>

This paper is posted at ScholarlyCommons. <http://repository.upenn.edu/edissertations/1456>
For more information, please contact libraryrepository@pobox.upenn.edu.

Regulation of Adipocyte Transcription by PPARgamma Ligands

Abstract

Rosiglitazone (rosi) is a powerful insulin sensitizer, but serious toxicities have curtailed its widespread clinical use. Rosi functions as a high-affinity ligand for PPARgamma, the adipocyte-predominant nuclear receptor (NR). The classic model of NR action, involving binding of ligand to the NR on DNA, explains positive regulation of gene expression, but both ligand-dependent transcriptional repression and indirect regulation are not well understood. We have addressed these issues by studying the direct effects of rosiglitazone on gene transcription, using global run-on sequencing (GRO-seq). Rosi-induced changes in gene body transcription were pronounced after 10 minutes and correlated with steady-state mRNA levels as well as with transcription at nearby enhancers (eRNAs). Up-regulated eRNAs occurred almost exclusively at PPARg binding sites, to which rosi treatment recruited coactivators including MED1, p300, and CBP, without changes in binding of the corepressor NCoR. By contrast, down-regulated eRNAs fell in sites devoid of PPARg but enriched for a variety of other TFs in the C/EBP and AP-1 families. These enhancers lost coactivator binding upon rosi treatment, suggesting that rosi treatment causes redistribution of coactivators to PPARg sites and away from enhancers containing other TFs, leading to transcriptional repression at these eRNAs and their target genes. We also investigated the function of MRL-24, a compound that has been shown to lack PPARg transactivation activity and regulate a distinct subset of PPARg target genes while functioning as an equally effective insulin sensitizer as rosi. Though our goal was to identify whether MRL-24 regulates the same functional enhancers marked by eRNAs as rosi, we instead found that MRL-24 does not control a distinct subset of target genes, but rather acts as a partial agonist for PPARg. Together, these studies further our understanding of transcriptional regulation by modulation of PPARg activity, including insights into determining functional enhancers and mechanisms of transcriptional repression by activation of a NR.

Degree Type

Dissertation

Degree Name

Doctor of Philosophy (PhD)

Graduate Group

Pharmacology

First Advisor

Mitchell A. Lazar

Subject Categories

Genetics | Molecular Biology

**REGULATION OF ADIPOCYTE TRANSCRIPTION BY PPAR γ
LIGANDS**

Sonia E. Step

A DISSERTATION

in

Pharmacology

Presented to the Faculties of the University of Pennsylvania

in

Partial Fulfillment of the Requirements for the
Degree of Doctor of Philosophy

2014

Supervisor of Dissertation:

Mitchell A. Lazar, M.D., Ph.D.
Sylvan Eisman Professor of Medicine

Graduate Group Chairperson:

Julie A. Blendy, Ph.D.
Professor of Pharmacology

Dissertation Committee:

Gerd Blobel, M.D., Ph.D., Frank E. Weise III Professor of Pediatrics
Klaus H. Kaestner, Ph.D., Thomas and Evelyn Butterworth Professor in Genetics
Patrick Seale, Ph.D., Assistant Professor of Cell and Developmental Biology
Kyoung-Jae Won, Ph.D., Research Assistant Professor of Genetics

ACKNOWLEDGMENTS

I would first like to thank my advisor Mitch for his guidance and mentorship over the last several years. His enthusiasm and support have pushed me to become a better student, scientist and critical thinker. I am also lucky to have had the opportunity to be a part of his lab, which is full of smart, passionate, and supportive scientists. I am grateful for these colleagues and friends in the Lazar Lab, past and present. Among them, I especially need to thank a few people who have contributed directly to this work. Andreas Prokesch began the troubleshooting and technical optimization of the GRO-seq protocol when I first started in the lab, and generously taught me everything he knew. Dave Steger mentored me during my rotation, and has continued to for four more years. He also performed a couple of the ChIP-seq experiments included here, and provided guidance with many others. Jill Marinis and I worked together on the eRNA knock-down experiments. Eric Chen provided valuable technical support and advice.

Our bioinformatics collaborators, Hee-woong Lim and Kyoung-Jae Won, did great computational work. Our partnership with them has been a great example of a fruitful collaboration between wet lab biologists and computational biologists.

I would also like to thank my thesis committee: Gerd Blobel who served as my chair, Klaus Kaestner, Patrick Seale, and Kyoung-Jae Won. I am grateful for their time, critical feedback, and advice.

I would like to acknowledge the Pharmacology Graduate Group, particularly Vlad Muzykantov and Julie Blendy, as well as Sarah Squire, for their help and support.

On the personal side, I first and foremost need to thank my parents for everything they have done for me over the past 28 years. From immigrating to the US 24 years ago, to helping me develop an interest and curiosity in science, to their constant love and support – everything they have done has helped me get to where I am today and I am truly grateful. I am indebted too to my grandparents, who helped raise me and taught me the values of hard work, dedication, and humility. I am also thankful that my brother has been, and will always be, by my side. Last, but certainly not least, I would like to thank Joel for his endless support and encouragement during the ups and downs of this journey, and for helping me in a million ways big and small to get to this point.

ABSTRACT

REGULATION OF ADIPOCYTE TRANSCRIPTION BY PPAR γ LIGANDS

Sonia E. Step
Mitchell A. Lazar

Rosiglitazone (rosi) is a powerful insulin sensitizer, but serious toxicities have curtailed its widespread clinical use. Rosi functions as a high-affinity ligand for PPAR γ , the adipocyte-predominant nuclear receptor (NR). The classic model of NR action, involving binding of ligand to the NR on DNA, explains positive regulation of gene expression, but both ligand-dependent transcriptional repression and indirect regulation are not well understood. We have addressed these issues by studying the direct effects of rosiglitazone on gene transcription, using global run-on sequencing (GRO-seq). Rosi-induced changes in gene body transcription were pronounced after 10 minutes and correlated with steady-state mRNA levels as well as with transcription at nearby enhancers (eRNAs). Up-regulated eRNAs occurred almost exclusively at PPAR γ binding sites, to which rosi treatment recruited coactivators including MED1, p300, and CBP, without changes in binding of the corepressor NCoR. By contrast, down-regulated eRNAs fell in sites devoid of PPAR γ but enriched for a variety of other TFs in the C/EBP and AP-1 families. These enhancers lost coactivator binding upon rosi treatment, suggesting that rosi treatment causes redistribution of coactivators to PPAR γ sites and away from enhancers containing other TFs, leading to transcriptional repression at these

eRNAs and their target genes. We also investigated the function of MRL-24, a compound that has been shown to lack PPAR γ transactivation activity and regulate a distinct subset of PPAR γ target genes while functioning as an equally effective insulin sensitizer as rosi. Though our goal was to identify whether MRL-24 regulates the same functional enhancers marked by eRNAs as rosi, we instead found that MRL-24 does not control a distinct subset of target genes, but rather acts as a partial agonist for PPAR γ . Together, these studies further our understanding of transcriptional regulation by modulation of PPAR γ activity, including insights into determining functional enhancers and mechanisms of transcriptional repression by activation of a NR.

TABLE OF CONTENTS

ACKNOWLEDGMENTS	II
ABSTRACT.....	III
LIST OF TABLES	X
LIST OF ILLUSTRATIONS.....	XI
CHAPTER 1: GENERAL INTRODUCTION.....	1
1.1 Diabetes and thiazolidinediones	2
1.2 The function of the nuclear receptor PPAR γ	3
1.2a Enhancer function and regulation	3
1.2b Nuclear receptors	4
1.2c The role of PPAR γ in TZD function and insulin sensitivity.....	6
1.2d Transcriptional regulation by PPAR γ	8
1.3 MRL-24 as a non-agonist ligand of PPAR γ	9
1.4 Mechanisms of nuclear receptor-mediated transcriptional repression.....	10
1.4a Transrepression	10
1.4b Ligand-dependent corepressor recruitment.....	11
1.4c Competitive binding.....	12
1.4d Coactivator redistribution	13
1.5 GRO-seq and non-coding RNAs	15
1.5a GRO-seq and nascent transcripts	15

1.5b lncRNA and eRNA function.....	16
1.5c eRNAs mark functional enhancers.....	20
1.6 Aims of thesis	21
CHAPTER 2: REGULATION OF NASCENT GENE TRANSCRIPTS AND MRNAS BY ROSIGLITAZONE	23
2.1 Introduction.....	24
2.2 Materials and Methods.....	25
2.2a Cell Culture	25
2.2b Gene expression analysis	26
2.2c GRO-seq library preparation.....	27
2.2d GRO-seq data processing.....	29
2.2e ChIP-seq data processing	29
2.2f Gene transcription analysis.....	30
2.3 Results.....	31
2.3a Rosiglitazone rapidly and robustly regulates gene transcription in adipocytes.	31
2.3b Regulation of nascent gene transcription by rosi correlates with changes in mRNA levels.....	31
2.3c Some target genes may be regulated non-transcriptionally or by secondary effects.....	32
2.3d Up-regulated genes are enriched for strength, number, and proximity of PPAR γ binding sites.	33

2.4 Conclusions.....	33
CHAPTER 3: THE ROLE AND ROSI-REGULATION OF ENHANCERS AND ERNAS	42
3.1 Introduction.....	43
3.2 Materials and Methods.....	44
3.2a Cell culture	44
3.2b GRO-seq library preparation.....	45
3.2c ChIP-qPCR and ChIP-seq.....	45
3.2d eRNA expression	46
3.2e ChIP-seq data analysis	46
3.2f FAIRE (Formaldehyde-Associated Isolation of Response Elements)	47
3.2g Transfection	47
3.2h eRNA analysis	47
3.3 Results.....	49
3.3a Adipocyte eRNAs are regulated by rosi treatment and correlated with regulation of the nearest gene.	49
3.3b Ablation of eRNA transcripts has no effect on transcription of nearby genes.	50
3.3c Down-regulated eRNAs are devoid of PPAR γ and are enriched for several C/EBP and AP-1 factors.	50
3.3d Rosi-mediated transcriptional repression may be mediated in part by redistribution of coactivators.	52

3.4 Conclusions.....	54
CHAPTER 4: REGULATION OF ADIPOCYTE TRANSCRIPTION BY MRL-24	74
4.1 Introduction.....	75
4.2 Materials and Methods.....	77
4.2a Cell culture	77
4.2b Gene expression analysis	77
4.3 Results.....	77
4.3a Previously identified MRL-24-specific gene targets are not differentially regulated in our model.	77
4.3b Microarray comparing effects of MRL-24 and rosi does not identify any MRL- 24-specific target genes.....	78
4.4 Conclusions.....	79
CHAPTER 5: DISCUSSION AND FUTURE DIRECTIONS.....	89
5.1 Summary and discussion.....	90
5.2 Future directions	92
5.2a Identifying secondary targets of rosi.....	92
5.2b Connecting coactivator redistribution to transcriptional regulation	94
5.2c Determinants of functional enhancers.....	96
5.2d Other compounds that differentially regulate PPAR γ	98
BIBLIOGRAPHY	101

LIST OF TABLES

Table 2.1 List of primers for gene expression	41
Table 3.1 List of primers for eRNA and gene expression	71
Table 3.2 List of primers for ChIP-qPCR and FAIRE-qPCR	72
Table 3.3 Sequences for ASO, LNA, and siRNA	73
Table 4.1 List of primers for eRNA and expression	87

LIST OF ILLUSTRATIONS

Figure 2.1 Rosiglitazone rapidly and robustly increases and represses gene transcription in adipocytes	37
Figure 2.2 Nascent gene transcript regulation by rosi correlates with regulation of steady-state mRNAs	38
Figure 2.3 Some steady-state mRNAs may also be regulated on different timescales or non-transcriptionally	39
Figure 2.4 Positive gene regulation by rosi is associated with number and proximity of nearby PPAR γ sites	40
Figure 3.1 eRNAs are transcribed in adipocytes	58
Figure 3.2 Adipocyte eRNAs are regulated by rosi	59
Figure 3.3 eRNA regulation and gene regulation are correlated on a genome-wide level	60
Figure 3.4 Examples of correlation between eRNA and gene regulation	61
Figure 3.5 Examples of intragenic eRNAs that correlate with gene regulation	62
Figure 3.6 Ablation of individual eRNAs has no effect on transcription of the nearest gene	63
Figure 3.7 Rosi-up-regulated eRNAs are enriched for PPAR γ binding, but down-regulated ones are depleted of it	64
Figure 3.8 Up- and down-regulated eRNAs are enriched for different motifs	65
Figure 3.9 Down-regulated eRNAs are enriched for binding of C/EBP α , C/EBP β , FOSL2, JUND, and ATF2	66
Figure 3.10 Strength of binding of C/EBP and AP-1 factors does not change upon rosi treatment	67
Figure 3.11 MED1 binding is increased upon rosi treatment at up-regulated eRNA sites and decreased at down-regulated sites	68

Figure 3.12 The coactivators CBP and P300 are also redistributed upon rosi treatment, but the corepressor NCoR is not	69
Figure 3.13 Rosi does not cause changes in levels of H3K27ac or open chromatin as measured by FAIRE	70
Figure 4.1 Previously defined MRL-24-specific genes are not specific targets in this model	82
Figure 4.2 Most classic adipogenic PPAR γ target genes are regulated by MRL-24 to comparable levels as by rosi	83
Figure 4.3 MRL-24 regulates most of the same gene targets as rosi on a genome-wide level	84
Figure 4.4 Potential MRL-24-specific genes from microarray are artifacts of the experiment	85
Figure 4.5 Preliminary evidence suggests that enhancers may be differentially regulated by MRL-24	86

CHAPTER 1: General Introduction

1.1 Diabetes and thiazolidinediones

Diabetes is a chronic disease that presents a growing burden on human health and the world economy. An estimated 347 million people worldwide have diabetes, and this number is expected to grow significantly in the coming decades (Danaei et al. 2011). Of the drugs used to treat diabetes, thiazolidinediones (TZDs) are the only class that functions primarily by improving insulin sensitivity. This class includes rosiglitazone (Avandia) and pioglitazone (Actos). Several large-cohort studies have demonstrated the efficacy of TZDs in improving glycemic control and preventing diabetes (Kahn et al. 2006; DeFronzo et al. 2011), but other trials showed an association with adverse effects, including cardiovascular risk, fractures, and bladder cancer (Nissen and Wolski 2007; Colhoun et al. 2012; Neumann et al. 2012). Based on these studies, in 2010 the FDA placed restrictions on the prescription and use of rosiglitazone (rosi), due primarily to concerns of increased risk of myocardial infarction. However, the FDA reversed this decision in 2013 after a randomized study designed specifically to assess cardiovascular risk on rosi was reanalyzed and no increased risk of heart attack or death was found (Mahaffey et al. 2013). These clinical studies demonstrate that TZDs have tremendous potential to aid in glycemic control, but their adverse effects have hindered widespread use. Gaining a better understanding of their mechanism of action may help in developing better drugs with fewer side effects.

1.2 The function of the nuclear receptor PPAR γ

1.2a Enhancer function and regulation

Specialization of cells in development and signal response is critical for organismal function. This regulation depends on the ability of cells to activate specific gene expression patterns in response to environmental cues. Enhancers are the key genetic elements that control cell-specific gene expression; they were first described as DNA elements that act over a distance and in any orientation to increase gene expression (Banerji et al. 1981). Though most of our knowledge about enhancer function comes from studies of individual loci, novel techniques have recently allowed for the detection of putative enhancer elements genome-wide and across cell types. Enhancers are usually a few hundred base pairs long, located in distal intergenic regions, and lack a unifying sequence composition (Buecker and Wysocka 2012). They do, however, contain specific recognition sequences for transcription factor (TF) binding. Tens of thousands of putative enhancers have been identified in different cell types, based on markers including histone modifications, coactivator occupancy, or TF binding (Xie and Ren 2013).

Such studies have also demonstrated that many different TFs tend to colocalize on a genome-wide scale in a given cell type (Chen et al. 2008), whereas the same factor in different cell types or across developmental stages binds in different locations (Odom et al. 2004). Enhancer activity appears to depend on relatively simple combinations of lineage-determining transcription factors (Heinz et al. 2010). Cooperative binding of

transcription factors to closely clustered response elements in closed chromatin regions increases chromatin accessibility to additional TFs, and causes the recruitment of coactivators such as histone remodeling complexes. Specific histone marks have been linked to active enhancers, including H3K4me1, H3K27ac, and H3K9ac (Buecker and Wysocka 2012). Thus, genome-wide studies that aim to define enhancer elements generally rely on the enrichment of these histone marks, the presence of coactivators such as CBP and p300, the occupancy of RNA Polymerase II, or the strong binding of a lineage-determining TF.

Though several mechanisms have been proposed for communication between a distal enhancer and its target promoter, the one with the most supporting evidence is the model of spatial colocalization, in which the enhancer and promoter are physically brought together, with the intervening chromatin looped out (Kleinjan and van Heyningen 2005). The presence of chromatin looping has now been tested in many models by experiments such as chromatin conformation capture (3C) (Dekker et al. 2002). These chromatin loops are believed to drive the specificity of enhancer-promoter interactions, as well as the phenomenon of transcription at enhancers, described below.

1.2b Nuclear receptors

Years after their anti-diabetic effects were established in animal models, TZDs were shown to be high-affinity ligands for the TF peroxisome proliferator-activated receptor γ

(PPAR γ) (Lehmann et al. 1995), a member of the nuclear receptor (NR) superfamily. NRs are a large family of mostly ligand-dependent transcription factors that regulate many aspects of physiology, including development and metabolism (Mangelsdorf et al. 1995).

All NRs share the same basic structure. The N-terminus contains the A/B domain, followed by the DNA binding domain (DBD), the hinge region, and the ligand binding domain (LBD) at the C-terminus (Helsen et al. 2012). The DBD consists of two zinc-finger elements, which confer sequence specificity to the hexanucleotide response element that each NR recognizes, known as a half-site. The LBD contains an interior pocket specific to the ligand it binds, as well as a ligand-dependent activation function domain (AF-2). AF-2 consists of several helices including helix 12, and is capable of recruiting transcriptional coactivators (Shiau et al. 1998). Ligands regulate the recruitment of coactivators via the LBD by altering the conformation of helix 12. In the absence of agonist, the conformation of the LBD creates a different binding surface, favoring corepressor recruitment (Bain et al. 2007).

The NR family is divided into three classes (Bain et al. 2007). The first class is steroid receptors, including estrogen receptor (ER), androgen receptor (AR), and glucocorticoid receptor (GR). These NRs are located in the cytoplasm in the absence of ligand, and the presence of ligand causes them to dissociate from heatshock proteins, translocate to the

nucleus, and bind to their response elements. The second class is the thyroid/retinoid family, which includes thyroid receptor (TR) and retinoic acid receptor (RAR). These NRs are constitutively bound to DNA, and the presence of ligand causes a conformational change in helix 12, leading to the recruitment of coactivators and activation of transcription. The last class is that of orphan nuclear receptors, such as REV-ERB and ROR, which were discovered based on sequence homology and have no known physiological ligands. Many orphan nuclear receptors have been “adopted” since their discovery when their ligands were identified.

NRs regulate transcription through ligand-controlled recruitment of coregulators. Most coregulators function as multi-unit protein complexes that regulate transcription by modifying chromatin (Millard et al. 2013). The best-understood chromatin modifications include histone acetylation and DNA methylation. Coactivator complexes often include histone acetyltransferases (HATs), such as CBP and p300, as well as other factors that recruit transcriptional machinery or favor promoter looping. Corepressor complexes often contain the nuclear corepressors NCoR and SMRT, as well as histone deacetylases (HDACs).

1.2c The role of PPAR γ in TZD function and insulin sensitivity

The expression of PPAR γ is dramatically induced during adipogenesis and the gene is expressed predominantly in adipose tissue (Chawla and Lazar 1994; Tontonoz et al.

1994a). PPAR γ is necessary (Rosen et al. 1999) and sufficient (Tontonoz et al. 1994b) for adipogenesis, and is also critical for the functions of mature adipocytes including lipid metabolism, adipokine secretion, and insulin sensitivity (Rangwala and Lazar 2004).

PPAR γ , like most NRs, is a ligand-dependent transcription factor (Glass and Rosenfeld 2000). TZDs contribute to insulin sensitivity by acting on adipose tissue PPAR γ to regulate gene transcription both positively and negatively. For example, TZDs induce insulin sensitizing factors adiponectin (Maeda et al. 2001) and FGF-21 (Moyers et al. 2007), while suppressing the expression of genes promoting insulin resistance, including TNF α (Hofmann et al. 1994), resistin (Steppan et al. 2001), and retinol binding protein 4 (Yang et al. 2005). The most potent TZD in the clinic is rosi (Lehmann et al. 1995), which has durable antidiabetic effects but, unfortunately, its use has been limited by its toxicities. Because PPAR γ expression in adipose tissue is required for the *in vivo* systemic insulin sensitizing effects of TZDs (Chao et al. 2000; He et al. 2003), it is critical to understand how rosi binding to PPAR γ modulates gene expression.

Among the antidiabetic drugs, TZDs are unique in their ability to effectively improve insulin sensitivity. The major organs that respond to insulin are skeletal muscle, liver, and adipose tissue but the direct effects of TZDs are believed to be mainly in adipose tissue for several reasons. First, adipose tissue has by far the highest levels of PPAR γ , about ten-fold higher than in muscle (Chawla et al. 1994). Second, mice lacking adipose tissue

or PPAR γ in adipose do not respond to TZD treatment (Chao et al. 2000; He et al. 2003). Fat-specific PPAR γ knock-out mice have almost complete lipoatrophy and severe insulin resistance (Wang et al. 2013). Mice lacking PPAR γ in liver or muscle, however, retain their response to the insulin sensitizing effects of PPAR γ (Matsusue et al. 2003; Norris et al. 2003). These results indicate that TZDs act primarily on adipose tissue, which in turn signals to the peripheral tissues to improve insulin sensitivity.

1.2d Transcriptional regulation by PPAR γ

There are two PPAR γ isoforms, γ 1 and γ 2. They are nearly identical except for different N-terminals due to different start sites and first exons (Chawla et al. 1994; Tontonoz et al. 1994a), and they are believed to have the same function. PPAR γ binds to specific DNA sequences known as PPAR response elements (PPREs) and heterodimerizes with another nuclear receptor, retinoid X receptor (RXR). Studies into the genome-wide binding of PPAR γ and members of the CCAAT/enhancer-binding protein (C/EBP) family demonstrated that these TFs bind cooperatively near most genes up-regulated during adipogenesis, suggesting that they coordinate the activation of genes that determine adipocyte biology (Lefterova et al. 2008; Nielsen et al. 2008). Bioinformatic analysis of PPAR γ :RXR binding sites in these studies showed that the heterodimer binds selectively to a degenerate direct repeat 1 (DR1) element, in which two direct repeats of the NR half-site (AGGTCA) are separated by one nucleotide. Binding of rosi to PPAR γ results in the increased recruitment of coactivators, including SRC-1, CBP, p300, and MED1, that

function to induce gene expression (Westin et al. 1998; Gelman et al. 1999; Ge et al. 2002; Bugge et al. 2009).

1.3 MRL-24 as a non-agonist ligand of PPAR γ

Some alternative mechanisms have been proposed to explain how TZDs exert their antidiabetic effects. In a mouse model of diet-induced obesity, Cdk5 was shown to specifically phosphorylate PPAR γ at Ser-273 in adipose tissue (Choi et al. 2010). Though this modification did not alter general PPAR γ transcriptional activity, it resulted in altered transcription of a subset of target genes. Treatment with TZDs inhibited this phosphorylation both *in vivo* and *in vitro*. The phosphorylation was also inhibited by MRL-24, a PPAR γ ligand that is a poor agonist in transactivation assays but an effective anti-diabetic agent in mice (Acton et al. 2005). Indeed, treating mice with MRL-24 in these studies improved glucose tolerance but only caused differential gene expression changes in a subset of PPAR γ target genes. These studies suggested that some PPAR γ pathways exist that may be able to dissociate the positive metabolic effects from the adverse effects seen with TZDs.

1.4 Mechanisms of nuclear receptor-mediated transcriptional repression

1.4a Transrepression

Though binding of rosi to PPAR γ results in recruitment of coactivators to increase gene expression, the mechanism by which rosi represses transcription is not well understood. Genes repressed by rosi are likely to play an important role in its metabolic effects, including genes such as TNF α and resistin. There are several mechanisms that may explain NR-mediated transcriptional repression.

One such suggested mechanism is transrepression, which has been demonstrated in the setting of rosi-treated macrophages (Pascual et al. 2005). In these cells, the corepressor NCoR is recruited to pro-inflammatory genes, including some chemokines and inducible nitric oxide synthase, by TFs such as AP-1 and NF- κ B. Treatment with the endotoxin lipopolysaccharide (LPS) causes activation of these genes through dismissal of the corepressor complex and recruitment of a coactivator complex. Co-treatment with rosi and LPS, however, causes transrepression: rosi causes SUMOylation of PPAR γ , which tethers to NCoR, prevents its dismissal from the gene promoter, and blocks gene activation. This mechanism, however, has not been shown in other cell types, has only been demonstrated at individual genes rather than genome-wide, and only explains the ability of rosi to block LPS-mediated gene induction, rather than the ability of rosi to repress genes directly (Glass and Saijo 2010).

A very similar transrepression mechanism was confirmed for liver X receptor (LXR) in macrophages, which represses an overlapping but separate set of inflammatory genes. Similar to PPAR γ , ligand-dependent SUMOylation of LXR blocks NCoR clearance from the promoter, preventing gene induction (Ghisletti et al. 2007).

A number of studies have also found that glucocorticoid receptor (GR) can have suppressive effects on immune function through transrepression. In one study, GR was able to suppress inflammatory gene activation by recruiting the coactivator GRIP1 (Rogatsky et al. 2002). Though usually a coactivator, GRIP1 functions as a corepressor in a complex with GR tethered to AP-1 or NF- κ B and blocks activation of immune genes. Other mechanisms for transrepression by GR have been suggested, including that GR tethering to NF- κ B blocks its ability to recruit the essential coactivator IRF3 (Ogawa et al. 2005) and positive transcription elongation factor b (pTEFb) (Luecke and Yamamoto 2005), both of which are required for activation of gene transcription.

1.4b Ligand-dependent corepressor recruitment

In some cases, nuclear receptors that normally function as transcriptional activators have been shown to repress transcription by recruiting corepressor complexes. For example, in microglia and astrocytes in the brain, the orphan nuclear receptor Nurr1 inhibits activation of inflammatory genes by docking to NF- κ B and recruiting the CoREST corepressor complex (Saijo et al. 2009). In another study more relevant to adipocyte

biology, TZDs were shown to repress certain “visceral white” genes (and promote the “browning” phenotype) by recruiting the corepressors CTBP1 and CTBP2 to C/EBP α , and PPAR γ was required for this process (Vernochet et al. 2009). Additionally, the cofactor RIP140 was shown to be able to function as a corepressor and inhibit transcription by binding to nuclear receptors including TR and ER α (Lopez et al. 1999).

1.4c Competitive binding

In another mechanism, nuclear receptors can inhibit transcription by competing for the same binding site as another transcription factor that may be a stronger transactivator in that context. For example, glucocorticoids antagonize E2-stimulated ER α gene expression in MCF-7 cells. When the cells were co-treated with dexamethasone and E2, GR was found to bind to estrogen binding sites, displacing ER α and its coactivator steroid receptor coactivator 3 (SRC3), leading to the repression of ER α target genes (Karmakar et al. 2013). Binding of GR to these sites requires protein-protein interactions with ER α , FOXA1, and AP1. Similarly, estrogen-related receptor alpha (ERR α) suppresses the expression of the hydroxysteroid sulfotransferase gene SULT2A1 in human liver carcinoma HepG2 cells by competing for binding to inverted repeat IR2 and DR4 elements with other nuclear receptors, including vitamin D receptor (VDR) and constitutive androstane receptor (CAR) (Huang et al. 2011). In other cases, a NR binds to a response element that overlaps the binding site for another TF, precluding binding and leading to transcriptional repression. This has been demonstrated at the osteocalcin

promoter, in which the GRE overlaps with the TATA box such that GR binding prevents binding of TFIID (Stromstedt et al. 1991). Similarly, during adipogenesis ROR α can block induction of the perilipin gene by binding to a response element that overlaps with the PPAR γ element in the promoter, thus blocking PPAR γ -mediated gene transcription (Ohoka et al. 2009).

1.4d Coactivator redistribution

Another important proposed mechanism to explain transcriptional repression driven by TFs is coactivator redistribution, also referred to as “squenching.” This model posits that general coactivators are at a limiting concentration in the nucleus such that when one TF is activated and recruits additional coactivators, those coactivators are necessarily lost from other TFs, leading to transcriptional repression. This idea has been around for more than 25 years, since Mark Ptashne demonstrated that overexpressing GAL4 in yeast inhibited transcription of genes lacking GAL4 binding sites (Gill and Ptashne 1988). They attributed this inhibition to the ability of GAL4 to sequester away key components of the transcriptional machinery and termed this phenomenon “squenching.” Since then, coactivator redistribution has been demonstrated in many models, though primarily in *in vitro* systems relying on overexpression.

It was later shown, for example, that activation of a number of nuclear receptors (including retinoic acid receptor [RAR], RXR, ER, and thyroid hormone receptor [TR])

and subsequent inhibition of AP-1 depend on the coactivators CBP and p300, apparently as a result of their limiting concentration (Kamei et al. 1996). Similarly, in LNCaP cells the coactivator CBP was shown to be necessary for androgen receptor (AR) function and its ability to inhibit AP-1 function, likely due to its limiting amount (Fronsdal et al. 1998). There is also evidence that PPAR γ may cause transcriptional repression through coactivator redistribution: in macrophages, PPAR γ inhibits gene induction by LPS, and this effect is dependent on the ability of PPAR γ to interact with CBP (Li et al. 2000). Another study demonstrated that RAR and RXR can inhibit transactivation by the TF serum response factor (SRF) because of competition for a limiting concentration of p300 and the coactivator SRC-1 (Kim et al. 2001).

All of the studies mentioned above were performed in *in vitro* systems, with methods including overexpression and pull-downs to determine binding interactions, and luciferase assays to measure transactivation, often at a single gene promoter. However, a more recent paper demonstrated this effect using chromatin immunoprecipitation (ChIP) for endogenous TFs and coactivators on DNA on a genome-wide scale (He et al. 2012). In this study, estradiol (E2) treatment of MCF-7 cells caused not only an increase in ER α binding, but also an increase in DNaseI hypersensitivity (DHS), a measure of chromatin accessibility, at the same sites, as well as increased transcription at nearby genes. Sites bound by the TF FOXA1 but not ER α , however, had a decrease in DHS. The change in DHS is linked not to changes in FOXA1 binding strength but to changes in binding of the

coactivator NCOA3. On a genome-wide level, sites with ER α binding and E2-increased DHS have increased NCOA3 binding, while sites with FOXA1 but not ER α and E2-decreased DHS have decreased NCOA3 levels. This supports a model in which E2 treatment causes recruitment of the coactivator NCOA3 to ER α sites, leading to a loss of coactivator from other TFs such as FOXA1 and subsequent transcriptional repression.

1.5 GRO-seq and non-coding RNAs

1.5a GRO-seq and nascent transcripts

Global run-on followed by sequencing (GRO-seq) is a technique that identifies nascent transcripts in a genome-wide manner (Core et al. 2008). This approach can detect near-instant changes in transcription levels, allowing the discrimination of direct transcriptional targets from secondary ones. It also provides stranded information to detect sense and anti-sense transcripts, including divergent transcription. Importantly, it also allows for the discovery of novel, un-annotated transcripts outside of RefSeq genes.

For example, GRO-seq was used to determine the immediate effects of estrogen on the transcriptome of MCF-7 cells (Hah et al. 2011). Estrogen was found to rapidly and transiently regulate 25% of the transcriptome, including many previously unannotated transcripts, with many transcripts regulated as early 10 minutes after treatment. One of the classes of regulated transcripts was intergenic transcripts; among those, the ones that

fell in ER α enhancers were mostly up-regulated by E2 treatment, while the others were mostly down-regulated. As expected, regulation of nascent protein-coding transcripts correlated with steady-state levels of the corresponding mRNA, as measured by microarray or RT-qPCR, but with temporal delay. rRNA and tRNA genes were also increased, suggesting an up-regulation of protein biosynthetic machinery in response to estrogen treatment. In addition, genes that were up-regulated after 10 or 40 minutes of treatment were significantly enriched for ER binding sites within 10kb of the transcription start site (TSS), whereas those up-regulated after 160 minutes were not, suggesting that these were in many cases secondary targets.

GRO-seq has also been used in several instances (Wang et al. 2011; Hah et al. 2013; Lam et al. 2013; Li et al. 2013) to identify enhancer RNAs, which are described in more detail below in section 1.5b and 1.5c.

1.5b lncRNA and eRNA function

Novel technologies of the genomic era have demonstrated that much more of the mammalian genome is transcribed than the 1-2% occupied by coding genes. These non-coding transcripts have been termed the “dark matter” of the genome (Johnson et al. 2005). One class of non-coding transcripts is long non-coding RNAs (lncRNAs), which are defined as intergenic transcripts longer than 200 bp. Thousands of lncRNAs have been identified so far and the number is growing (Cabili et al. 2011). There are many

examples of well-characterized lncRNAs that play an important role in development or disease, including *Xist* in X-inactivation (Sotomaru et al. 2002) and *HOTAIR* in trans-acting gene regulation (Gupta et al. 2010). Nevertheless, the vast majority of lncRNAs are not evolutionarily conserved, are expressed at very low levels, and may represent transcriptional noise (Struhl 2007).

For the lncRNAs that have been shown to have a biological function, several mechanisms have been demonstrated, including interactions with protein, RNA, and DNA. lncRNAs can recruit protein complexes via specific RNA:protein interactions, such as in the case of *Xist*, which interacts with the polycomb repressive complex to silence one of the X chromosomes in vertebrates (Zhao et al. 2008). A lncRNA can also act as a scaffold, bringing two or more proteins together into a complex; for example, *HOTAIR* brings together several components of a repressive complex through specific modular interactions with its 5' and 3' ends (Tsai et al. 2010). lncRNAs can also interact with other RNAs, including by binding to an mRNA in an antisense manner to regulate its translation or degradation (Carrieri et al. 2012), or by acting as a “sponge” for a miRNA and thereby regulating expression of the corresponding mRNA (Cesana et al. 2011). Lastly, lncRNAs can act as guides or decoys to regulate transcription or epigenetic modifications. For example, the lncRNA *NeST* acts as a guide for the histone H3 lysine 4 methyltransferase complex and brings it to specific loci (Gomez et al. 2013), whereas *Lethe* functions as a decoy by binding to components of the NF- κ B complex and preventing them from binding to gene promoters (Rapicavoli et al. 2013).

A sub-family of lncRNAs that are transcribed from enhancer elements, known as enhancers RNAs (eRNAs), have also been of particular interest. Enhancers depend on the binding of lineage-determining TFs, which recruit chromatin remodeling complexes to activate transcription (Heinz et al. 2010).

Though transcription originating from an enhancer element was first demonstrated close to 25 years ago at the locus control region near the *beta-globin* gene (Collis et al. 1990), the genome-wide pervasiveness of enhancer transcription only became clear in 2010 due to high-throughput techniques (De Santa et al. 2010; Kim et al. 2010). eRNAs can be poly-adenylated or non-polyadenylated and can be either unidirectional or bidirectional (Kim et al. 2010; Hah et al. 2011; Wang et al. 2011). They are transcribed from putative enhancer regions, which can be characterized by high levels of H3K4me1 and H3K27ac, binding of CBP and p300, and binding of lineage-determining TFs (Heintzman et al. 2009).

Interestingly, eRNAs are dynamically regulated in a signal-dependent manner, including in response to depolarization of neurons (Kim et al. 2010) or estrogen treatment in breast cancer cells (Hah et al. 2011). Additionally, signal-dependent changes in eRNA levels are highly correlated with corresponding changes in transcription of nearby genes. Several hypotheses for the role or function of eRNAs have been postulated (Natoli and Andrau

2012), some or all of which may be true for different eRNAs. The first is that eRNAs are noise, reflecting the collision of transcriptional machinery with accessible genomic regions, or with regions that are brought close to promoters through chromatin looping. The second is that the process of eRNA transcription may be important in changing chromatin accessibility at specific sites. Lastly, the eRNA transcripts themselves may be functional, by interacting with RNA or protein in *cis* or *trans* to regulate transcription similarly to lncRNAs.

In the past two years, there has been mounting evidence for the last hypothesis: that eRNAs may function to promote transcription of nearby genes. Targeted ablation of eRNAs by small interfering RNA (siRNA), antisense oligonucleotides (ASO), and locked nucleic acids (LNA) caused decreased expression of nearby genes in several models (Lam et al. 2013; Li et al. 2013; Melo et al. 2013; Mousavi et al. 2013). Furthermore, artificially tethering an eRNA to a promoter increased transcription of the target gene (Melo et al. 2013). The question of how eRNAs may be contributing to enhancer function or increasing gene transcription still remains open, though potential mechanisms include increased chromatin looping and increased recruitment of transcriptional machinery, chromatin modifiers, or coregulators (Lam et al. 2014).

1.5c eRNAs mark functional enhancers

Despite several examples of eRNAs functioning to promote target gene transcription, controversy remains as to whether the vast majority of eRNAs have a functional role. Independent of the question of whether eRNA transcripts serve a function, however, there is increasing evidence that eRNA transcription marks functional enhancers. For example, ER α binding sites containing eRNAs are enriched for enhancer elements compared to binding sites without eRNAs, including coactivator binding, H3K4me1, DNase I hypersensitivity, and chromatin looping by chromatin interaction analysis by paired-end tag sequencing (ChIA-PET) (Hah et al. 2013). Furthermore, using eRNAs as predictors of enhancer function is more effective than using H3K4me1 or H3K27ac, where the measure of enhancer function is either chromatin looping or CBP occupancy. Additionally, blocking eRNA elongation with flavopiridol does not affect enhancer function, suggesting that at least in the case of the specific enhancers tested in this experiment, the eRNA transcript is not critical for enhancer function. The first paper to describe genome-wide eRNA transcription also noted that knocking out a gene promoter ablates the associated eRNA, which suggests that an interaction with the promoter, such as a chromatin loop, is necessary for eRNA production (Kim et al. 2010). Lastly, another study also showed in both IMR90 and mESC cells that eRNA transcription is a more reliable indicator of enhancer activity than H3K27ac is, where enhancer activity was defined by transcription of the nearest gene (Zhu et al. 2013). Together these studies suggest that in the context of tens of thousands of putative enhancers defined by TF binding or chromatin marks, eRNA production can serve as a useful marker of functional

enhancers that are actually playing a role in regulating gene transcription in a signal-dependent manner.

1.6 Aims of thesis

It has been known for many years that TZDs bind to PPAR γ in adipose tissue, causing an improvement in insulin sensitivity. Though their molecular target is known, however, the molecular mechanism of TZD action is still not well understood. The aim of this thesis is to expand our understanding of the transcriptional regulation of adipocytes by TZDs and PPAR γ .

Previous methods to identify gene targets of rosi treatment relied on microarray or RNA-seq, which measure steady-state mRNA levels after a longer period of time. This conflates immediate transcriptional targets with secondary, indirect targets. In Chapter 2, direct transcriptional targets of rosi treatment are identified by using GRO-seq after short time points of rosi treatment. This allows us to determine the relationship between nascent pre-mRNA targets and steady-state mRNAs, identify gene targets that are likely due to secondary effects, and confirm that virtually all direct transcriptional up-regulation is due to PPAR γ activity.

In Chapter 3, eRNAs are identified and used to determine functional regulatory elements that are important to rosi-regulation. Though rosi has previously been shown to cause a dismissal of corepressors and a recruitment of coactivators at certain sites (Guan et al. 2005), changes in coregulator occupancy has never been demonstrated genome-wide, and the effects of rosi on histone marks were unknown. Furthermore, there has been very little insight into rosi-mediated repression of gene transcription. In this aim, the regulation of eRNAs is used to focus on functional enhancers and correlated with other changes – coactivator and corepressor recruitment, histone marks, and binding of other TFs – to gain a better understanding of the mechanisms of transcriptional regulation by rosi in a dynamic manner.

The promise of insulin-sensitizing effects of TZDs along with concern for their serious adverse effects have driven a continued interest in studying selective PPAR γ modulators, or SPPARMs. For example, the compound MRL-24 has been demonstrated to improve insulin sensitivity in mice despite lacking agonist ability in transactivation studies and activating a distinct subset of PPAR γ target genes (Choi et al. 2010). In Chapter 4, transcriptional regulation by MRL-24 is studied in a different model of adipocytes in an attempt to confirm its unique set of target genes and determine whether it acts by regulating a distinct group of PPAR γ enhancers. In this aim, we demonstrate that at least in the 3T3-L1 model of adipocytes, MRL-24 does not in fact up-regulate a unique set of target genes, but rather acts as a partial agonist to regulate many of the same genes as rosi but to a lesser degree. Chapter 5 summarizes the studies and discusses future directions.

CHAPTER 2: Regulation of nascent gene transcripts and mRNAs by rosiglitazone

Published in part in *Genes & Development*, 2014 May 1;28(9):1018-28.

The text, figures, and legends in this chapter were the work of Sonia Step with the following exceptions. Andreas Prokesch performed the gene expression microarray experiment. Hee-wong Lim conducted the data processing and bioinformatics analyses.

2.1 Introduction

PPAR γ is a nuclear receptor that is dramatically induced during adipogenesis and expressed predominantly in adipose tissue (Chawla and Lazar 1994; Tontonoz et al. 1994a). It is necessary (Rosen et al. 1999) and sufficient (Tontonoz et al. 1994b) for adipogenesis, and also critical for the functions of mature adipocytes, including lipid metabolism, adipokine secretion, and insulin sensitivity (Rangwala and Lazar 2004). PPAR γ binds near most adipogenic genes as a heterodimer with RXR (Lefterova et al. 2008; Nielsen et al. 2008).

PPAR γ , like most NRs, is a ligand-dependent transcription factor (Glass and Rosenfeld 2000). High affinity ligands for PPAR γ include the TZDs (Lehmann et al. 1995), which are insulin-sensitizing drugs (Nolan et al. 1994). TZDs contribute to insulin sensitization by acting on adipose tissue to regulate gene transcription both positively and negatively. For example, TZDs induce insulin sensitizing factors adiponectin (Maeda et al. 2001) and FGF-21 (Moyers et al. 2007), while suppressing the expression of genes promoting insulin resistance, including TNF α (Hofmann et al. 1994), resistin (Steppan et al. 2001), and retinol binding protein 4 (Yang et al. 2005). The most potent TZD in the clinic is rosiglitazone (rosi) (Lehmann et al. 1995), which has durable antidiabetic effects but, unfortunately, has toxicities that limit its widespread use (Kung and Henry 2012; Ahmadian et al. 2013). Because PPAR γ expression in adipose tissue is required for the *in vivo* systemic insulin sensitizing effects of TZDs (Chao et al. 2000; He et al. 2003), it is critical to understand how rosi binding to PPAR γ modulates gene expression.

Many studies have used transcriptome analysis to infer the effects of rosi on steady state gene expression in adipocytes (Li and Lazar 2002; Sears et al. 2007; Choi et al. 2010; Rong et al. 2011). However, steady state mRNAs levels are determined both by their rates of transcription and degradation. Here, for the first time, we have directly measured rates of adipocyte transcription genome-wide, using global run-on followed by sequencing (GRO-seq) (Core et al. 2008). We find that rosi rapidly up- or downregulates the transcription of thousands of adipocyte genes, and this regulation correlates highly with steady state mRNA regulation. We can also separate out direct gene targets that are up-regulated within 30 minutes or 1 hour of treatment from other genes that are not direct targets but are up-regulated at later time points, suggesting indirect or non-transcriptional regulation.

2.2 Materials and Methods

2.2a Cell Culture

3T3-L1 cells were obtained from American Type Culture Collection and grown in DMEM (Invitrogen) supplemented with 10% fetal bovine serum (Tissue Culture Biologics), 100 U/ml penicillin and 100 µg/ml streptomycin (Invitrogen). Two days post-confluence differentiation media was added, consisting of growth media with 1 µM dexamethasone, 10 µg/ml human insulin, and 0.5 mM 3-isobutyl-1-methylxanthine (Invitrogen). Cells were differentiated as described previously (Lefterova et al. 2008), by

growth in differentiation media for 2 days, followed by growth media with insulin for 2 days, followed by growth media only. When indicated, mature 3T3-L1 adipocytes were treated with 1 μ M rosiglitazone (Biomol) dissolved in DMSO.

2.2b Gene expression analysis

RNA was isolated from cells using TRIzol (Invitrogen), followed by the RNeasy Mini Kit (Qiagen). RT-PCR was performed using 1 μ g RNA (Applied Biosystems) following manufacturer's instructions, and qPCR was performed using primers listed in Table 2.1 using Power SYBR Green Master Mix (Applied Biosystems) on the PRISM 7500 and 7900HT instruments (Applied Biosystems). Analysis was performed using the standard curve method, and all genes were normalized to the housekeeping gene *Arbp*. For the microarray, RNA integrity was examined using an Agilent 2100 Bioanalyzer. RNA samples (150 ng) with RNA integrity number >7 were used for target amplification and labeling via the Ambion WT Expression kit (#4411974) and Affymetrix WT Terminal Labeling kit (#900671) following manufacturer's protocol. Mouse Gene 1.1 ST Array Plates (#901418, Affymetrix) were used for microarray hybridization, wash, stain and scan with GeneTitan hyb-wash-stain kits (#901622, Affymetrix) and a GeneTitan instrument. GeneTitan scanner data were collected with default parameters and further analyzed using Partek Genomics Suite. Data were normalized using default RMA method. For each gene, an average was taken across replicates for the comparative analysis with GRO-seq gene transcriptional level.

2.2c GRO-seq library preparation

GRO-seq was performed as previously described (Core et al. 2008; Wang et al. 2011). Cells were washed twice with ice-cold PBS, then swelled in swelling buffer (10 mM Tris pH 7.5, 2 mM MgCl₂, 3 mM CaCl₂) for 5 min on ice. Cells were centrifuged at 400g for 10 min, then resuspended in lysis buffer (swelling buffer with 10% glycerol and 1% Igepal) and incubated on ice for 5 min. Nuclei were washed twice with lysis buffer, then resuspended in freezing buffer (50 mM Tris pH 8.3, 40% glycerol, 5 mM MgCl₂, 0.1 mM EDTA). Nuclei were counted, pelleted, and 5×10^6 nuclei were resuspended in 100 μ l freezing buffer. For each library, run-on was performed on 4 tubes of 5×10^6 nuclei.

For the run-on, cells were mixed with an equal volume of run-on buffer (10 mM Tris pH 8.0, 5 mM MgCl₂, 1 mM DTT, 300 mM KCl, 20 units of SUPERase-In, 1% Sarkosyl, 500 μ M ATP, GTP and Br-UTP, 2 μ M CTP) and incubated for 5 min at 30°C. Nuclear RNA was extracted with TRIzol (Invitrogen) and precipitated with NaCl and ethanol overnight. The pellet was resuspended in water and the RNA was DNase treated (Ambion) for 30 min. RNA was hydrolyzed using fragmentation reagents (Ambion) for 13 min at 70°C and purified through a Micro Bio-Spin p-30 column (Bio-Rad) according to manufacturer's instructions. RNA was treated with 1.5 μ l T4 polynucleotide kinase (New England Biolabs) for 1h at 37°C, then with an additional 1 μ l for 1h more. RNA was denatured for 5 min at 65°C.

Anti-BrU agarose beads (Santa Cruz) were rotated for 1h in blocking buffer (0.5x SSPE, 1 mM EDTA, 0.05% Tween-20, 0.1% PVP, and 1 mg/ml BSA). Run-on RNA was rotated with beads for 1h, followed by washes twice in binding buffer (0.5x SSPE, 1 mM EDTA, 0.05% Tween-20), twice in low salt buffer (0.2x SSPE, 1 mM EDTA, 0.05% Tween-20), once in high salt buffer (0.5x SSPE, 1 mM EDTA, 0.05% Tween-20, 150 mM NaCl), and twice in TET buffer (TE pH 7.4, 0.05% Tween-20). BrU-labeled RNA was eluted from the beads four times for 15 min with 100 μ l elution buffer pre-heated to 42°C. RNA was ethanol-precipitated overnight.

Precipitated RNA was resuspended in water, denatured, and treated with poly(A)-polymerase (NEB) for 30 min at 37°C. cDNA synthesis was performed as described previously (Wang et al, Nature 2011) using oNTI223 primer ((5'-pGATCGTCGGACTGTAGAACTCT;CAAGCAGAAGACGGCATAACGATTTTTTTTTTTTTTTTTTTTTTVN-3') where the p indicates 5' phosphorylation, ';' indicates the abasic dSpacer furan and VN indicates degenerate nucleotides. The reaction was treated with 3 μ l exonuclease I (Fermentas) for 15 min at 37°C, followed by 2 μ l 1M NaOH for 20 min at 98°C, and neutralized with 1 μ l 2M HCl. cDNA was run on 10% TBE-urea gel, then products were excised and eluted from shredded gel pieces for 4h in TE + 0.1% Tween and precipitated in ethanol overnight. First-strand cDNA was circularized with CircLigase (Epicentre), denatured for 10 min at 80°C, and relinearized with APE I (NEB). Linearized DNA was amplified by PCR using Phusion Hot Start II Kit, according to manufacturer's instructions. The oligonucleotide primers oNTI200 (5'-

CAAGCAGAAGACGGCATA-3') and oNTI201 (5'-AATGATACGGCGACCACCGACAGGTTTCAGAGTTCTACAGTCCGACG-3') were used for amplification. The PCR product was run on a 10% TBE gel and eluted as before. Libraries were sequenced on an Illumina hi-Seq2000 with sequencing primer 5'-CGACAGGTTTCAGAGTTCTACAGTCCGACGATC-3'.

2.2d GRO-seq data processing

First, adapter and poly-A sequence were trimmed off from the raw tags, then remaining tags were converted into FASTA format before alignment. Trimmed tags were aligned to the mouse genome, mm8, using Bowtie (Langmead et al. 2009) with the following options: inputs were in FASTA format (-f), three mismatches were allowed for each tags (-v 3), and only uniquely mapped tags were retained (-m 1). All the alignments were adjusted to 50bp by extending toward 3'-end if their size is shorter than that to make libraries comparable. For the visualization of GRO-seq data, we pooled two replicates for each time point then extended each tag to 150bp to make smooth profiles. bedGraph files were generated first using genomeCoverageBed command in BEDTools suite (Quinlan and Hall 2010) for plus and minus strands separately and they were converted to bigwig format using bedGraphToBigWig command in BLAT suite (Kent et al. 2010).

2.2e ChIP-seq data processing

For PPAR γ , we used two public PPAR γ ChIP-seq data sets, GSM340799 and GSM678393 (Nielsen et al. 2008; Schmidt et al. 2011) from Gene Expression Omnibus,

where all the redundant tags were eliminated in each data set and then the remaining tags were pooled into a single data set. Peak-calling was performed using findPeaks command in Homer (Heinz et al. 2010). After initial calling, all the peaks were resized to 200 bp, then a 2 RPM cut-off was applied to select strong peaks.

2.2f Gene transcription analysis

To determine rosi-induced regulation of gene transcription, we used normalized tag counts within a window between +0.5 kb and 12 kb of transcription start site (TSS) to capture acute changes and yet minimize the bias from paused signal at promoters. When counting tags, we ignored the tags aligned onto rRNA, snoRNA, snRNA, or tRNA to avoid any false contribution to gene body GRO-seq signal due to these highly abundant elements. To identify rosi-regulated genes, we performed an exact test with edgeR package (Robinson et al. 2010) for each time point, 10 min, 30 min, 1h, and 3h using 0 min as a control. Genes were considered rosi-regulated if $FDR < 0.05$ at any time point, but those with low GRO-seq signal (< 0.5 RPKM) or poor gene body coverage ($< 70\%$) at every time point were discarded before downstream analysis. Temporal patterns of rosi-induced regulation were graphically presented by hierarchical clustering, where GRO-seq levels were RPKM-normalized and $1 - (\text{correlation coefficient})$ were used as a distance measure between genes. Initial dendrogram was first created based on Ward's criterion using fastcluster R package (Müllner 2011) then subjected to optimal leaf ordering (Bar-Joseph et al. 2001). In the visualization of clustering heatmaps, RPKM

values were converted into $\log_2(\text{fold-change over 0 min})$ for intuitive color representation of up or down regulation.

2.3 Results

2.3a Rosiglitazone rapidly and robustly regulates gene transcription in adipocytes.

GRO-seq (Core et al. 2008; Wang et al. 2011) was used to measure nascent gene transcription in mouse 3T3-L1 adipocytes and after treatment with rosi for 10 min, 30 min, 1h and 3h. The *Fabp4* locus, a classic adipocyte PPAR γ gene target (Spiegelman and Green 1980; Rival et al. 2004), showed increased transcription with rosi treatment (**Figure 2.1A**). By contrast, transcription from the *Rgs2* gene body was rapidly repressed by rosi (**Figure 2.1B**), consistent with the behavior of the mRNA (Sears et al. 2007). Overall, 1,951 annotated RefSeq genes were transcriptionally regulated by rosi at one or more of the time points tested (**Figure 2.1C**). Interestingly, 71% of regulated nascent transcripts were repressed whereas only 29% were activated by rosi.

2.3b Regulation of nascent gene transcription by rosi correlates with changes in mRNA levels.

To assess the temporal and gene-specific relationship between nascent gene transcription and steady-state mRNA levels, we determined the adipocyte transcriptome using gene expression microarrays after 30 min, 1h, 2h, 6h, 12h, 24h, 36h, and 48h of rosi treatment, with 3 biological replicates at each time point (**Figure 2.2**). While the nascent

transcription of many genes was regulated as early as 10 and 30 minutes after rosi, very few mRNA transcripts changed during this time period and for at least 2 hours after rosi treatment. This was not surprising, as the time required to reach new steady state levels is related to the rate of degradation rather than the rate of synthesis (Schimke and Doyle 1970). However, the correlation between nascent transcription and steady-state mRNA levels was high at later time points, with the greatest correlation noted between the transcription regulation at 3h and the mRNA regulation measured 6h after rosi. The lower correlation with later microarray time points suggests that steady-state regulation at these later times may be dependent on secondary transcriptional changes occurring later than 3h of treatment.

2.3c Some target genes may be regulated non-transcriptionally or by secondary effects.

Comparing rosi-regulation of pre-mRNAs and their corresponding steady-state mRNAs by RT-qPCR suggests that despite the high correlation between transcription and mRNA (**Figure 2.2**), many genes may also be regulated by different mechanisms or on different timescales. While *Fabp4* pre-mRNA is rapidly induced, *Gyk* pre-mRNA is not significantly regulated despite induction of the mRNA, and *Acaa1b* pre-mRNA is not significantly induced until later time points (**Figure 2.3**). These results suggest alternative mechanisms that may regulate a subset of PPAR γ target genes, such as induction of secondary transcription factors, or non-transcriptional regulation of mRNA degradation.

2.3d Up-regulated genes are enriched for strength, number, and proximity of PPAR γ binding sites.

PPAR γ binding is critical for the regulation of gene body transcription. Upregulated genes were statistically significantly enriched for PPAR γ sites closer to the transcription start site (TSS) compared to downregulated or unregulated genes (**Figure 2.4A**). Furthermore, upregulated genes had significantly more PPAR γ binding sites within 100kb of the TSS (**Figure 2.4B**).

2.4 Conclusions

These studies provide a higher resolution and more dynamic portrait of rosi-regulated gene transcription than previously possible. Earlier reports of rosi-regulated gene expression using microarray or PolIII ChIP-seq found a few hundred regulated genes, with half or slightly more than half of those being upregulated by rosi (Choi et al. 2010; Haakonsson et al. 2013). In contrast, we find that transcription is regulated at almost 2,000 gene bodies, more than two-thirds of which are repressed in response to ligand treatment. We believe this increased sensitivity arises from the GRO-seq technique, as well as from the use of multiple time points to capture various dynamics of direct transcriptional regulation.

Rosi regulates nascent gene transcription within 10 minutes of treatment, and this correlates well with steady state mRNA regulation. The correlation is delayed, as

expected, since changes in gene body transcription precede those of the mRNAs, and because the time to reach a new steady state mRNA level is independent of the rate of synthesis and dependent solely on the mRNA half-life (Schimke and Doyle 1970). Thus, while transcription changes quickly, very few changes in steady state mRNA levels are seen earlier than 2h of rosi treatment. Interestingly, the highest correlation between transcription and steady state mRNA is seen at the 3h GRO-seq and 6h microarray time point, with a correlation coefficient of 0.773. Comparing the transcriptional regulation after 3h of rosi with later microarray time points leads to lower and lower correlations at later time points, suggesting that changes in mRNA levels after 24h or 36h are controlled in part by early transcriptional changes, but also by other effects that we cannot detect by GRO-seq after 3h of rosi treatment.

One phenomenon that may contribute to later mRNA changes that are not explained by early transcriptional changes is secondary transcriptional regulation. It is possible that among the many targets that rosi regulates, there may be genes that encode TFs. Even if these are among its directly up-regulated targets, it would still take hours until their protein levels increase. These TFs may then bind to DNA and regulate transcription after 12 to 24h of rosi treatment or later. This kind of secondary transcriptional regulation may be important to the effects of longer rosi treatments on mRNA levels, and thus critical for the physiological effects of rosi. As discussed in Section 5.2a, future studies could investigate these presumed secondary effects that may contribute to the effects of rosi. GRO-seq at later time points such as 24 or 36 hours would provide important additional

information, such as which genes are regulated at later time points, and the mechanism of these effects. Analysis of regulated eRNAs at later time points, similar to the work described in Chapter 3, may suggest which enhancers and therefore which transcription factors play a role in secondary effects of *rosi*.

In Figure 2.4, qPCR of pre-mRNAs and their corresponding mRNAs suggests that some important targets may be regulated non-transcriptionally. Mechanisms to explain this post-transcriptional regulation could include regulation of mRNA degradation pathways. For example, both microRNAs and lncRNAs have been implicated in regulating mRNA stability and degradation. miRNAs function as components of RNA-induced silencing complexes (RISCs) by base pairing to mRNAs and either targeting them for degradation or blocking their translation into protein (Filipowicz et al. 2008). In order for the changes we are interested in to be detectable by microarray, they would have to involve the first pathway: the mRNAs being targeted for degradation. Mechanisms for this effect include the ability of the RISC complex to cause deadenylation or decapping of the transcript, which ultimately leads to mRNA degradation by general machinery (Eulalio et al. 2008). lncRNAs have also been shown to be involved in regulation of mRNA stability. They can act as a miRNA “sink” by binding to it and blocking its ability to bind and degrade its mRNA target (Mercer et al. 2009), or bind complementarily to the mRNA itself to regulate its stability (Atianand and Fitzgerald 2014).

Therefore, a possible mechanism for post-transcriptional regulation by rosi is the direct regulation of miRNA or lncRNA transcripts by rosi treatment, which in turn would regulate mRNA stability and degradation. We did not investigate whether miRNAs or lncRNAs are regulated by rosi, though it is possible because at least one class of non-coding RNAs – eRNAs – are. In another model of NR-mediated transcriptional regulation, estrogen treatment of breast cancer cells caused regulation of 37% of annotated miRNA precursor transcripts (Hah et al. 2011) at early time points of treatment. These mechanisms could be explored further to better understand regulation of steady state mRNAs by secondary or non-transcriptional means.

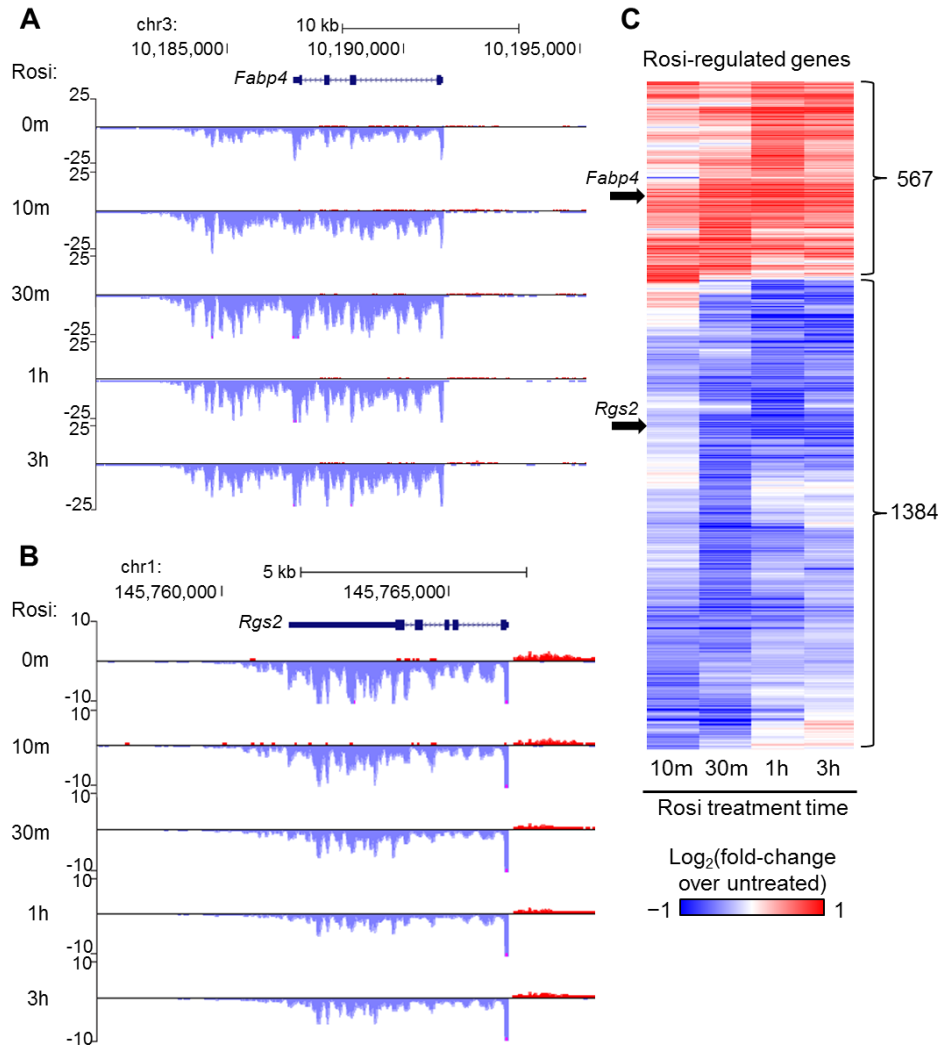


Figure 2.1 Rosiglitazone rapidly and robustly increases and represses gene transcription in adipocytes.

Rosi regulation of RefSeq adipocyte gene transcription as measured by GRO-seq. GRO-seq was performed on mature 3T3-L1 adipocytes treated for 0, 10m, 30m, 1h, or 3h with rosi. (A) Increased transcription at the *Fabp4* locus with rosi treatment. (B) The *Rgs2* gene shows repressed transcription upon rosi treatment. (C) Heatmap shows 1,951 genes that displayed a significant change in transcription (FDR <.05) due to rosi treatment in at least one time point.

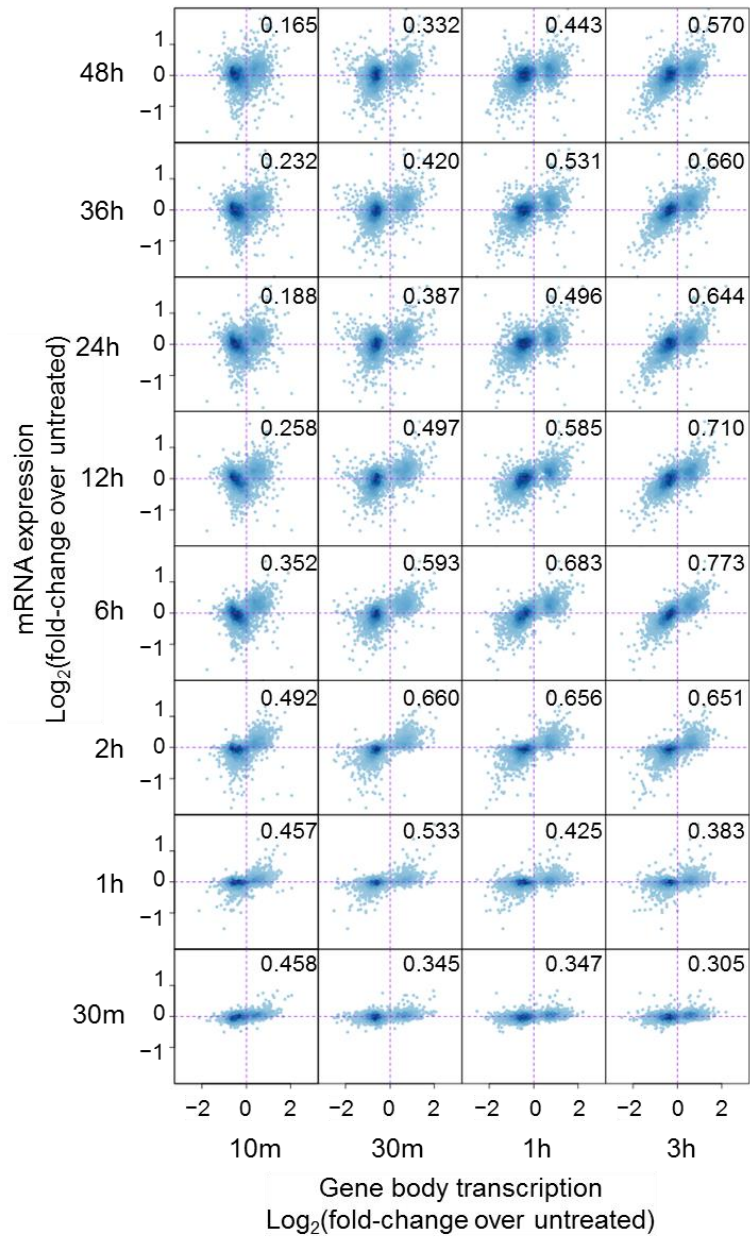


Figure 2.2 Nascent gene transcript regulation by rosi correlates with regulation of steady-state mRNAs.

Level of mRNA regulation (from microarray data) vs. gene body transcript regulation (from GRO-seq) is plotted at each time point. The Pearson correlation coefficient is given for each pair of time points.

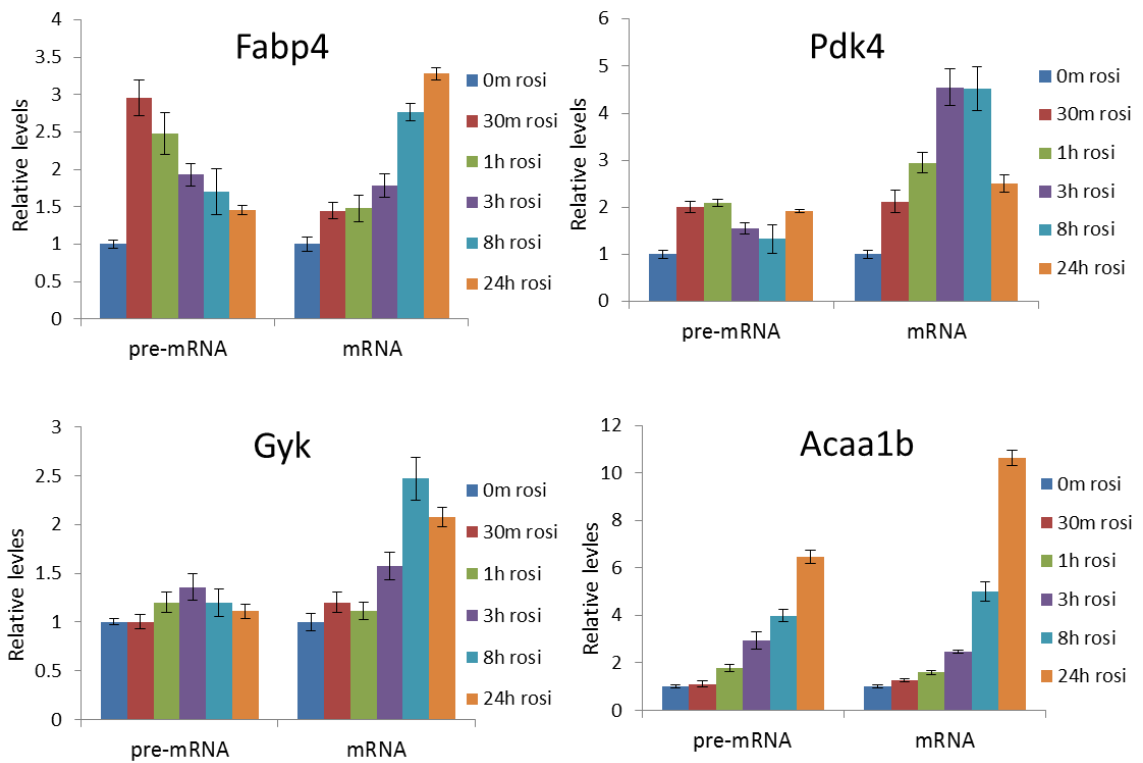


Figure 2.3 Some steady-state mRNAs may also be regulated on different timescales or non-transcriptionally.

Levels of pre-mRNA and steady-state mRNA for several genes of interest as measured by RT-PCR.

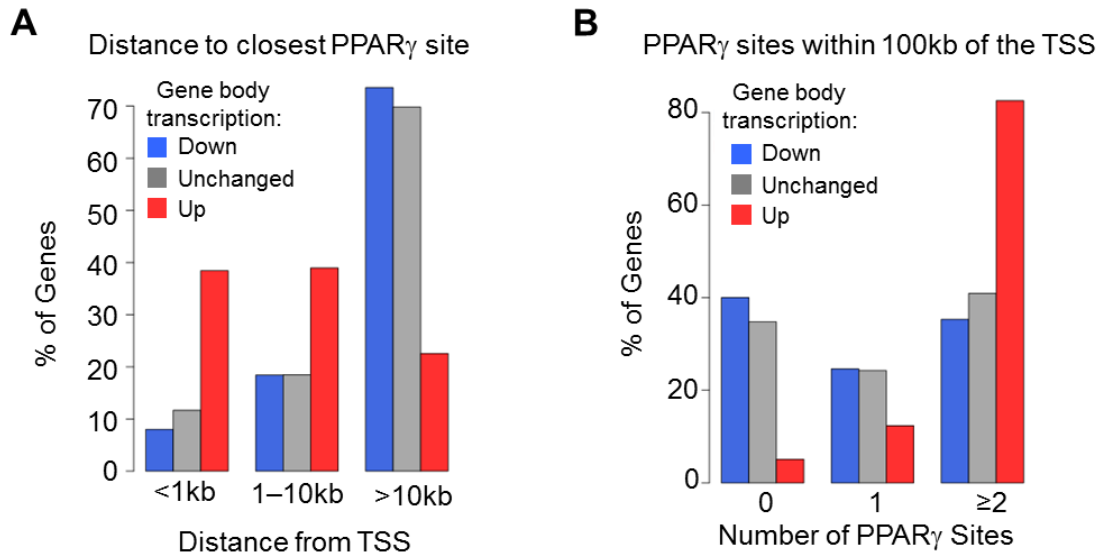


Figure 2.4 Positive gene regulation by rosi is associated with number and proximity of nearby PPAR γ sites.

(A) Distance from TSS to the nearest called PPAR γ site in genes that are up-regulated by rosi, down-regulated by rosi, and unchanged. $p < 10^{-10}$ for up-regulated versus unchanged genes by χ^2 test. (B) Number of PPAR γ sites within 100kb of the TSS for the three groups of genes. $p < 10^{-10}$ for up-regulated versus unchanged genes by χ^2 test.

Table 2.1 List of primers for gene expression

Name	Forward Sequence	Reverse Sequence
Fabp4 mRNA	CACTTTCCTTGTGGCAAAGC	AATGTGTGATGCCTTTGTGG
Fabp4 pre-mRNA	ATCGGGAATTCAGCATGAC	TCAAGCCCTGGTATTTCTGG
Pdk4 mRNA	ATCATCTTTGGTGGCCGTAG	CATGGCTGCTCCTACAAACA
Pdk4 pre-mRNA	TAACTATGCCGTGCACCAAA	AAAGGCTCAAGGGGAAGAGA
Gyk mRNA	CCCATCCTTCTCTTGGGAAT	GTACCAGCTCGACACGTTTTT
Gyk pre-mRNA	TGCTTGCTCACAGCTAGGAA	GAAGCATGGGCTTTTAGCAG
Acaa1b mRNA	ATTCCCATGGTTCCTCTCT	GCTGGTGGCATCAGAAATG
Acaa1b pre-mRNA	GCAGCAGTTCAGGGATTCTC	CCCAAACCCTTGACTGACAT
Arbp mRNA	CCGATCTGCAGACACACACT	ACCCTGAAGTGCTCGACATC

CHAPTER 3: The role and rosi-regulation of enhancers and eRNAs

Published in part in *Genes & Development*, 2014 May 1;28(9):1018-28.

The text, figures, and legends in this chapter were the work of Sonia Step with the following exceptions. Jill Marinis performed the eRNA ablation experiments shown in Figure 3.6. The C/EBP α and C/EBP β ChIP-seq experiments are the work of David Steger, and the NCoR ChIP-seq was performed by Seo-Hee You. Hee-woong Lim conducted the data processing and bioinformatics analyses.

3.1 Introduction

PPAR γ binds at many thousands of sites in the genome (Lefterova et al. 2008; Nielsen et al. 2008), yet it is difficult to determine which of these sites play an important role in regulating gene transcription in response to rosi. Previous studies have relied on mapping every PPAR γ binding site to its nearest gene to determine trends of regulation (Haakonsson et al. 2013). These studies also showed that PPAR γ binding is largely unaffected by rosi treatment, though occupancy at some sites is slightly increased. This leaves the question of what causes rosi-dependent transcriptional changes.

There has been some evidence that changes in coactivator and corepressor occupancy may be involved in rosi-mediated regulation. Early studies showed that rosi causes dismissal of corepressors and recruitment of coactivators to individual sites in the genome (Guan et al. 2005). More recently, a paper demonstrated that binding of the coactivators MED1 and CBP is increased at PPAR γ sites near genes that are up-regulated by rosi (Haakonsson et al. 2013). However, about half of rosi-regulated genes are actually repressed rather than increased, and none of these studies contributed any insight into rosi-mediated transcriptional repression.

eRNAs have garnered much interest in the last few years, as they have been shown to contribute to transcription of their target gene (Lam et al. 2013; Li et al. 2013; Melo et al.

2013). Additionally the production of eRNAs have been demonstrated to mark functional enhancers, as measured by other markers of enhancers or by transcription of the nearest gene (Hah et al. 2013; Zhu et al. 2013).

We use GRO-seq to identify thousands of bidirectional, intergenic eRNAs, detect those that are regulated by rosi, and use these to categorize functional enhancers of rosi-mediated transcription. By focusing exclusively on these functional enhancers rather than all PPAR γ sites, we examine the contributions of coactivator occupancy and other TFs to transcriptional regulation. We find that rosi-upregulated eRNAs occur at sites of strong PPAR γ binding to which coactivators such as MED1, CBP, and p300 are recruited. Remarkably, however, downregulation of eRNA transcription occurs at sites that are devoid of PPAR γ but enriched for C/EBP and AP-1 family members. MED1 and other coactivators are dismissed at these downregulated sites, strongly supporting a mechanism of negative regulation involving coactivator redistribution upon rosi binding to PPAR γ .

3.2 Materials and Methods

3.2a Cell culture

3T3-L1 cells were cultured as described in Chapter 2.

3.2b GRO-seq library preparation

GRO-seq libraries were prepared as described in Chapter 2.

3.2c ChIP-qPCR and ChIP-seq

ChIP was performed as described previously (Steger et al. 2008). Cells were crosslinked with 1% formaldehyde for 15 minutes, followed by quenching with 1/20th volume of 2.5M glycine and washed with 1x PBS. Cells were scraped down, transferred to a 1.5ml tube, and pelleted by centrifugation for 5 minutes at 300g at 4°C. Cells were resuspended in 1ml ChIP buffer (50mM Tris-HCl, 500mM NaCl, 1mM EDTA, 1% Triton X-100, 0.1% NaDOC, 0.1% SDS, and complete protease inhibitor tablet) and probe sonicated 3 times for 10 seconds at power 4, rested on ice, then probe sonicated 3 times for 10 seconds at power 6. Samples were centrifuged at maximum speed for 5 minutes at 4°C, and the interlayer was removed to a fresh tube, avoiding the lipid top layer. This clarification was repeated twice. Immunoprecipitation was performed at 4°C overnight with the appropriate antibody, then bound to Sepharose A beads. Crosslinking was reversed at 65°C overnight, then samples were digested with Proteinase K, and the DNA was isolated using phenol/chloroform. Precipitated DNA was analyzed by qPCR. The following antibodies were used in this study: C/EBP α (sc-61x, Santa Cruz), C/EBP β (sc-150x, Santa Cruz), FOSL2 (sc-13017x, Santa Cruz), JUND (sc-74x, Santa Cruz), ATF2 (sc-6233x, Santa Cruz), MED1 (A300-793A, Bethyl), H3K27ac (ab4729, Abcam), CBP (sc-369x, Santa Cruz), p300 (sc-585x, Santa Cruz), and NCoR (rabbit polyclonal, generated in-lab). Primer sequences used for ChIP-qPCR are provided in Table 3.2. ChIP

DNA was prepared for sequencing according to the amplification protocol provided by Illumina. Next generation sequencing of ChIP-seq libraries were performed by the Functional Genomics Core at the University of Pennsylvania, including preprocessing and alignment of the raw tags.

3.2d eRNA expression

RNA isolation, reverse transcription, and qRT-PCR were performed as described in Chapter 2. Primer sequences used to detect eRNA levels are listed in Table 3.1.

3.2e ChIP-seq data analysis

All the ChIP-seq tags for *C/EBP α* , *FOSL2*, *ATF2*, *JUND*, *NCoR* and *MED1* were aligned to mouse genome, mm8, using Bowtie with options, '-k 1 -m 1 --best --strata', and all the redundant tags were eliminated except one before downstream analysis. Peak-calling was performed using findPeaks command in Homer (Heinz et al. 2010). After initial calling, all the peaks were resized to 200 bp, then 2 RPM cut-off was applied for *C/EBP α* , *FOSL2*, *ATF2*, and *JUND* to select strong peaks and 1 RPM cut-off was applied for *MED1*, *CBP*, *p300* and *NCoR* because of their indirect genomic binding.

3.2f FAIRE (Formaldehyde-Associated Isolation of Response Elements)

Cells were crosslinked as for ChIP, and nuclei were isolated by probe sonication. Nuclei were sonicated in the Bioruptor (7.5 minutes on/30 seconds off). Samples were spun for 10 minutes at maximum speed, then lysates were pooled. An aliquot was removed for input, then lysates were extracted 3 times with phenol/chloroform in PhaseLock tubes. The aqueous phase was removed, and incubated at 65°C overnight. Samples were digested with Proteinase K, and then DNA was precipitated as during ChIP and analyzed by qPCR. Primer sequences are listed in Table 3.2.

3.2g Transfection

For ablation of eRNA by siRNA, antisense oligo (ASO), and locked nucleic acid (LNA), mature differentiated 3T3-L1 adipocytes were electroporated using Amaxa Cell Line L (program A-033, Lonza). One quarter of a 10-cm dish of cells was treated with 200 pmol of ASO or LNA, or 350 or 700pmol siRNA as indicated (sequences in Table 3.3) and plated onto one well of a 12-well dish. Cells were harvested 24-30h post-transfection and RNA was isolated.

3.2h eRNA analysis

For eRNA analysis, we defined an enhancer as an intergenic center of a bidirectional transcript. After pooling both replicates to improve transcript coverage for each time

point, we identified all the putative transcripts in plus and minus strands using the findPeaks command in Homer. Two start sites of a plus transcript and a minus transcript were paired together if their distance is less than 1kb, and then their midpoint was defined as a center of a bidirectional transcript. Any of these centers were discarded if they are located within 2kb from RefSeq genes or Satellite regions to avoid potential bias from gene body transcripts or abundant signal from Satellite regions. To investigate rosi-induced eRNA regulation, we used a similar pipeline as the gene transcript analysis described in Chapter 2, with the following differences. When counting tags for eRNA, we considered 2kb window only around the previously defined enhancer and summed plus and minus tags. Coverage cut-off was not applied, but the 0.5RPKM cut-off was still applied. Among eRNAs that passed the cut-off, those with $FDR < 0.05$ was considered rosi-regulated and the others were considered non-regulated. For the clustering analysis, we used $\log_2(\text{fold-change over untreated})$ in each time point and Euclidean distance. Initial dendrogram was created by Ward's criterion then further subjected to optimal leaf ordering. De novo motif search was performed using HOMER more than once for a given set of genomic loci, and the consensus motifs were considered for downstream analysis only if they appear consistently with significant p-value.

3.3 Results

3.3a Adipocyte eRNAs are regulated by rosi treatment and correlated with regulation of the nearest gene.

In addition to gene body transcription, GRO-seq revealed robust bidirectional transcripts at enhancers, or eRNAs (Core et al. 2008; Kim et al. 2010), which were identified and quantified in an unbiased, genome-wide analysis (**Figure 3.1**). For example, bidirectional eRNAs were identified at enhancers upstream of the *Fabp4* locus, and their transcription was observed to be upregulated by rosi (**Figure 3.2A**). Indeed, unbiased de novo calling of bidirectional intergenic transcripts confirmed that the transcription of many eRNAs was strongly and rapidly regulated by rosi, and downregulated eRNAs greatly outnumbered upregulated eRNAs (**Figure 3.2B**). This was similar to the effect of rosi on gene body transcription and, as has been observed in other systems (De Santa et al. 2010; Kim et al. 2010), the effect of rosi on eRNA transcription correlated strongly with transcription at the nearby gene bodies (**Figure 3.3**). The correlation was confirmed at eRNA/gene body pairs by qPCR, which also demonstrated that eRNA induction often preceded gene induction (**Figure 3.4A**). The correlation was validated at repressed eRNA/gene pairs as well (**Figure 3.4B**). Though intragenic eRNAs were excluded from downstream analysis because of difficulties in identifying them reliably, we observed that many follow a similar pattern of correlation with the target gene (**Figure 3.5**).

3.3b Ablation of eRNA transcripts has no effect on transcription of nearby genes.

To test whether the eRNA transcript has a functional role in increasing gene transcription, we ablated eRNAs using several methods and tested levels of the eRNA, its target gene, and a distant non-target gene as a control using qRT-PCR. Targeting an eRNA near the *Tusc5* gene (a relatively well-conserved eRNA) for degradation using an antisense oligonucleotide (ASO) led to robust suppression of eRNA levels, but no statistically significant effect on *Tusc5* mRNA (**Figure 3.6A**). Similarly, targeting an eRNA upstream of *Fabp4* for degradation by locked nucleic acid (LNA) gapmers resulted in a large decrease in eRNA levels, and though a small decrease was measured in *Fabp4* mRNA, this decrease was seen in off-target genes as well, such as *Pparg2* (**Figure 3.6B**). Using siRNA to ablate the same *Fabp4* eRNA had some minor effects on *Fabp4* mRNA at higher concentrations, but again off-target effects were seen at the *Pparg2* gene as well (**Figure 3.6C**).

3.3c Down-regulated eRNAs are devoid of PPAR γ and are enriched for several C/EBP and AP-1 factors.

Since *rosi* is known to positively regulate PPAR γ activity and transcription of its target genes, we investigated the differential regulation of eRNAs by PPAR γ and other transcription factors. Indeed, upregulated eRNAs were extremely likely to have PPAR γ bound nearby (85%), much more so than unregulated or downregulated eRNAs (**Figure 3.7A**). In fact, downregulated eRNAs were relatively devoid of PPAR γ binding, as will

be discussed below. Furthermore, strong PPAR γ binding as measured by total normalized tag counts from ChIP-seq was enriched at upregulated eRNAs, but not at downregulated eRNAs, relative to unregulated eRNAs (**Figure 3.7B**). PPAR γ binding sites that overlap with eRNAs had higher PPAR γ occupancy than those that lack eRNAs, further suggesting that enhancers with eRNAs are more likely to be functional (**Figure 3.7C**).

In contrast to the upregulation of transcription by rosi, PPAR γ strength of binding was not enriched at rosi-repressed eRNAs. Though 23.6% of downregulated eRNAs had PPAR γ bound (**Figure 3.7A**), this percent was far less than at unregulated eRNAs, and the binding tended to be extremely weak (**Figure 3.7B**). Moreover, unlike upregulated genes, the number, strength, and proximity of PPAR γ binding were not enriched near the TSS of downregulated genes relative to unchanged genes (**Figures 2.4A, 2.4B**). Together these data strongly suggest that PPAR γ does not mediate the repression of eRNA and gene body transcription by rosi directly, i.e., by binding in *cis* with the regulated gene body, as was the case at the majority of rosi-upregulated eRNAs.

To investigate which transcription factors may be involved in rosi-mediated transcriptional repression, we performed motif analysis at sites containing regulated eRNAs. Consistent with enrichment of PPAR γ at upregulated eRNAs, *de novo* motif finding analysis at sites of rosi-induced eRNAs revealed strong enrichment for a sequence that is highly similar to the canonical PPAR γ /RXR binding site (**Figure 3.8A**).

In contrast, *de novo* motif analysis of sites with downregulated eRNAs produced two highly enriched motifs that most resembled a C/EBP:AP-1 hybrid motif and the canonical AP-1 motif (**Figure 3.8B**). ChIP-seq analysis for C/EBP and AP-1 factors that are abundant in adipocytes revealed significant enrichment at downregulated eRNAs of C/EBP α , C/EBP β , FOSL2, JUND, and ATF2. (**Figure 3.9A**). A higher percentage of downregulated eRNAs, compared to upregulated and nonregulated, had these C/EBP and AP-1 factors bound (**Figure 3.9B**). Interestingly, although C/EBP α has been shown to be enriched near genes repressed after rosi treatment (Vernochet et al. 2009; Haakonsson et al. 2013), in our data the enrichment was higher for other factors, including FOSL2 and JUND (**Figure 3.9**). The finding that both C/EBP factors and all three AP-1 factors are enriched at downregulated sites suggests that each of these factors, potentially along with other TFs but notably not PPAR γ , is located at eRNAs in *cis* with gene bodies whose transcription is negatively regulated by rosi and may be involved in transcriptional repression.

3.3d Rosi-mediated transcriptional repression may be mediated in part by redistribution of coactivators.

The strength of C/EBP and AP-1 binding did not change upon rosi treatment (**Figure 3.10**), suggesting that it was not a change in TF occupancy that was driving rosi-mediated transcriptional repression. Instead, we hypothesized that the repression could be related to coactivator redistribution to the rosi-bound PPAR γ . ChIP-seq for the general coactivator MED1 was performed in the presence and absence of rosi. We then determined the sites

of MED1 occupancy that contained eRNAs, and whether these eRNAs were up- or downregulated by rosi. As expected, MED1 recruitment to sites of PPAR γ binding at upregulated eRNAs was increased by rosi (**Figure 3.11A**).

Remarkably, 1h of rosi treatment decreased MED1 recruitment at sites of downregulated eRNA transcription despite the general absence of PPAR γ at these sites (**Figure 3.11B**). These results were confirmed at several representative sites of up- and downregulated eRNAs by MED1 ChIP-qPCR (**Figure 3.11C**). On average, upon rosi treatment MED1 recruitment significantly decreased at downregulated eRNAs and increased at upregulated eRNAs relative to unregulated eRNAs (**Figure 3.11D**). Furthermore, redistribution of a coactivator to upregulated sites and away from repressed sites was not limited to only MED1. ChIP-seq for the coactivators CREB-binding protein (CBP) and p300 in the presence and absence of rosi showed a modest but consistent and statistically significant redistribution upon rosi treatment similar to MED1 (**Figures 3.12A, 3.12B**). Notably, occupancy of the corepressor NCoR was not altered upon rosi treatment (**Figure 3.12C**), suggesting that transcriptional repression may be driven by redistribution of coactivators, rather than replacement of coactivators with corepressors. Surprisingly, we did not observe significant changes in H3K27ac or chromatin accessibility by FAIRE at sites of eRNAs regulated after 1h of rosi treatment, although we cannot rule out changes in chromatin marks at later time points (**Figure 3.13**).

3.4 Conclusions

eRNAs are of great interest, as they have been shown to contribute to enhancer function and influence transcription at the target gene body (Kaikkonen et al. 2013; Lam et al. 2013; Li et al. 2013; Melo et al. 2013). However, we found no effect of eRNA ablation – whether by siRNA, LNA, or ASO – on transcription of nearby genes. This suggests that at least not all eRNAs have a functional role in promoting gene transcription. It is possible that those that resemble long non-coding eRNAs more closely – longer, unidirectional, poly-A tailed, etc – are more likely to play a functional role in transcription.

We were able to detect adipocyte eRNAs, on a genome-wide level, and quantification of their basal and rosi-regulated rates of transcription revealed a high correlation between eRNA transcription and transcription at the nearby genes. At rosi-upregulated eRNAs, PPAR γ binding was highly enriched and was actually required for eRNA transcription. Upregulation of gene body transcription by rosi was correlated with recruitment of the coactivators MED1, CBP, and p300 to the site of eRNA transcription, in agreement with a recent study that found MED1 was recruited to PPAR γ binding sites (Haakonsson et al. 2013). Thus, activation of gene transcription by rosi fits a general model of NR function in which ligand binding facilitates the recruitment of coactivators to PPAR γ bound in *cis* with a regulated gene body. The site of PPAR γ binding functions as an enhancer, generating eRNAs that correlate with the level of gene body transcription. The effect is

greatest when multiple strong PPAR γ binding events occur in relatively close proximity to the TSS.

In contrast, rosi-downregulated eRNAs are quite different. They are depleted of PPAR γ binding compared to background levels, but are enriched for other TFs, especially members of the C/EBP and AP-1 TF families. Nevertheless, despite the fact that PPAR γ is not bound in the vicinity, rosi treatment leads to dismissal of the coactivators from these sites. This suggests that a primary mechanism of rosi-dependent transcriptional repression involves squelching of essential coactivators from enhancers lacking PPAR γ . Consistent with this, the induction of the PPAR γ -dependent, rosi-induced eRNAs preceded the downregulation of non-PPAR γ -dependent eRNAs.

In contrast to upregulated enhancers, which depend upon activation of PPAR γ and recruitment of coactivators such as MED1, downregulated sites where MED1 binding was lost were enriched for TFs other than PPAR γ . This suggests that, in principle, any TF driving transcription at a PPAR γ -independent enhancer would be susceptible to the repressive effects of rosi redistributing coactivators to PPAR γ . Indeed, this may explain why the downregulated enhancers are enriched for binding of multiple factors, including C/EBP α , C/EBP β , FOSL2, ATF2, and JUND. Of these, only C/EBP α has previously been implicated in rosi-mediated transcriptional repression (Vernochet et al. 2009; Haakonsson et al. 2013), and notably, in our studies C/EBP α was less enriched at downregulated sites relative to the AP-1 TFs.

A role for coactivator redistribution, or squelching, has been previously suggested to explain transcriptional repression by NRs, but most of those studies were performed using transfection to overexpress receptors or coactivators, and used reporter genes as readouts (Kamei et al. 1996; Fronsdal et al. 1998; Lee et al. 2000; Li et al. 2000; Kim et al. 2001; Zhang and Teng 2001; Manna and Stocco 2007; He et al. 2012; Pascual-Garcia et al. 2013). This model gained further support recently with evidence that the endogenous coactivator NCOA3 is lost from sites of diminished DNase I hypersensitivity upon E2 hormone treatment in MCF-7 cells (He et al. 2012). Here our analysis of eRNAs has allowed us to focus on regulated enhancers and interrogate this mechanism in the context of the endogenous genome and TFs in adipocytes, where the only manipulation was treatment with the PPAR γ ligand, and to link the coactivator redistribution to changes in transcriptional levels of both eRNAs and genes.

We found five C/EBP and AP-1 transcription factors enriched at down-regulated eRNAs, and the coactivator redistribution mechanism we propose suggests that any transcription factor other than PPAR γ could lose its coactivators and drive transcriptional repression upon rosi treatment. Further studies should investigate whether all of these transcription factors, and others, indeed play an equal role in transcriptional down-regulation. Furthermore, the fact that eRNA regulation correlates so highly with regulation of the target gene may be evidence of a physical interaction between enhancer and promoter,

such as a chromatin loop. Studies such as chromatin conformation capture (3C) could determine whether the strength of looping is altered at sites with regulated eRNAs.

The strength of our approach lies in using regulated eRNAs to identify functional enhancers, which allows unbiased, *de novo* detection of novel important factors. In fact, our lab has recently used a very similar approach to identify enhancers and factors that drive circadian transcription in the liver (Fang et al. 2014). These methods could be extended to many other systems and questions.

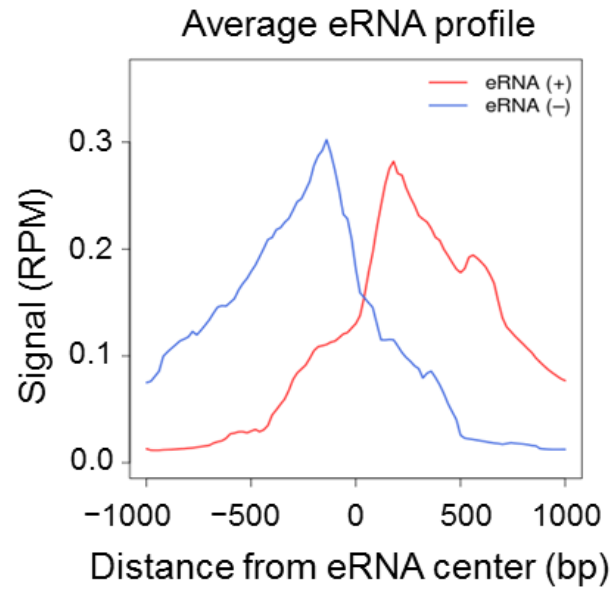


Figure 3.1 eRNAs are transcribed in adipocytes.

Genome-wide average signal of intergenic bidirectional transcripts in untreated adipocytes from the plus and minus strands.

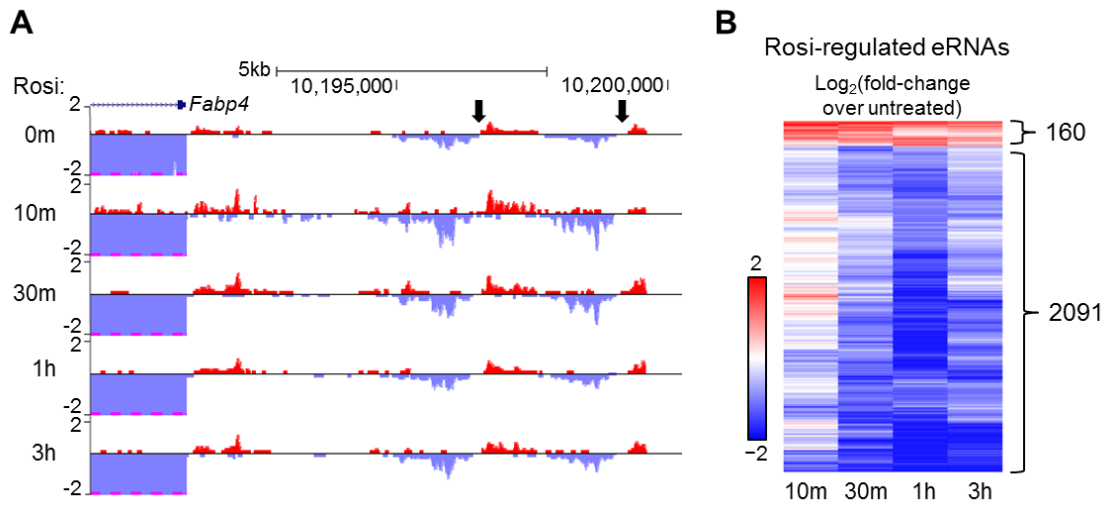


Figure 3.2 Adipocyte eRNAs are regulated by rosi.

(A) Two bidirectional eRNAs are transcribed at enhancers upstream of the *Fabp4* TSS and up-regulated by rosi treatment. eRNA centers are indicated by arrows. (B) Heatmap showing all rosi-regulated eRNAs found in an unbiased manner (N=2251).

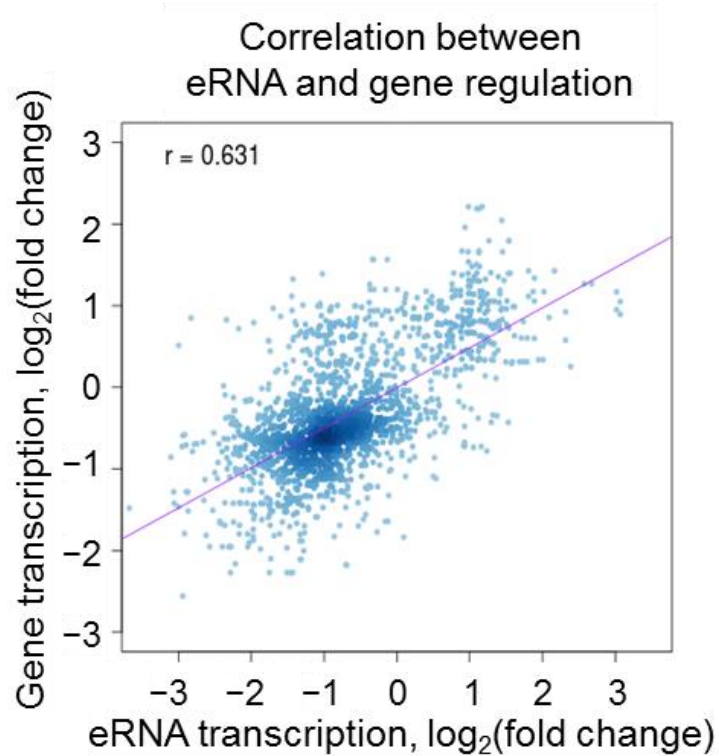
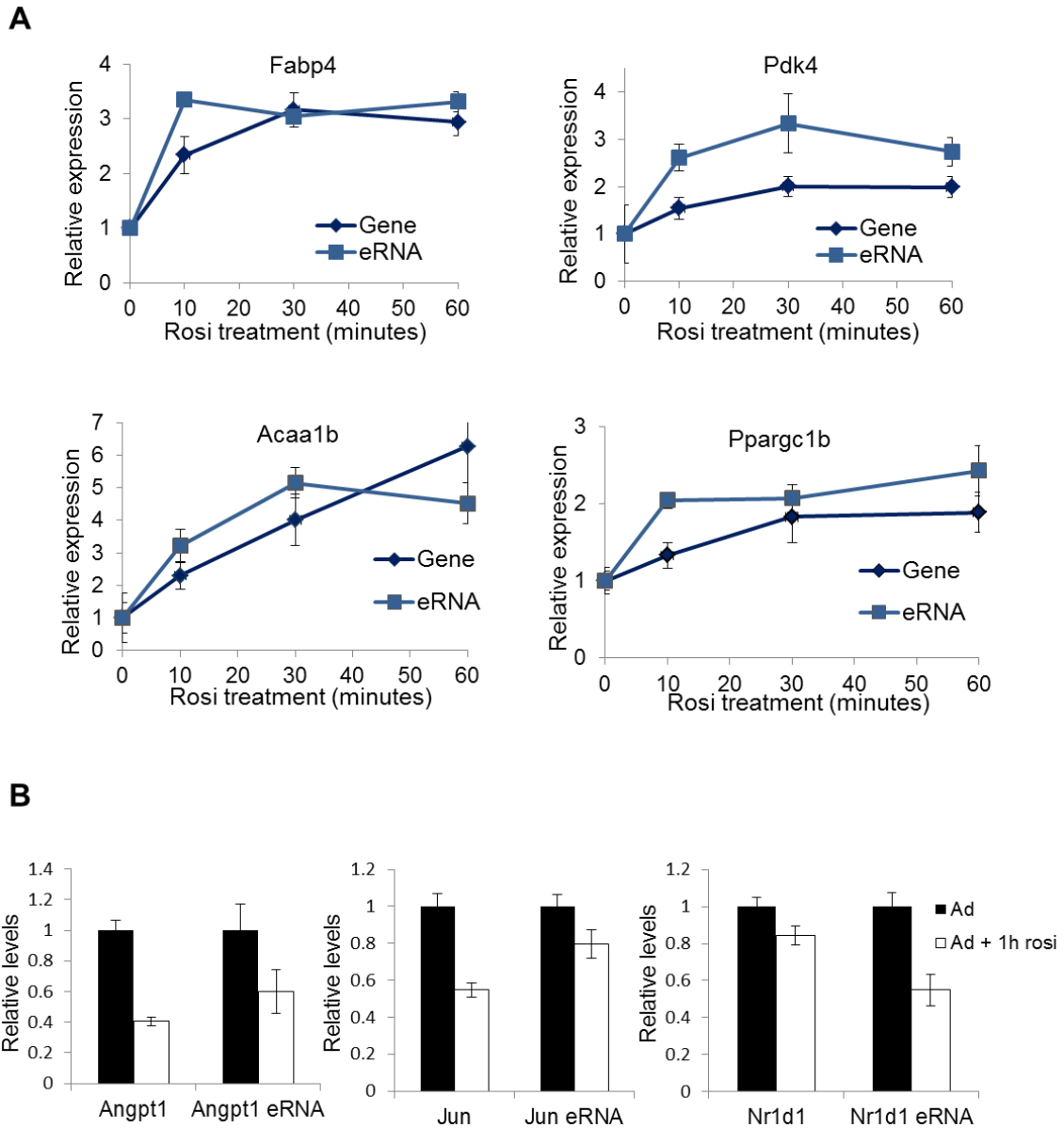


Figure 3.3 eRNA regulation and gene regulation are correlated on a genome-wide level.

Correlation between rosi-regulated eRNAs and the regulation of the nearby gene for all pairs of matching time points (N=462). For each gene, eRNAs within 100kb of the TSS were included in the analysis.



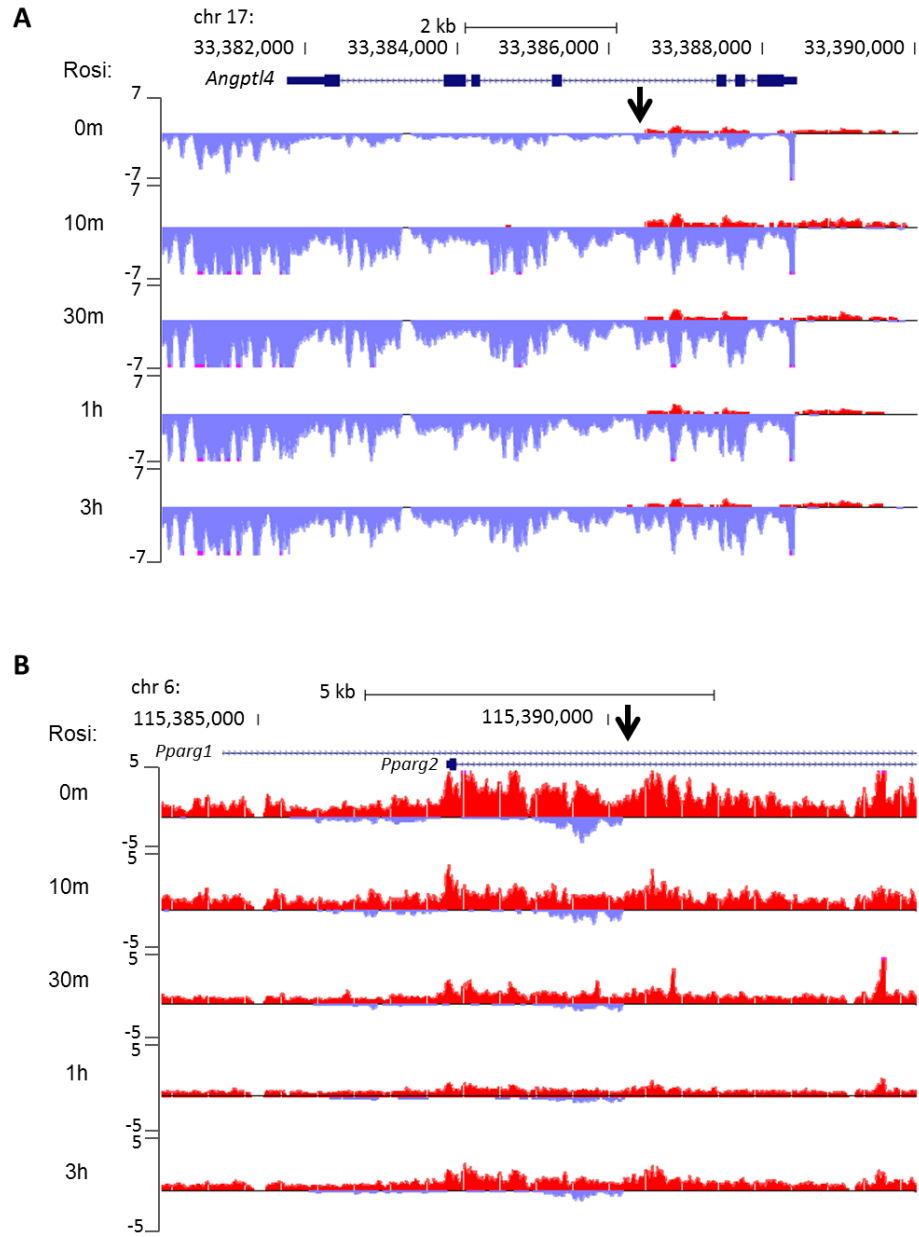


Figure 3.5 Examples of intragenic eRNAs that correlate with gene regulation.

(A) Screenshot of the *Angptl4* gene locus. Approximate eRNA center is indicated by the arrow. (B) Screenshot of the *Pparg* gene locus. Approximate eRNA center is indicated by the arrow.

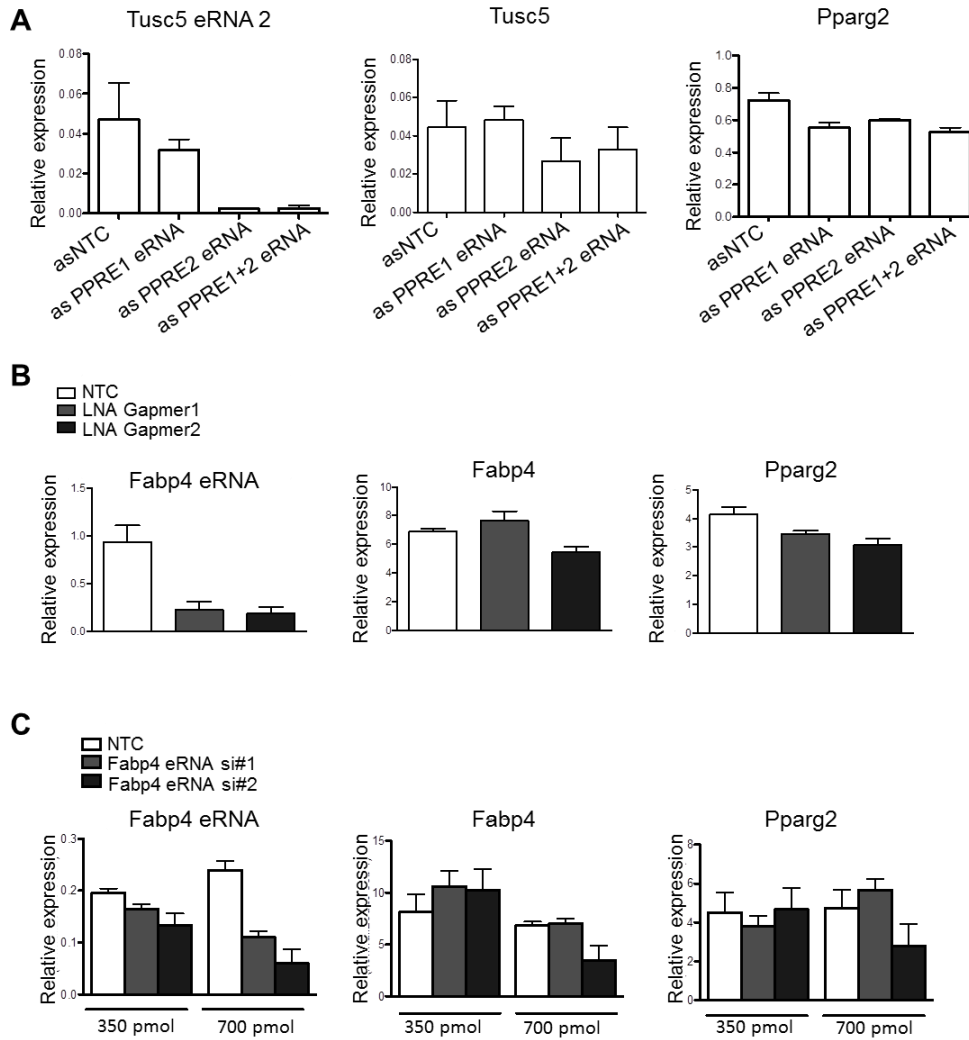


Figure 3.6 Ablation of individual eRNAs has no effect on transcription of the nearest gene.

(A) qRT-PCR for the eRNA near *Tusc5*, *Tusc5* mRNA, and *Pparg2* mRNA as a control after ablation of the eRNA with an antisense oligonucleotide. (B) qRT-PCR for the eRNA upstream of *Fabp4*, *Fabp4* mRNA, and *Pparg2* mRNA after ablation of the eRNA with locked nucleic acid (LNA) gapmers. (C) qRT-PCR for the eRNA upstream of *Fabp4*, *Fabp4* mRNA, and *Pparg2* mRNA after ablation of the eRNA with siRNA.

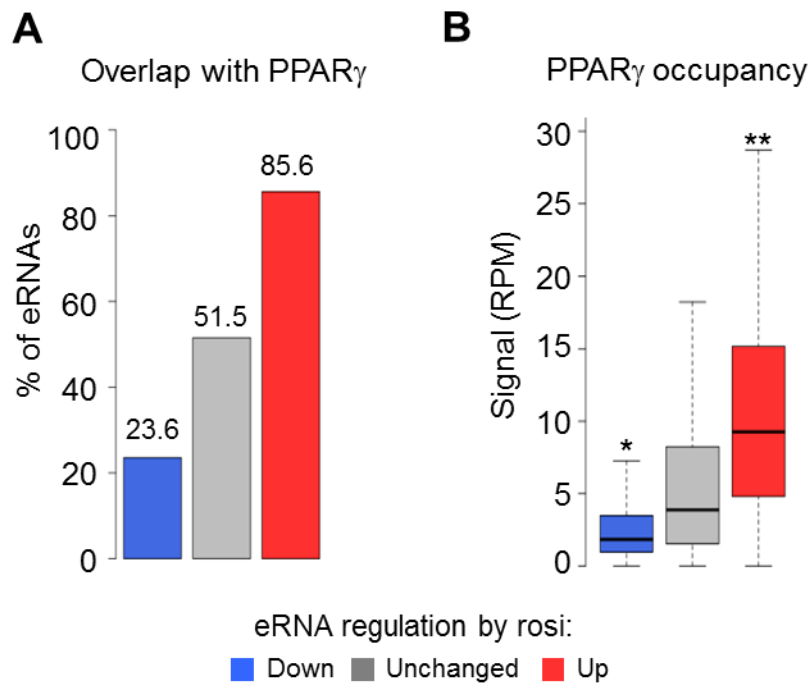


Figure 3.7 Rosi-up-regulated eRNAs are enriched for PPAR γ binding, but down-regulated ones are depleted of it.

(A) Percentage of up-regulated, down-regulated, and unregulated eRNA sites that overlap with a called PPAR γ peak from ChIP-seq. (B) Total PPAR γ tag count, in reads per million (RPM), within 1kb of up-regulated, down-regulated, and unregulated eRNA sites.

(*) $p = 7.7 \times 10^{-95}$ versus unregulated sites; (**) $p = 1.8 \times 10^{-20}$ versus unregulated sites.

(C) Occupancy of PPAR γ in RPM is plotted at sites that contain or do not contain an eRNA.

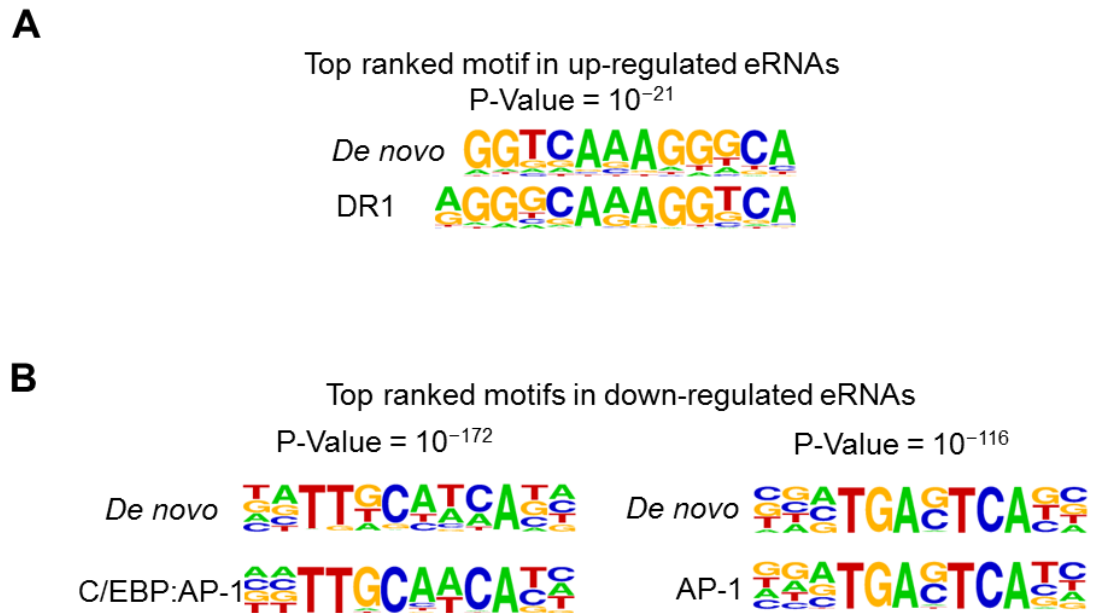


Figure 3.8 Up- and down-regulated eRNAs are enriched for different motifs.

(A) Top hit from HOMER de novo motif search at up-regulated eRNAs. The closest known motif, the DR1 motif, is shown for reference. The enrichment for this motif was 45% at the target sites and 13.5% in the background sites. (B) Top two hits from HOMER de novo motif search at down-regulated eRNAs. The closest known motif for each is shown for reference.

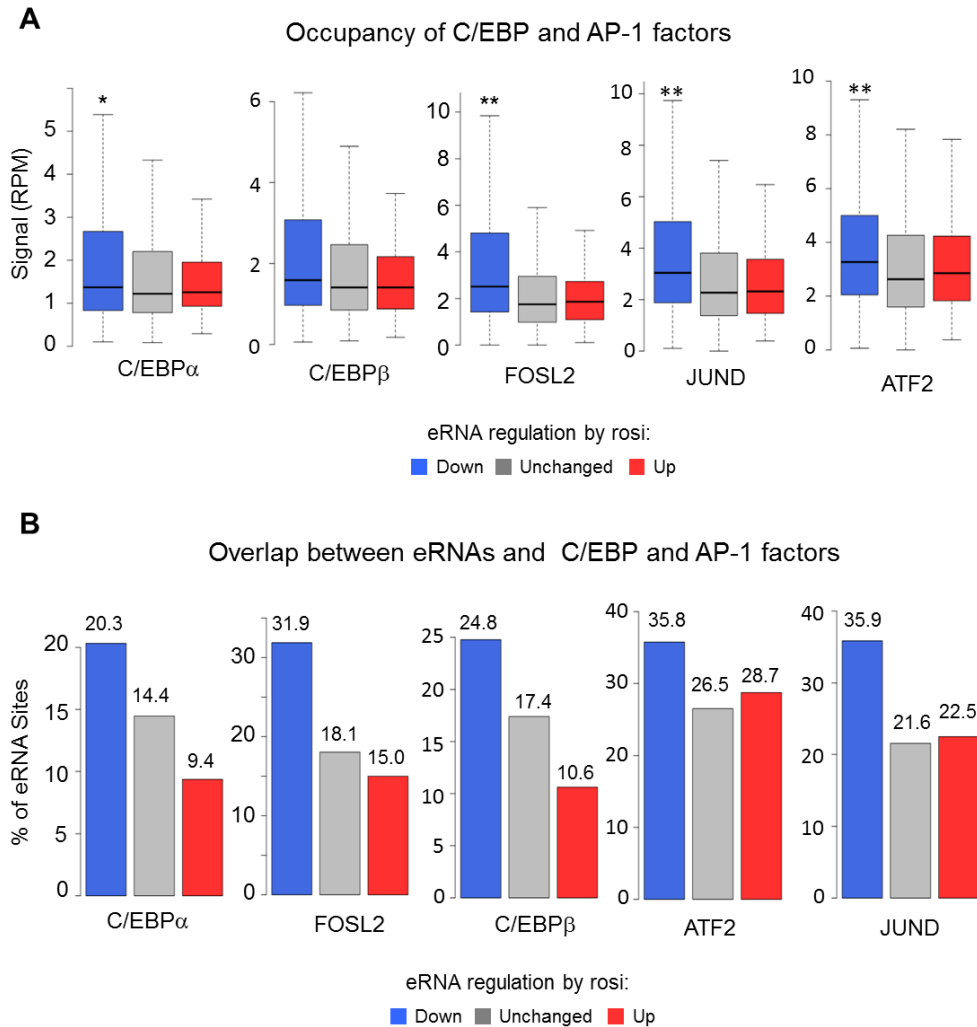


Figure 3.9 Down-regulated eRNAs are enriched for binding of C/EBP α , C/EBP β , FOSL2, JUND, and ATF2.

(A) Total tag counts in reads per million (RPM) within 1kb of the center of the regulated eRNAs from ChIP-seq for the following factors: C/EBP α , C/EBP β , FOSL2, JUND, and ATF2. (*) $p < 4.6 \times 10^{-5}$. (**) $p < 10^{-10}$. (B) Percentage of regulated eRNAs that overlap with called peaks of C/EBP α , C/EBP β , FOSL2, JUND, and ATF2.

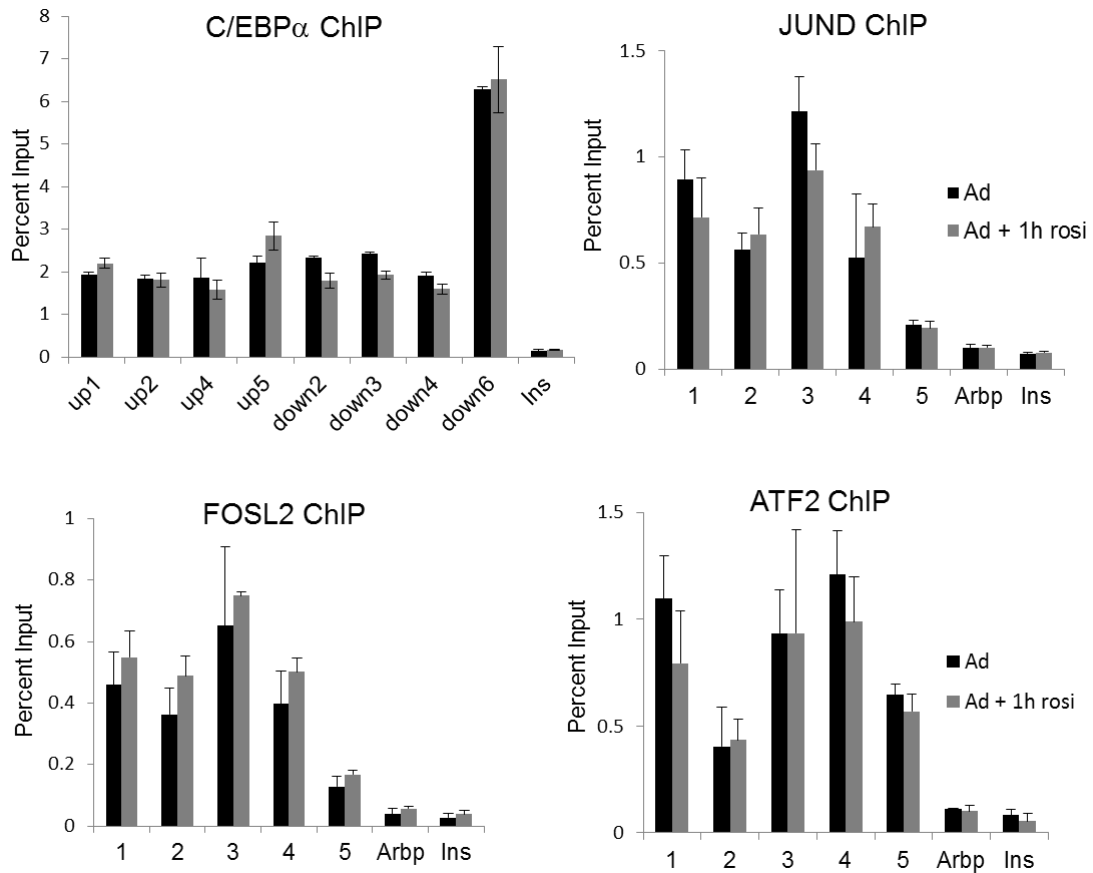


Figure 3.10 Strength of binding of C/EBP and AP-1 factors does not change upon rosi treatment.

ChIP-qPCR at several strong binding sites for C/EBP α , C/EBP β , FOSL2, JUND, and ATF2 before and after 1h of rosi treatment. Primer sequences are listed in Table 3.2.

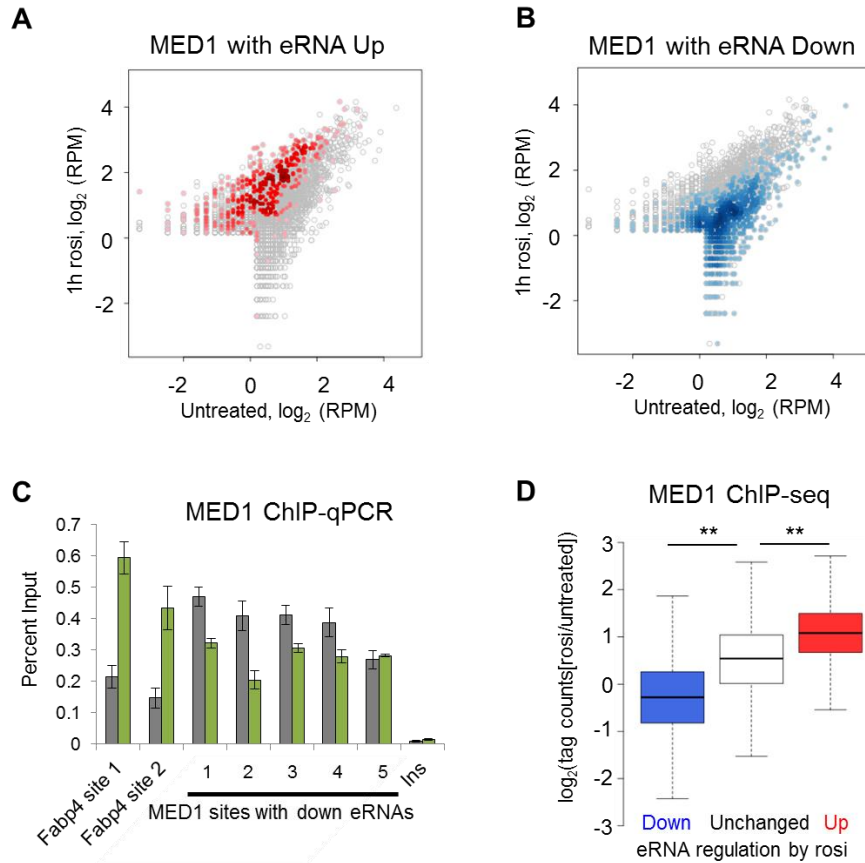


Figure 3.11 MED1 binding is increased upon rosi treatment at up-regulated eRNA sites and decreased at down-regulated sites.

(A) Scatter plot comparing MED1 binding strength in reads per million (RPM) with and without 1h of rosi treatment, with sites containing an up-regulated eRNA highlighted in red. (B) Scatter plot comparing MED1 binding strength with and without 1h of rosi treatment, with sites containing a down-regulated eRNA highlighted in blue. (C) MED1 ChIP-qPCR at sites with up-regulated or down-regulated eRNAs. N = 5. Error bars indicate SEM. (*) $p < 0.05$; (**) $p < 0.01$; (***) $p < 0.005$ by paired t -test. (D) Box plot showing average \log_2 of fold change in MED1 occupancy upon rosi treatment at sites of regulated eRNAs. (**) $p < 10^{-15}$.

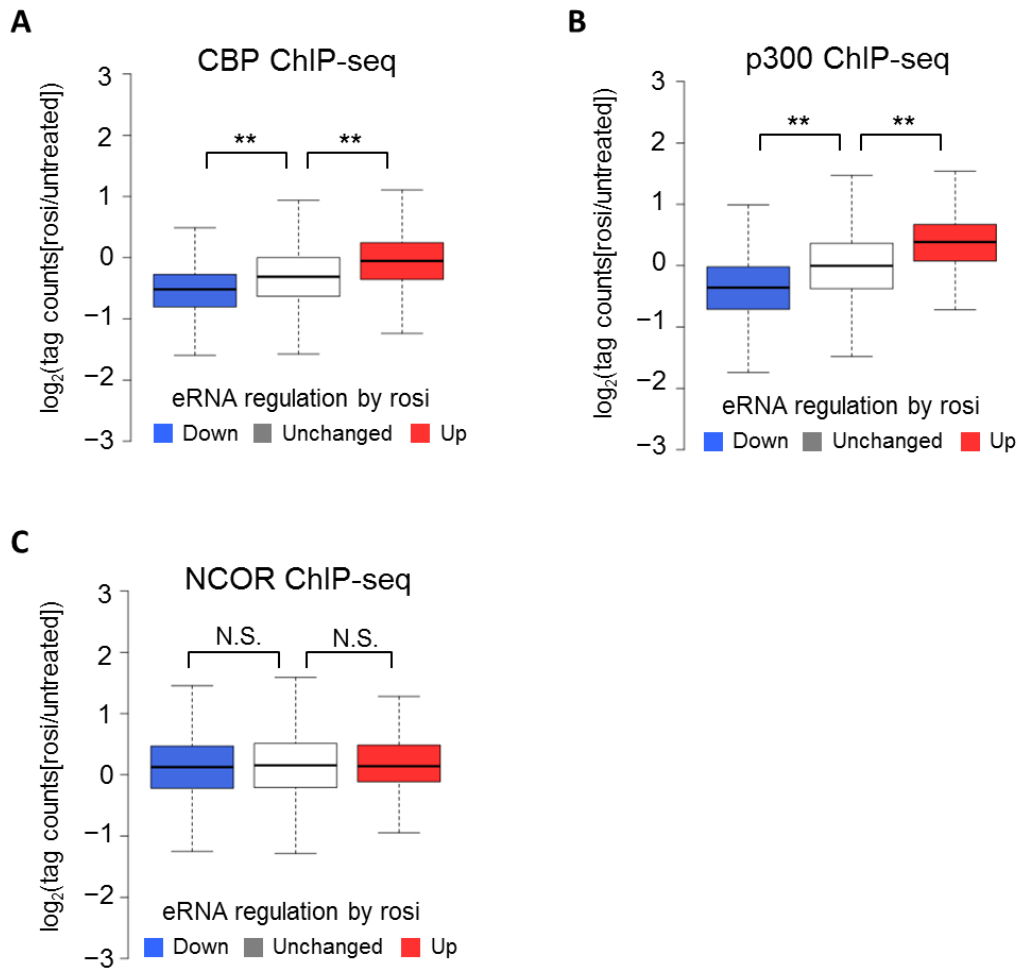


Figure 3.12 The coactivators CBP and P300 are also redistributed upon rosi treatment, but the corepressor NCoR is not.

(A) Box plot showing average \log_2 of fold change in CBP occupancy at up-regulated, down-regulated, and unregulated eRNA sites. (**) $p < 10^{-15}$. (B) Box plot showing average \log_2 of fold change in P300 occupancy at up-regulated, down-regulated, and unregulated eRNA sites. (**) $p < 10^{-15}$. (C) Box plot showing average \log_2 of fold change in NCoR occupancy at up-regulated, down-regulated, and unregulated eRNA sites. N.S. = not statistically significant.

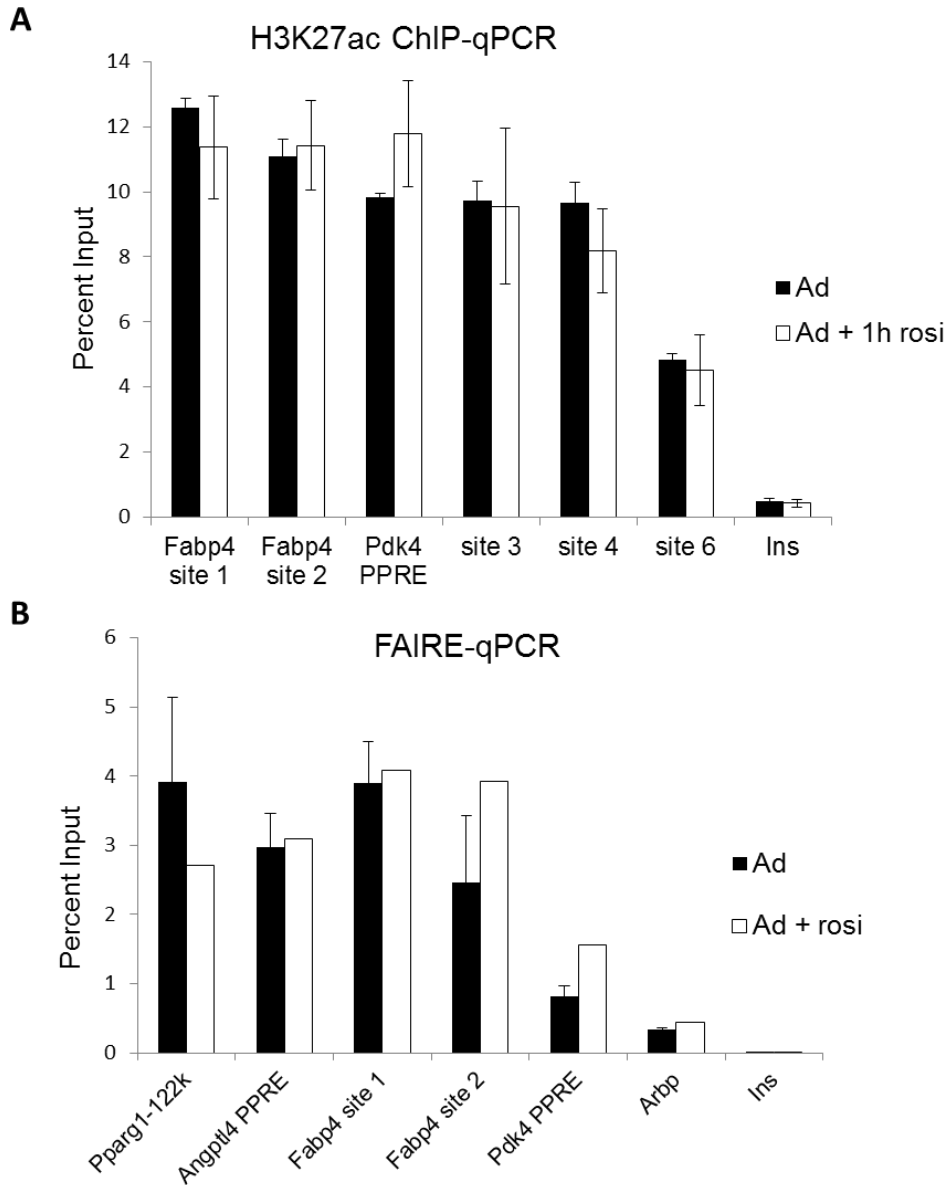


Figure 3.13 Rosi does not cause changes in levels of H3K27ac or open chromatin as measured by FAIRE.

(A) ChIP-qPCR for H3K27ac at enriched sites before and after 1h of rosi treatment. Primers sequences are listed in Table 3.2. (B) FAIRE-qPCR at several regulated sites before and after 1h of rosi treatment. Primer sequences are listed in Table 3.2.

Table 3.1 List of primers for eRNA and gene expression

Name	Forward Sequence	Reverse Sequence
Fabp4 pre-mRNA	ATCGGGAATTCAGCATGAC	AATGTGTGATGCCTTTGTGG
Fabp4 eRNA	TGAGTCCCCCACTTGCTTTA	CACCCTGTAAGGCTGGTGAT
Pdk4 pre-mRNA	TAACTATGCCGTGCACCAAA	AAAGGCTCAAGGGGAAGAGA
Pdk4 eRNA	TTAACAAAGAAAACAGGCAACA	CATCAGTACCCTCAAAACACAAA
Acaa1b pre-mRNA	GCAGCAGTTCAGGGATTCTC	CCCAAACCCTTGACTGACAT
Acaa1b eRNA	ACAGCAGGTGTGGTGACTTG	TGCATCCTTGAGGAACAAGA
Ppargc1b pre-mRNA	TGAATGCACAGTGGTTTGGT	TGTACCCGCCACACAAGTAA
Ppargc1b eRNA	TCTATTGTTAGGCTGTGAAACATT	TATGCATCCCCAGTCCTCAT
Angpt1 pre-mRNA	ACGATGTAAGTCCGGCAGAA	TGCTTTAAGCGTACAACCAAAA
Angpt1 eRNA	CCATTTACAGCCAACGGTCT	CCAAACTATTTGCTCCTGGTG
Jun pre-mRNA	GGTCCCTGCTTTGAGAATCA	GCAGACACTTTGGTTGAAAGC
Jun eRNA	GAAGTTGAGCGGGTTTGAGA	TTCCAGGTACAGCACACTGC
Nr1d1 pre-mRNA	AGGCAGGGCAACCTTAAAAT	TGAAACCATAGCCGGGTAAC
Nr1d1 eRNA	CAGAAGATTCTCCTCCCGTAA	AGAGCATCCAAGCCTGACAA
Tusc5 eRNA 2	TTCAAACAAAACCCCTTT	GAATTATTCCTCCGTGATCCA
Tusc5	CCCCTGCTGCACACTACTTC	TTACCTGGTCCTTGCCATTG
Fabp4 eRNA	GGAAACCCACACAAGCTGTT	GGGCATGGCATAACAGAACT
Fabp4	CACTTTCCTTGTGGCAAAGC	AATGTGTGATGCCTTTGTGG

Pparg2	TGGGTGAAACTCTGGGAGAT TC	GAGAGGTCCACAGAGCTGATTC C
Arbp	CCGATCTGCAGACACACT	ACCCTGAAGTGCTCGACATC

Table 3.2 List of primers for ChIP-qPCR and FAIRE-qPCR

Name	Forward Sequence	Reverse Sequence
C/EBP up1	AGCCAGGGAATCTGCTTAG G	TGGCATTGCATGTTATTGCT
C/EBP up2	TGTCACAATACTAACCCT GTTGA	TGTCCCCATGACAATAATGA
C/EBP up4	GCCTCTCGAAATGTTTGTC C	GCCAGACAGAATGGAAGCA
C/EBP up5	CTGTACCTTTTTGGCCTTG	CTCACATGCTGGAAACCTCA
C/EBP down2	GGCCAAATCAGTTCCTGAA A	GTTGTGGGGAGTGAAGCAAT
C/EBP down3	GGGCTTGGAGACTGTAGCT G	CTCTGGCTCCTTGAGCAATC
C/EBP down4	CTCAGTTGCTCCCTTTCACC	GGCAACTCTTTTCCCTCCTC
C/EBP down6	AGCGCAGACTCCCTCTAAT G	CAACGGTTTCAAACCCAGA
ATF2 site 1	CATCAGGAAGTTGGCCTCT G	GGCTTTCCTCTGCTTCTCCT
ATF2 site 2	CGAACTCCAGGGATTTTCT G	GCAAACCGTGGTCCTTTCTA
ATF2 site 3	GGACAGCGGAGTTCTCTAG C	TGAGAATAGCATGCAGTGTGC
ATF2 site 4	CGCGTCTTGATTGGTCACT	AGGCAGGTGTCCTGGTCTC
ATF2 site 5	TCATCCTGTGAGCCTGATT G	CATCCCACATTCATCCACTG
FOSL2/JUND site 1	GGAAAAGCCACACCCTACA A	GGGACTTTCTTCAGGAGCCTA
FOSL2/JUND site 2	GCCAGAGCATGGGTTTTTCT A	TTGGACAGGCCATGTGACTA
FOSL2/JUND site 3	AGCTACCAAGTGACTGCCA AG	TTGAGCAGCGTGATGAAATC
FOSL2/JUND site 4	GACTCATTTCCCAGCTGAC C	CAATTCAAAGGGGAACTCG
FOSL2/JUND site 5	ATGATGCAATTGGGCTCCT	CTGACTGTGCTGGCTGACTC
Fabp4 site 1	AATGTCAGGCATCTGGGAA	GACAAAGGCAGAAATGCACA

	C	
Fabp4 site 2	GTGGAAGCTGAAGCTGCTG T	GTCCCTGGGAATGATTTGTG
MED1 site 1	CCCCACTGTTGCAAAAATC T	CCCTGGCCTACAAGAGCTTA
MED1 site 2	TTAAAAGAACGAGCCCCAA A	AATGGCTTGCAAAACTCCAC
MED1/H3K27 site 3	AATGGTTGGAGGCCAGTAA A	AGTTGGAAGCGTTCATTGCT
MED1/H3K27 site 4	TTCCCCAGGAAAGTTCAG A	CCCTGAGATGAGGTTGGTTG
MED1 site 5	GCATTTCTCAGCCAGGAGT C	GGCACAGAGGAAGCTCAGTC
MED1/H3K27 site 6	GCACTATTGCGTTCCTTTC	TGGCTAGGTCCAAGGACAAC
Pparg-122k	AGCTTTGCTGGCTAGAGGT G	TTTCGCAGAACTGAGGTTGA
Angptl4 PPRE	CTGAAACTGCATGCCTCAA G	TTCCTGTCTGCCTGTCACTG
Pdk4 PPRE	AGAGTTCTCTGGGGGAAAG G	CCACTTGGGCAACAGAATTT
Arbp	TCATCCAGCAGCAGGTGTT TGACA	GGCACCGAGGCAACAGTT
Ins	TGCTTGCTGATGGTTTTTGA	CAGAGAGGAGGTGCTTTGGT

Table 3.3 List of sequences for ASO, LNA, and siRNA

Name	Sequence
asNTC	TAGCGACTAAACACATCA
as Tusc5 PPRE1 eRNA	GTTATCTCTCCAGTGCCCA
as Tusc5 PPRE2 eRNA	GCATTCGTCTCCAGGCTTT
LNA gapmer1	ATCAGGCCACCACTATGTA
LNA gapmer 2	TGCTTTCAGAAACGGGAACT
NTC si	UAGCGACUAAACACAUCA
Fabp4 eRNA si1	AUGGCAUACAGAAACUGCCCCUUGAGCAGUUUCUU
Fabp4 eRNA si2	AAAUUUGUUAUUGGCAGAAAGUCCCUCUGCCAAUA A

CHAPTER 4: Regulation of adipocyte transcription by MRL-24

4.1 Introduction

Alternative mechanisms have been suggested to explain the dysregulation of PPAR γ signaling in obesity or diabetes and subsequent improvement by TZD treatment. In one such model, PPAR γ is phosphorylated at Ser273 by Cdk5. This phosphorylation is increased in adipose tissue by high fat diet or pro-inflammatory treatments such as TNF α , but blocked by TZDs (Choi et al. 2010). The phosphorylation is also effectively blocked by a compound called MRL-24, which binds to PPAR γ and improves glucose tolerance but lacks agonist activity in a PPAR γ transactivation assay. In both the adipose tissue of MRL-24-treated mice and in a cell culture model of differentiated fibroblasts treated with MRL-24, the compound did not activate the majority of expected PPAR γ target genes that are up-regulated with rosi, but instead up-regulated a unique subset of target genes. Understanding these differentially regulated gene targets may be critical to dissociating the positive anti-diabetic effects of these drugs from the adverse effects.

The same group followed up this work with another paper in which they created other novel synthetic compounds that bind to PPAR γ and block its Cdk5-mediated phosphorylation, but lack classical transcriptional agonism (Choi et al. 2011). They showed that one such compound, SR1664, had potent anti-diabetic activity *in vivo* without causing some of the adverse effects that plague TZDs, including weight gain, fluid retention, and inhibiting bone formation in culture. A separate group developed another compound, called GQ-16, that retains similar insulin-sensitizing effects to rosi

without causing weight gain or edema (Amato et al. 2012). It acts as a partial PPAR γ agonist in transactivation and adipogenesis studies and inhibits Cdk5-mediated phosphorylation of PPAR γ *in vivo*. Hydrogen/deuterium exchange studies and molecular dynamics modeling suggest that GQ-16 binds differently than rosi, and is less effective at stabilizing helix 12 in its active conformation. Lastly, a compound called INT131 was shown clinically to improve blood glucose in diabetic patients without associated weight gain or fluid retention (DePaoli et al. 2014). This is discussed in more detail in Section 5.2d.

These studies still leave many questions unanswered about the mechanistic link between phosphorylation of PPAR γ and its transcriptional activity. This mechanism may still involve regulated recruitment of coregulators, similar to the way rosi functions as described in Chapter 3. We sought to further explore the regulation of transcription by MRL-24, with the eventual goal of using MRL-24-regulated eRNAs to identify whether it functions by regulating the same group of enhancers as rosi or distinct ones, and whether the altered phosphorylation of PPAR γ causes differential recruitment of coactivators to drive transcriptional changes. However, we find that in the 3T3-L1 model of adipocytes, MRL-24 does not up-regulate the previously described unique set of target genes distinct from rosi. Instead, its function resembles that of a partial agonist: it regulates many of the same targets as rosi, but less robustly.

4.2 Materials and Methods

4.2a Cell culture

Cells were cultured as described in Chapter 2, and treated with 1 μ M rosiglitazone (Biomol) or 1 μ M MRL-24 (Merck) when stated.

4.2b Gene expression analysis

RNA was isolated from cells and analyzed by microarray or qRT-PCR as described in Chapter 2. Primer sequences used for qPCR are listed in Table 4.1.

4.3 Results

4.3a Previously identified MRL-24-specific gene targets are not differentially regulated in our model.

MRL-24 was previously demonstrated to selectively increase transcription of a subset of PPAR γ target genes (Choi et al. 2010). To test these findings in our model, adipocytes were treated for 24h with 1 μ M rosi or MRL-24, and then gene expression levels of the putative MRL-24-specific genes were tested by qRT-PCR. Unexpectedly, none of these genes were robustly increased by MRL-24 (**Figure 4.1**). To confirm that the treatments worked, and to investigate whether MRL-24 is able to agonize classical PPAR γ target genes similar to rosi, qRT-PCR was performed with gene expression primers to known rosi target genes. MRL-24 increased expression of these genes to a comparable level as

did rosi (**Figure 4.2**), suggesting that both drugs were active and had many of the same transcriptional effects.

4.3b Microarray comparing effects of MRL-24 and rosi does not identify any MRL-24-specific target genes.

To further investigate whether there were any gene targets specific to MRL-24 and not rosi, microarray was performed on untreated adipocytes as well as those treated with 1 μ M rosi or MRL-24 for 24h (**Figure 4.3**). Each point represents a gene regulated by at least one drug, with fold-change over the untreated control plotted for rosi on the x-axis and for MRL-24 on the y-axis. The very high correlation between the two treatments ($r = 0.79$) suggests that on a genome-wide level, the two drugs regulate most of the same gene targets. The relatively low slope of 0.47 suggests that while MRL-24 targets many of the same genes as rosi, it up-regulates them to lower degree, similar to a partial agonist.

To further test whether any of the genes that fall above the best-fit line may in fact be robust MRL-24-specific targets, the samples were tested by qRT-PCR with primers to those genes. When performed on the same cDNA samples as used for the microarray, qRT-PCR confirmed MRL-24-specific regulation (**Figure 4.4A**), but when repeated in an independent experiment the result was not replicated (**Figure 4.4B**), suggesting that the MRL-24-specific regulation was an artifact of the original experiment, and no robustly MRL-24-specific genes could be found by microarray.

Since the results in Chapter 3 support the idea that eRNA regulation can provide valuable insight into which enhancers are regulated by a TF ligand, we examined whether MRL-24 regulates any eRNAs differently than rosi, and whether this could provide any information about its mechanism. Very preliminary evidence suggests that while rosi up-regulates eRNAs associated with its target genes (such as Pdk4 and Fabp4), MRL-24 may not be regulating these eRNAs (**Figure 4.5**) despite regulating the same target genes (**Figure 4.2**).

4.4 Conclusions

Much attention has been devoted to the development and study of selective PPAR γ modulators, or SPPARMs, with the hope that we may be able to dissociate the positive metabolic effects of TZDs from their adverse effects. MRL-24 has been shown to regulate only a selective subset of PPAR γ target genes, and this was thought to explain its favorable risk/benefit profile. We were unable to confirm any of its unique target genes, though this could be due in part to different cell culture models. The experiments we performed were all done in the 3T3-L1 cell culture model of adipocytes. In contrast, the published studies on MRL-24 were performed either *in vivo*, in which mice were treated with MRL-24 and then their white adipose tissue was harvested and studied, or *in vitro* but in a different cell culture model (Choi et al. 2010). Their gene expression studies were performed in a cell culture model in which mouse embryonic fibroblasts from

PPAR γ -null mice were cultured, FLAG-PPAR γ was retrovirally overexpressed, cells were selected, and the cells were differentiated into adipocytes with the hormonal cocktail of dexamethasone, insulin, and isobutylmethylxanthine. Clearly this cell culture model is considerably different from the model of 3T3-L1 adipocytes, and it is thus not surprising that many genes may be regulated differently in the two models. What is surprising, however, is that MRL-24, which was shown to selectively regulate a group of genes in differentiated MEFs, did not uniquely regulate any genes at all in our model. Not only were we unable to identify any robustly selective MRL-24 gene targets, but the drug behaved very similar to a partial agonist, regulating most of the same genes as rosi but to a lesser extent.

Despite the lack of MRL-24 specific genes, the drug could still be functioning through a different mechanism than rosi. GRO-seq on MRL-24-treated cells followed by identification of regulated eRNAs could identify differentially regulated or selective enhancers. We could not identify any MRL-24-specific genes, though this could be in part due to our model, 3T3-L1 cells, which may not adequately reflect the behavior of adipocytes *in vivo*. Nevertheless, this preliminary data suggests that MRL-24 may not truly be a selective enough ligand to dissociate favorable physiologic effects from adverse ones.

We could not confirm any unique target genes for MRL-24, or find any evidence that it behaves as a SPPARM. Nevertheless, there are other SPPARMs currently being studied or in clinical development that hold more promise. For example, a compound called INT131 has shown promise in early clinical studies for improvement of blood glucose without the associated toxicities of TZDs (DePaoli et al. 2014), and biochemical studies suggest that it functions as a SPPARM. Studies investigating how this compound and others regulate transcription using GRO-seq and ChIP-seq could shed more light on their mechanisms of action, including which functional enhancers they regulate and whether they drive transcriptional changes through the redistribution of coactivators. This is discussed in more detail in Section 5.2d.

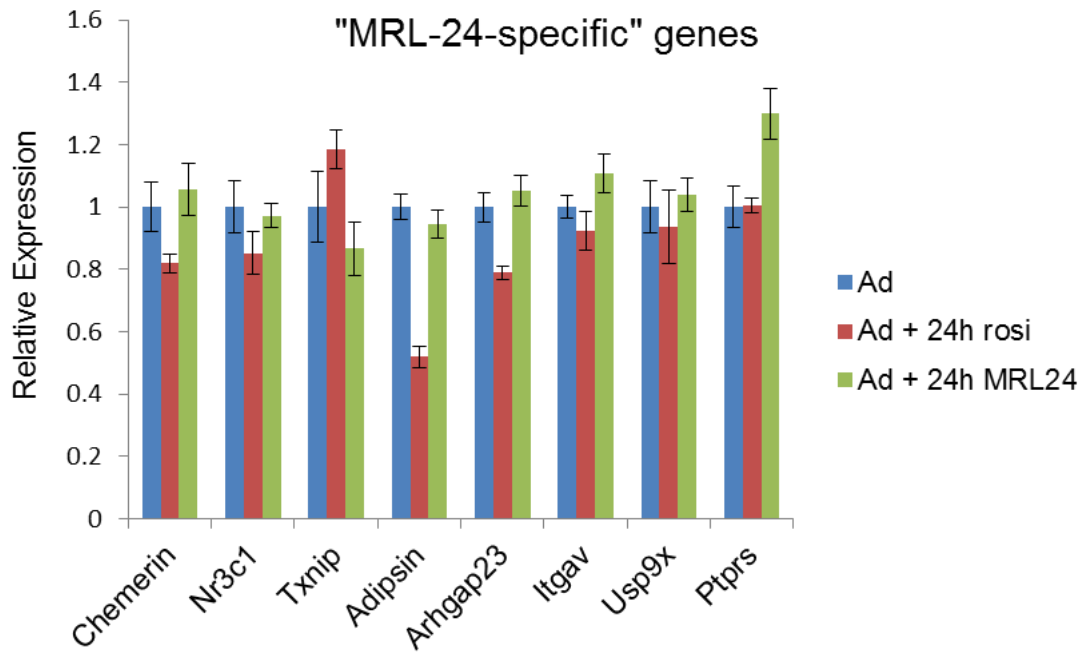


Figure 4.1 Previously defined MRL-24-specific genes are not specific targets in this model.

mRNA levels of genes previously identified as selectively up-regulated by MRL-24 but not rosi were measured by qRT-PCR in control adipocytes and adipocytes treated for 24h with rosi or MRL-24.

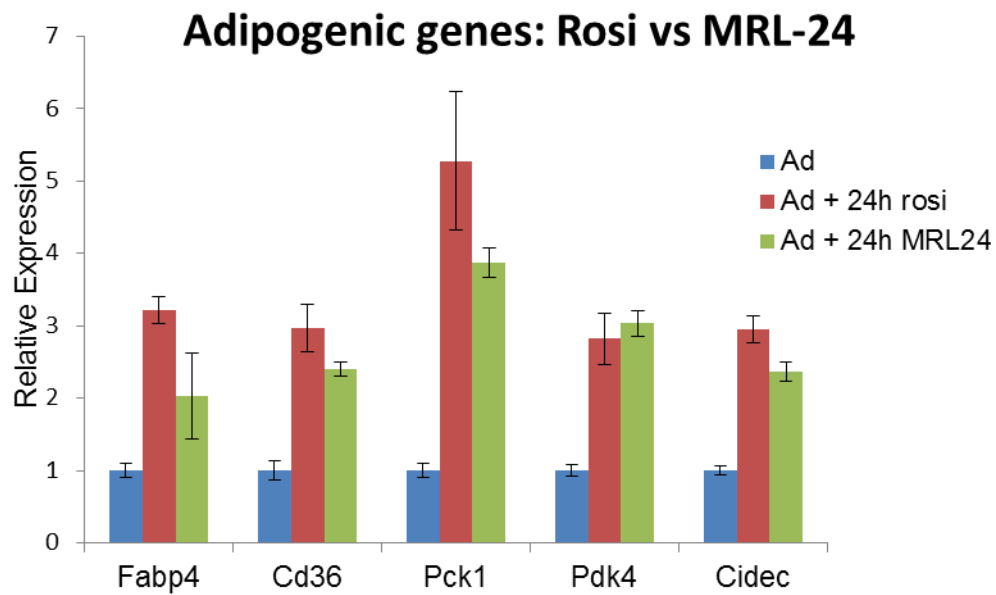


Figure 4.2 Most classic adipogenic PPAR γ target genes are regulated by MRL-24 to comparable levels as by rosi.

Levels of classic PPAR γ target genes were measured by qRT-PCR in adipocytes and adipocytes treated for 24h with rosi or MRL-24.

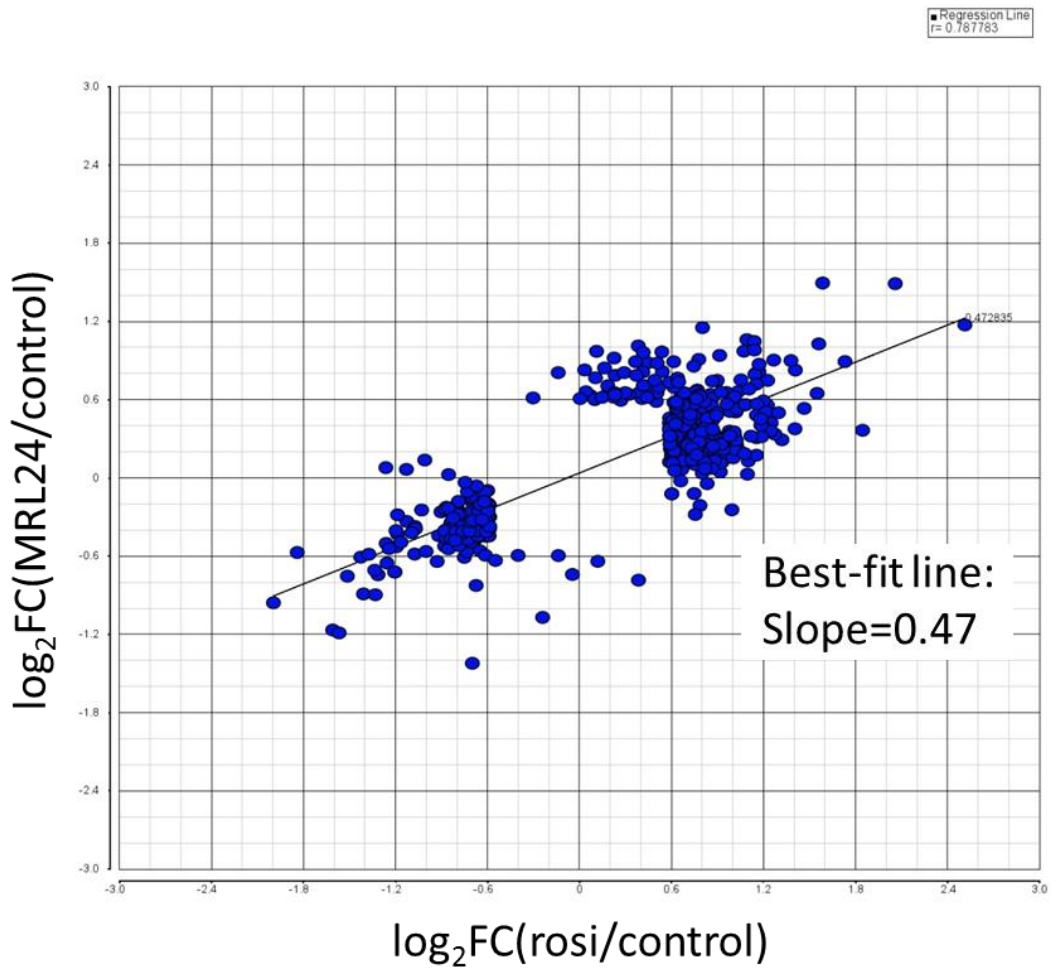


Figure 4.3 MRL-24 regulates most of the same gene targets as rosi on a genome-wide level.

Scatterplot representing mRNA regulation in adipocytes treated for 24h with rosi or MRL-24 over control as measured by microarray. The slope of the best-fit line is 0.47.

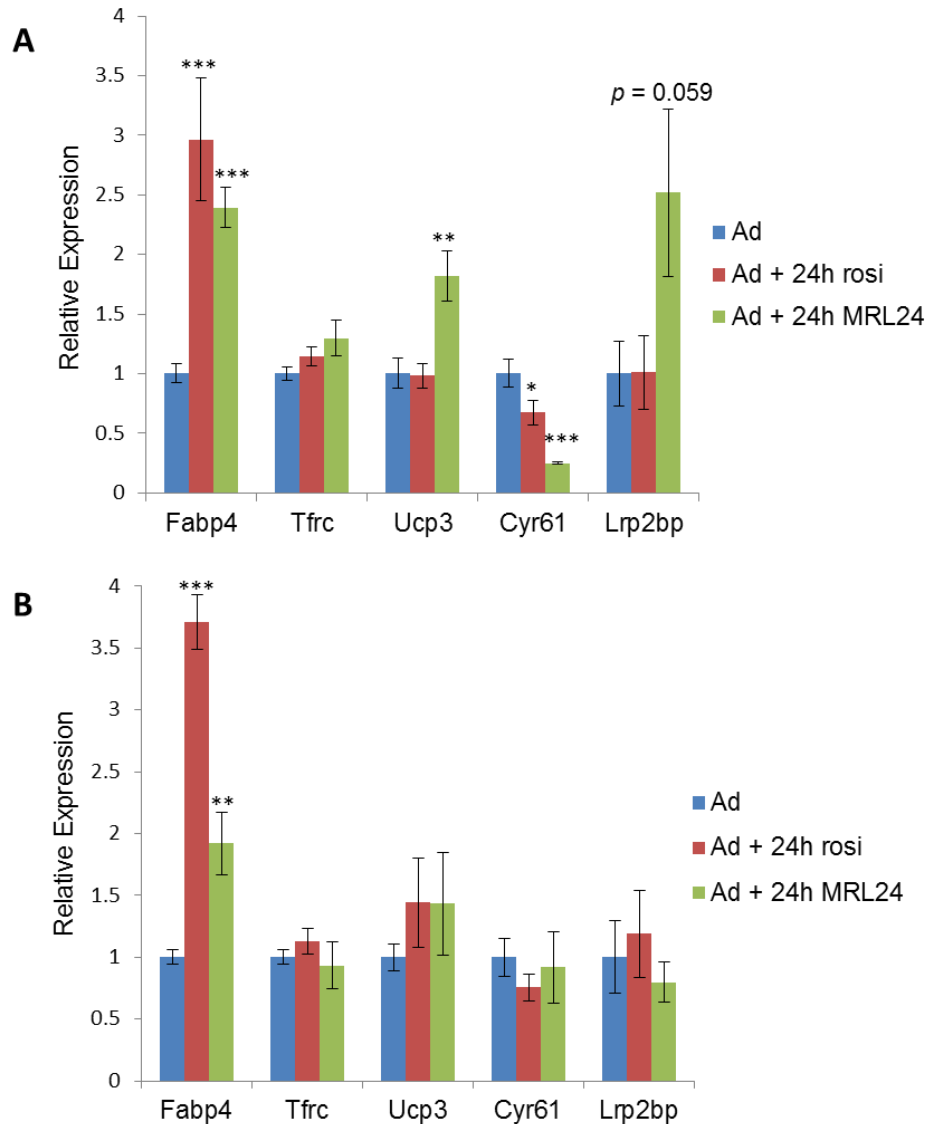


Figure 4.4 Potential MRL-24-specific genes from microarray are artifacts of the experiment.

(A) qRT-PCR for several genes determined to be MRL-24-specific from the microarray in Figure 4.3 in the same RNA samples used for the microarray. Fabp4 was used as a control. (B) qRT-PCR for the same genes in an independent experiment of adipocytes treated for 24h with rosi MRL-24. (*) $p < 0.05$; (**) $p < 0.01$; (***) $p < 0.005$.

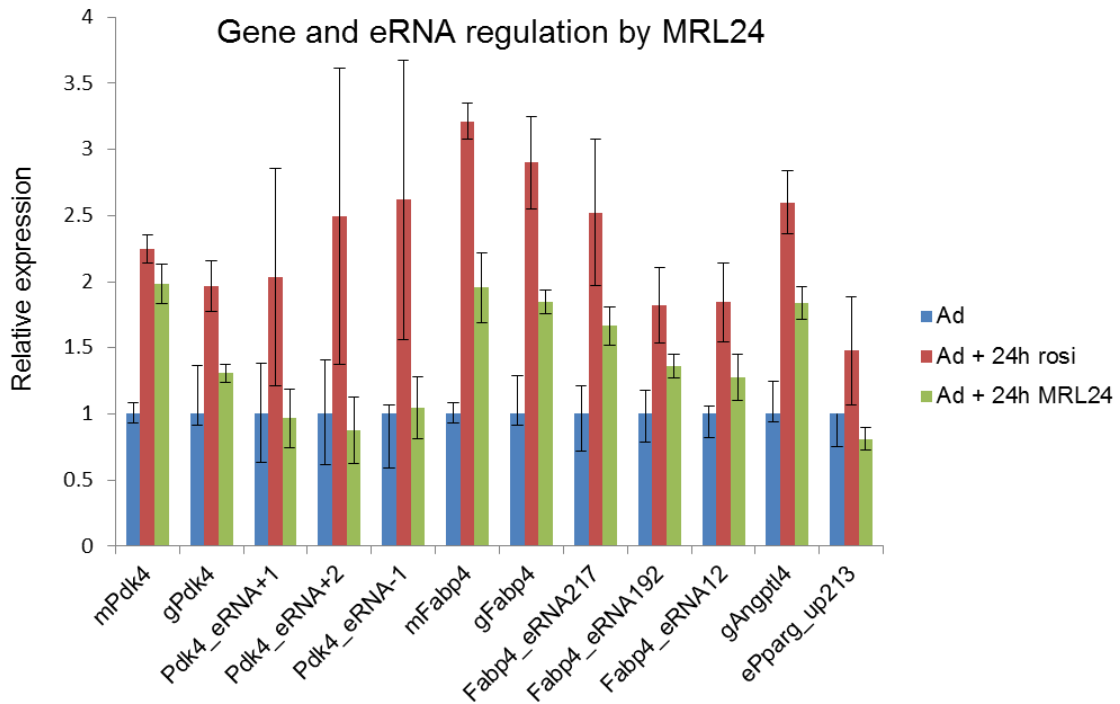


Figure 4.5 Preliminary evidence suggests that enhancers may be differentially regulated by MRL-24.

qRT-PCR for mRNAs (mPdk4, mFabp4), pre-mRNAs (gPdk4, gFabp4, gAntpl4) and nearby eRNAs in adipocytes treated for 24h with rosi or MRL-24.

Table 4.1 List of primers for eRNA and gene expression

Name	Forward Sequence	Reverse Sequence
Chemerin	GTGGACTATCCGGCCTA GAA	GTGCACAATCAAACCAAAC G
Nr3c1	CTGGACGGAGGAGAAC TCAC	GGACAACCTGACTTCCTTGG
Txnip	AGGCCTCATGATCACCA TCT	GGTCTCAGCAGTGCAAACA G
Adipsin	CTCCTGGCCACCCAGAA T	GCTGTCAGAATGCACAGCTC
Arhgap23	GTTGACCGCAGAGATGA AGG	CCTGTAGCTCAGCCAAGTCC
Itgav	TTGCCCTCCTTCTACAAT CC	ATTCGCCGTGGACTTCTTC
Usp9x	CATCTTGCAGAGACCAT TGC	TTTGTGGGTTTCGCCATATT
Ptprs	TGATATTCACATTCCCA CCG	ATCACCTGCCAACCTCTACG
Fabp4	CACTTTCCTTGTGGCAA AGC	AATGTGTGATGCCTTTGTGG
Cd36	TCAGAAGCAGGAAGGG AGTG	ATTGCACAAGGCACACAAA G
Pck1	AGGCCTCCCAACATTCA TTA	GATCATAGCCATGGTCAGCA
Pdk4	ATCATCTTTGGTGGCCG TAG	CATGGCTGCTCCTACAAACA
Cidec	ATTGTGCCATCTTCTCTC AG	ATCATGGCTCACAGCTTGG
Tfrc	CAGTCCAGCTGGCAAAG ATT	GTCCAGTGTGGGAACAGGT C
Ucp3	GTCCTTTGCTGCCTATG GA	TACCCAACCTTGGCTAGACG
Cyr61	TTTACAGTTGGGCTGGA AGC	CACCGCTCTGAAAGGGATCT
Lrp2bp	TTTCAAGTGCATTGTCT GGG	TATTATGATGGGCTGGGGAC
gPdk4	TAACTATGCCGTGCACC AAA	AAAGGCTCAAGGGGAAGAG A
Pdk4_eRNA+1	GGACAGAGGCCCAAAT GTTA	CTTGTGAAGCAGACCCAGTG
Pdk4_eRNA+2	AGAGTTCTCTGGGGGAA AGG	CCACTTGGGCAACAGAATTT

Pdk4_eRNA-1	CTATGGCTGGCACTGGA GTT	TCCCCTCCTTTTGACTCTCA
gFabp4	ATCGGGAATTTTCAGCAT GAC	AATGTGTGATGCCTTTGTGG
Fabp4_eRNA217	AACATCCGAATCAACCG TTC	GGTGGGACAAACAAAATTC C
Fabp4_eRNA192	TGAGTCCCCCACTTGCT TTA	CACCCTGTAAGGCTGGTGAT
gAngptl4	ACCCAAGGCCAGAATCT CTT	TTGCTGTCATCTGGCAACTC
ePparg_up213	AGAGCTCTTACCCAGCA GAGA	GCACACCAGGCAAGTGCTA T
Arbp	CCGATCTGCAGACACAC ACT	ACCCTGAAGTGCTCGACATC

CHAPTER 5: Discussion and future directions

5.1 Summary and discussion

In the studies summarized above, we have further elucidated the effects of PPAR γ ligands on adipocyte transcription. In Chapter 2, we examined the immediate and direct effects of rosi on gene transcription using GRO-seq. We found thousands of rapidly regulated genes, 2/3 of which were down-regulated by rosi. These regulated nascent transcripts are highly correlated with changes in steady-state mRNA levels as identified by microarray, but with a temporal delay. Interestingly, the correlation between nascent transcript and steady-state mRNA level waned at later microarray time points, after 12 or 24h, suggesting that steady-state levels likely have other contributing factors besides direct transcriptional changes, as discussed in Section 5.2a below.

In Chapter 3, we used GRO-seq to identify regulated eRNAs. We could not demonstrate any role for these eRNAs in promoting transcription of the target gene, despite several recent studies that suggest this function (Lam et al. 2013; Li et al. 2013; Melo et al. 2013; Mousavi et al. 2013). We did, however, use these regulated eRNAs to determine functional enhancers. By focusing exclusively on the functional enhancers, we were able to identify changes in coactivator occupancy that would not have been identifiable by determining all TF binding sites genome-wide. We found that enhancers containing an up-regulated eRNA are driven by PPAR γ , while enhancers with down-regulated eRNAs are depleted of PPAR γ but are enriched for other TFs, including members of the C/EBP and AP-1 families. Additionally, in response to rosi treatment the coactivators MED1,

CBP, and p300 are recruited to sites of up-regulated eRNAs and lost from sites with down-regulated eRNAs. These findings suggest a mechanism wherein rosi treatment causes increased recruitment of coactivators to PPAR γ sites and away from sites containing other TFs, leading to transcriptional repression at these sites and at their target genes. This suggests that, in principle, any TF driving transcription at an enhancer lacking PPAR γ would be susceptible to the loss of coactivators and subsequent transcriptional repression. Indeed, this may explain why the down-regulated enhancers are enriched for binding of multiple factors, including C/EBP α , C/EBP β , FOSL2, ATF2, and JUND.

These studies shed light onto the mechanisms by which rosi affects adipocyte transcription, especially the ways in which it leads to transcriptional repression, a phenomenon of which we previously had very little understanding. In addition, we believe that the approach we took in these studies – using regulated eRNAs to identify functional enhancers, and focusing on these sites to identify enriched motifs, critical TFs, and changes in coactivators – could be applied to many other questions of transcriptional regulation. In other systems in which a signal or cue causes transcriptional changes through unknown mechanisms, this method can be taken to discover key enhancers and TFs that are driving the changes. For example, the Lazar lab recently used a similar approach to identify enhancers and TFs that are important for circadian regulation of transcription in the liver (Fang et al. 2014).

In Chapter 4, we sought to determine whether differential gene regulation by MRL-24 was driven by differential use of enhancers, and whether the mechanism of its transcriptional regulation was distinct from that of rosi. However, we found that in our adipocyte model MRL-24 did not regulate a unique subset of gene targets, but rather functioned similarly to a partial PPAR γ agonist. This difference in results is likely attributable to differences in cell culture models, and studying it further *in vivo* may clarify its effects.

5.2 Future directions

5.2a Identifying secondary targets of rosi

In Chapter 2, we determined that although nascent gene transcription is highly correlated with steady-state mRNA levels after 6 to 12 hours of rosi treatment, this correlation is weaker when nascent transcription from GRO-seq is compared to later microarray time points. This suggests that steady-state mRNA levels that are reached after 24h of rosi treatment are determined not only by direct transcriptional changes due immediately to rosi treatment, but by other factors as well, which may include secondary transcriptional changes and non-transcriptional regulation such as changes in mRNA degradation rates. Though we gained many mechanistic insights by examining early direct changes due to rosi treatment, studying later, secondary effects is equally important because these are the changes that ultimately contribute to the function and phenotype of rosi treatment. Thus,

determining which genes are controlled by rosi at later, steady-state time points and the mechanisms of this regulation are important future directions.

An important follow-up experiment would be to perform GRO-seq on adipocytes treated with rosi for a longer period of time, such as 24 or 36 hours. First of all, this would identify genes that are transcribed as a downstream response to rosi treatment, and these would be expected to correlate more strongly with later time points from the microarray experiment. It would also distinguish genes that are secondary transcriptional targets from those that are regulated in a non-transcriptional manner, such as through degradation rates. Lastly, analysis of eRNAs at later time points of rosi treatment would identify functional enhancers that are regulating these downstream gene targets. Similar to the approach we took in Chapter 3, motif analysis of the enhancers that are regulated at later time points may help identify TFs that are induced by rosi treatment and control downstream gene transcription. If such a TF is identified that putatively controls long-term steady-state response to rosi, its role could be verified by ablating its expression and testing whether this blocks secondary responses to rosi treatment. It would also be interesting to explore how these downstream regulated enhancers control both transcriptional activation as well as repression, and whether repression of secondary gene targets is through an effect similar to coactivator redistribution as shown in Chapter 3, or through a different mechanism.

5.2b Connecting coactivator redistribution to transcriptional regulation

In Chapter 3 we demonstrated that rosi treatment causes a redistribution of coactivators (including MED1, CBP, and p300) to enhancers containing PPAR γ and away from enhancers containing other TFs. We observed no change in the occupancy of the corepressor NCoR or in levels of the histone mark H3K27ac at those sites where coactivator levels changed. A clear next question is how exactly changes in coactivator occupancy are leading to changes in transcription.

Coactivators are known to promote transcription mainly through a few different functions: modifying chromatin, recruiting components of the transcriptional machinery, and promoting long-range looping between the enhancer and promoter (Carlsten et al. 2013; Grunberg and Hahn 2013). When coactivators are redistributed in response to rosi, one of these mechanisms – or a novel one – must be at play to regulate subsequent changes in transcription. The coactivators CBP and p300, which we showed were redistributed, are known to function as histone acetyltransferases (Schiltz et al. 1999), suggesting a role for histone acetylation in connecting coactivator occupancy to transcription. However, our finding that H3K27ac levels do not change at a few enhancers where eRNAs are regulated suggests that chromatin modification may not be the primary mechanism of transcriptional regulation, although this is far from conclusive. We only tested levels of this chromatin mark at a few sites, so making genome-wide conclusions could be premature. We also only tested one time point – after 1h of rosi treatment – but this mark may be changing later, or it may in fact be changing even

earlier (since we see eRNA changes as soon as after 10 minutes of rosi), then normalizing back to basal levels. Testing other chromatin marks, as well as at more enhancer sites and at different time points may elucidate a role for chromatin modifications in the link between coactivator occupancy and transcriptional changes.

The other mechanisms, including differential recruitment of transcriptional machinery should be tested as well. For example, the Mediator complex has been shown to interact directly with Pol II, and is required for transcription (Soutourina et al. 2011). CBP and p300 interact with the basal transcription factors TATA-binding protein (TBP) and TFIIB (Yuan et al. 1996). This suggests the mechanism that upon redistribution of these coactivators, they in turn differentially bind and recruit elements of the basal transcriptional machinery, leading to changes in transcription. Binding of Pol II, TBP, TFIIB, and other factors could be tested by ChIP. However, most of the regulated functional enhancers we identified were distal from genes, tens or even hundreds of kilobases away from the TSS. Therefore, changes in recruitment of the transcriptional machinery to these sites would explain regulation of eRNA transcription, but would not explain changes in gene transcription without additional information about long-range chromatin interactions between enhancers and gene promoters.

Thus, studying chromatin loops between enhancers and promoters, and how they may change upon rosi treatment, would be an important component of further understanding

this transcriptional regulation. The first goal would be to determine which enhancers loop to which gene promoters, to identify each enhancer's target gene. This would be a much more conclusive way of determining enhancer-gene pairs, compared to relying on using the nearest regulated gene for each enhancer, as we had to do in Chapter 3 due to the lack of chromatin looping data. The existence and regulation of chromatin loops could be explored at a few select enhancers and promoters by chromatin conformation capture (3C) or circular chromosome conformation capture (4C), although ideally all chromatin loops in the genome would be identified by Hi-C (Dekker et al. 2013). Another important question would be whether rosi modifies gene transcription levels by regulating the strength of the chromatin loops, or whether the loops stay the same but recruitment of additional transcription factors is what drives the transcriptional changes. Since the Mediator complex has been implicated in the formation of chromatin loops (Carlsten et al. 2013), and we demonstrated a rosi-dependent redistribution of the Mediator subunit MED1 at regulated enhancers, we would hypothesize that rosi treatment may indeed strengthen enhancer-promoter loops at up-regulated sites, and weaken them at down-regulated sites. These studies would mechanistically link changes in coactivator binding to changes in eRNA and gene transcription.

5.2c Determinants of functional enhancers

In Chapter 3, we identified 2,251 distal enhancers with regulated eRNAs; these are the enhancers we termed “functional.” However, they make up a relatively small fraction of all putative enhancers as defined by TF binding sites. For example, we had 14,604

PPAR γ binding sites in our data set, in which sites were called after pooling reads from two published cistromes (Nielsen et al. 2008; Schmidt et al. 2011), and similar numbers for other TFs bound in adipocytes, including the members of the C/EBP and AP-1 families described in Chapter 3. Only a small number of these sites produce eRNAs. This can be explained in part by the fact that we only called eRNAs at intergenic sites for technical reasons, while TFs bind at many intronic sites. Nevertheless, even when considering just intergenic TF binding sites, those with eRNAs make up only about half of the total in the case of PPAR γ (Step et al. 2014).

Thus, an important follow-up question is: what distinguishes the relatively small number of “functional” enhancers from the rest of the thousands of TF binding sites? What feature determines whether a putative enhancer produces an eRNA? We know that part of the answer involves strength of binding of the TF: PPAR γ sites with eRNAs tend to be strong sites than those without eRNAs (Step et al. 2014). However, this is unlikely to be the whole explanation, since the trend is strong but not overwhelming. Perhaps there is a factor that is able to bind to certain TF binding sites but not others, and is able to act together with the TF to recruit coactivators and other factors to drive eRNA transcription. To investigate this, all putative enhancers could be divided into two groups: those that produce an eRNA and those that do not. Then, the presence of an eRNA can be correlated with binding of other known TFs in adipocytes, to determine whether colocalization of another factor with PPAR γ is necessary for the production of an eRNA at an enhancer.

Motif searches could also be performed around enhancers that do or do not contain eRNAs to determine if response elements for a given TF are enriched around one group or the other. Identifying what distinguishes functional enhancers from other TF binding sites would be important not only in understanding rosi-mediated regulation of adipocytes, but also transcription in any other cell type in response to a stimulus.

5.2d Other compounds that differentially regulate PPAR γ

As discussed in Chapter 1, TZDs are able to potently improve insulin sensitivity and lower glucose levels, but have been linked to multiple safety issues. Because of these effects, there has been much interest in the development of selective PPAR γ modulators, or SPPARMs, small molecules that would agonize the TF in a way that would lead to differential gene expression. The goal of these SPPARMs would be to retain the insulin-sensitizing effects of TZDs but without the unwanted side effects of full receptor activation (Higgins and Depaoli 2010).

In Chapter 4, we studied MRL-24, which had been described as a ligand of PPAR γ that regulates a distinct subset of target genes yet still functions as an effective insulin sensitizer *in vivo*. Instead, we found that in our cell culture model of adipocytes, MRL-24 did not have any unique gene targets, but rather functioned by regulating most of the same genes as rosi but to a lesser degree. Nevertheless, other SPPARMs are still being investigated, including a compound called INT131. A clinical study recently showed that

INT131 demonstrated reductions in HbA1c (glycated hemoglobin, a time-averaged measure of blood glucose levels) comparable to pioglitazone, with less fluid accumulation and weight gain (DePaoli et al. 2014). This exciting result suggests that PPAR γ may still be a relevant target for new drug development for diabetes treatment. Biochemical and cell-based studies suggest that INT131 may be acting as a SPPARM: treatment of 3T3-L1 preadipocytes with this drug caused very little adipogenesis or lipid accumulation, whereas rosi treatment caused full differentiation. It also induced most adipogenic genes to a much smaller extent than did rosi. Finally, an in vitro assay that measures the strength of interaction between the PPAR γ LBD and coactivators demonstrated that while rosi causes a large increase in recruitment of coactivators such as SRC2, CBP, and p300, INT131 had a much smaller effect (Motani et al. 2009).

However, it should be noted that all of these effects are equally consistent with INT131 acting as a partial agonist. Genome-wide transcriptional studies of its effects would be better able to discern between a partial agonist and a SPPARM. GRO-seq should be performed on adipocytes treated briefly with INT131, and its direct transcriptional effects compared to that of rosi. If it is truly a SPPARM, a distinct group of immediate gene targets should be differentially regulated by the two compounds, whereas if it is a partial agonist, most of the same genes would be regulated but to different degrees. Additionally, it would be interesting to analyze eRNAs in this GRO-seq experiment to determine whether INT131 is regulating the same group of functional enhancers as rosi, or a distinct subset. This would also contribute to the understanding of INT131 as either a SPPARM

or a partial agonist. Finally, measuring changes in coactivator occupancy upon INT131 treatment would demonstrate whether it acts similarly to rosi, by redistributing coactivator binding genome-wide to regulate transcription both positively and negatively. It would also be crucial to investigate whether any differences between the mechanisms of action of the two compounds are related to the differences in their toxicity profiles.

BIBLIOGRAPHY

- Acton JJ, 3rd, Black RM, Jones AB, Moller DE, Colwell L, Doebber TW, Macnaul KL, Berger J, Wood HB. 2005. Benzoyl 2-methyl indoles as selective PPAR γ modulators. *Bioorganic & medicinal chemistry letters* **15**: 357-362.
- Ahmadian M, Suh JM, Hah N, Liddle C, Atkins AR, Downes M, Evans RM. 2013. PPAR γ signaling and metabolism: the good, the bad and the future. *Nat Med* **19**: 557-566.
- Amato AA, Rajagopalan S, Lin JZ, Carvalho BM, Figueira AC, Lu J, Ayers SD, Mottin M, Silveira RL, Souza PC et al. 2012. GQ-16, a novel peroxisome proliferator-activated receptor gamma (PPAR γ) ligand, promotes insulin sensitization without weight gain. *The Journal of biological chemistry* **287**: 28169-28179.
- Atianand MK, Fitzgerald KA. 2014. Long non-coding RNAs and control of gene expression in the immune system. *Trends in molecular medicine*.
- Bain DL, Heneghan AF, Connaghan-Jones KD, Miura MT. 2007. Nuclear receptor structure: implications for function. *Annual review of physiology* **69**: 201-220.
- Banerji J, Rusconi S, Schaffner W. 1981. Expression of a beta-globin gene is enhanced by remote SV40 DNA sequences. *Cell* **27**: 299-308.
- Bar-Joseph Z, Gifford DK, Jaakkola TS. 2001. Fast optimal leaf ordering for hierarchical clustering. *Bioinformatics* **17 Suppl 1**: S22-29.
- Buecker C, Wysocka J. 2012. Enhancers as information integration hubs in development: lessons from genomics. *Trends in genetics : TIG* **28**: 276-284.
- Bugge A, Grontved L, Aagaard MM, Borup R, Mandrup S. 2009. The PPAR γ 2 A/B-domain plays a gene-specific role in transactivation and cofactor recruitment. *Molecular endocrinology* **23**: 794-808.
- Cabili MN, Trapnell C, Goff L, Koziol M, Tazon-Vega B, Regev A, Rinn JL. 2011. Integrative annotation of human large intergenic noncoding RNAs reveals global properties and specific subclasses. *Genes & development* **25**: 1915-1927.
- Carlsten JO, Zhu X, Gustafsson CM. 2013. The multitasking Mediator complex. *Trends in biochemical sciences* **38**: 531-537.
- Carrieri C, Cimatti L, Biagioli M, Beugnet A, Zucchelli S, Fedele S, Pesce E, Ferrer I, Collavin L, Santoro C et al. 2012. Long non-coding antisense RNA controls Uchl1 translation through an embedded SINEB2 repeat. *Nature* **491**: 454-457.
- Cesana M, Cacchiarelli D, Legnini I, Santini T, Sthandier O, Chinappi M, Tramontano A, Bozzoni I. 2011. A long noncoding RNA controls muscle differentiation by functioning as a competing endogenous RNA. *Cell* **147**: 358-369.
- Chao L, Marcus-Samuels B, Mason MM, Moitra J, Vinson C, Arioglu E, Gavrilova O, Reitman ML. 2000. Adipose tissue is required for the antidiabetic, but not for the hypolipidemic, effect of thiazolidinediones. *The Journal of clinical investigation* **106**: 1221-1228.
- Chawla A, Lazar MA. 1994. Peroxisome proliferator and retinoid signaling pathways co-regulate preadipocyte phenotype and survival. *Proceedings of the National Academy of Sciences of the United States of America* **91**: 1786-1790.

- Chawla A, Schwarz EJ, Dimaculangan DD, Lazar MA. 1994. Peroxisome proliferator-activated receptor (PPAR) gamma: adipose-predominant expression and induction early in adipocyte differentiation. *Endocrinology* **135**: 798-800.
- Chen X, Xu H, Yuan P, Fang F, Huss M, Vega VB, Wong E, Orlov YL, Zhang W, Jiang J et al. 2008. Integration of external signaling pathways with the core transcriptional network in embryonic stem cells. *Cell* **133**: 1106-1117.
- Choi JH, Banks AS, Estall JL, Kajimura S, Bostrom P, Laznik D, Ruas JL, Chalmers MJ, Kamenecka TM, Bluher M et al. 2010. Anti-diabetic drugs inhibit obesity-linked phosphorylation of PPARgamma by Cdk5. *Nature* **466**: 451-456.
- Choi JH, Banks AS, Kamenecka TM, Busby SA, Chalmers MJ, Kumar N, Kuruvilla DS, Shin Y, He Y, Bruning JB et al. 2011. Antidiabetic actions of a non-agonist PPARgamma ligand blocking Cdk5-mediated phosphorylation. *Nature* **477**: 477-481.
- Colhoun HM, Livingstone SJ, Looker HC, Morris AD, Wild SH, Lindsay RS, Reed C, Donnan PT, Guthrie B, Leese GP et al. 2012. Hospitalised hip fracture risk with rosiglitazone and pioglitazone use compared with other glucose-lowering drugs. *Diabetologia* **55**: 2929-2937.
- Collis P, Antoniou M, Grosveld F. 1990. Definition of the minimal requirements within the human beta-globin gene and the dominant control region for high level expression. *The EMBO journal* **9**: 233-240.
- Core LJ, Waterfall JJ, Lis JT. 2008. Nascent RNA sequencing reveals widespread pausing and divergent initiation at human promoters. *Science* **322**: 1845-1848.
- Danaei G, Finucane MM, Lin JK, Singh GM, Paciorek CJ, Cowan MJ, Farzadfar F, Stevens GA, Lim SS, Riley LM et al. 2011. National, regional, and global trends in systolic blood pressure since 1980: systematic analysis of health examination surveys and epidemiological studies with 786 country-years and 5.4 million participants. *Lancet* **377**: 568-577.
- De Santa F, Barozzi I, Mietton F, Ghisletti S, Polletti S, Tusi BK, Muller H, Ragoussis J, Wei CL, Natoli G. 2010. A large fraction of extragenic RNA pol II transcription sites overlap enhancers. *PLoS biology* **8**: e1000384.
- DeFronzo RA, Tripathy D, Schwenke DC, Banerji M, Bray GA, Buchanan TA, Clement SC, Henry RR, Hodis HN, Kitabchi AE et al. 2011. Pioglitazone for diabetes prevention in impaired glucose tolerance. *The New England journal of medicine* **364**: 1104-1115.
- Dekker J, Marti-Renom MA, Mirny LA. 2013. Exploring the three-dimensional organization of genomes: interpreting chromatin interaction data. *Nature reviews Genetics* **14**: 390-403.
- Dekker J, Rippe K, Dekker M, Kleckner N. 2002. Capturing chromosome conformation. *Science* **295**: 1306-1311.
- DePaoli AM, Higgins LS, Henry RR, Mantzoros C, Dunn FL, Group INTS. 2014. Can a selective PPARgamma modulator improve glycemic control in patients with type 2 diabetes with fewer side effects compared with pioglitazone? *Diabetes care* **37**: 1918-1923.

- Eulalio A, Huntzinger E, Izaurralde E. 2008. Getting to the root of miRNA-mediated gene silencing. *Cell* **132**: 9-14.
- Fang B, Everett LJ, Jager J, Briggs E, Armour SM, Feng D, Roy A, Gerhart-Hines Z, Sun Z, Lazar MA. 2014. Circadian Enhancers Coordinate Multiple Phases of Rhythmic Gene Transcription In Vivo. *Cell*.
- Filipowicz W, Bhattacharyya SN, Sonenberg N. 2008. Mechanisms of post-transcriptional regulation by microRNAs: are the answers in sight? *Nature reviews Genetics* **9**: 102-114.
- Fronsdal K, Engedal N, Slagsvold T, Saatcioglu F. 1998. CREB binding protein is a coactivator for the androgen receptor and mediates cross-talk with AP-1. *The Journal of biological chemistry* **273**: 31853-31859.
- Ge K, Guermah M, Yuan CX, Ito M, Wallberg AE, Spiegelman BM, Roeder RG. 2002. Transcription coactivator TRAP220 is required for PPAR gamma 2-stimulated adipogenesis. *Nature* **417**: 563-567.
- Gelman L, Zhou G, Fajas L, Raspe E, Fruchart JC, Auwerx J. 1999. p300 interacts with the N- and C-terminal part of PPARgamma2 in a ligand-independent and -dependent manner, respectively. *The Journal of biological chemistry* **274**: 7681-7688.
- Ghisletti S, Huang W, Ogawa S, Pascual G, Lin ME, Willson TM, Rosenfeld MG, Glass CK. 2007. Parallel SUMOylation-dependent pathways mediate gene- and signal-specific transrepression by LXRs and PPARgamma. *Molecular cell* **25**: 57-70.
- Gill G, Ptashne M. 1988. Negative effect of the transcriptional activator GAL4. *Nature* **334**: 721-724.
- Glass CK, Rosenfeld MG. 2000. The coregulator exchange in transcriptional functions of nuclear receptors. *Genes & development* **14**: 121-141.
- Glass CK, Saijo K. 2010. Nuclear receptor transrepression pathways that regulate inflammation in macrophages and T cells. *Nature reviews Immunology* **10**: 365-376.
- Gomez JA, Wapinski OL, Yang YW, Bureau JF, Gopinath S, Monack DM, Chang HY, Brahic M, Kirkegaard K. 2013. The NeST long ncRNA controls microbial susceptibility and epigenetic activation of the interferon-gamma locus. *Cell* **152**: 743-754.
- Grunberg S, Hahn S. 2013. Structural insights into transcription initiation by RNA polymerase II. *Trends in biochemical sciences* **38**: 603-611.
- Guan HP, Ishizuka T, Chui PC, Lehrke M, Lazar MA. 2005. Corepressors selectively control the transcriptional activity of PPARgamma in adipocytes. *Genes & development* **19**: 453-461.
- Gupta RA, Shah N, Wang KC, Kim J, Horlings HM, Wong DJ, Tsai MC, Hung T, Argani P, Rinn JL et al. 2010. Long non-coding RNA HOTAIR reprograms chromatin state to promote cancer metastasis. *Nature* **464**: 1071-1076.
- Haakonsson AK, Stahl Madsen M, Nielsen R, Sandelin A, Mandrup S. 2013. Acute genome-wide effects of rosiglitazone on PPARgamma transcriptional networks in adipocytes. *Molecular endocrinology* **27**: 1536-1549.

- Hah N, Danko CG, Core L, Waterfall JJ, Siepel A, Lis JT, Kraus WL. 2011. A rapid, extensive, and transient transcriptional response to estrogen signaling in breast cancer cells. *Cell* **145**: 622-634.
- Hah N, Murakami S, Nagari A, Danko CG, Kraus WL. 2013. Enhancer transcripts mark active estrogen receptor binding sites. *Genome research* **23**: 1210-1223.
- He HH, Meyer CA, Chen MW, Jordan VC, Brown M, Liu XS. 2012. Differential DNase I hypersensitivity reveals factor-dependent chromatin dynamics. *Genome research* **22**: 1015-1025.
- He W, Barak Y, Hevener A, Olson P, Liao D, Le J, Nelson M, Ong E, Olefsky JM, Evans RM. 2003. Adipose-specific peroxisome proliferator-activated receptor gamma knockout causes insulin resistance in fat and liver but not in muscle. *Proceedings of the National Academy of Sciences of the United States of America* **100**: 15712-15717.
- Heintzman ND, Hon GC, Hawkins RD, Kheradpour P, Stark A, Harp LF, Ye Z, Lee LK, Stuart RK, Ching CW et al. 2009. Histone modifications at human enhancers reflect global cell-type-specific gene expression. *Nature* **459**: 108-112.
- Heinz S, Benner C, Spann N, Bertolino E, Lin YC, Laslo P, Cheng JX, Murre C, Singh H, Glass CK. 2010. Simple combinations of lineage-determining transcription factors prime cis-regulatory elements required for macrophage and B cell identities. *Molecular cell* **38**: 576-589.
- Helsen C, Kerkhofs S, Clinckemalie L, Spans L, Laurent M, Boonen S, Vanderschueren D, Claessens F. 2012. Structural basis for nuclear hormone receptor DNA binding. *Molecular and cellular endocrinology* **348**: 411-417.
- Higgins LS, Depaoli AM. 2010. Selective peroxisome proliferator-activated receptor gamma (PPARgamma) modulation as a strategy for safer therapeutic PPARgamma activation. *The American journal of clinical nutrition* **91**: 267S-272S.
- Hofmann C, Lorenz K, Braithwaite SS, Colca JR, Palazuk BJ, Hotamisligil GS, Spiegelman BM. 1994. Altered gene expression for tumor necrosis factor-alpha and its receptors during drug and dietary modulation of insulin resistance. *Endocrinology* **134**: 264-270.
- Huang C, Zhou T, Chen Y, Sun T, Zhang S, Chen G. 2011. Estrogen-related receptor ERRalpha-mediated downregulation of human hydroxysteroid sulfotransferase (SULT2A1) in Hep G2 cells. *Chemico-biological interactions* **192**: 264-271.
- Johnson JM, Edwards S, Shoemaker D, Schadt EE. 2005. Dark matter in the genome: evidence of widespread transcription detected by microarray tiling experiments. *Trends in genetics : TIG* **21**: 93-102.
- Kahn SE, Haffner SM, Heise MA, Herman WH, Holman RR, Jones NP, Kravitz BG, Lachin JM, O'Neill MC, Zinman B et al. 2006. Glycemic durability of rosiglitazone, metformin, or glyburide monotherapy. *The New England journal of medicine* **355**: 2427-2443.
- Kaikkonen MU, Spann NJ, Heinz S, Romanoski CE, Allison KA, Stender JD, Chun HB, Tough DF, Prinjha RK, Benner C et al. 2013. Remodeling of the enhancer

- landscape during macrophage activation is coupled to enhancer transcription. *Molecular cell* **51**: 310-325.
- Kamei Y, Xu L, Heinzl T, Torchia J, Kurokawa R, Gloss B, Lin SC, Heyman RA, Rose DW, Glass CK et al. 1996. A CBP integrator complex mediates transcriptional activation and AP-1 inhibition by nuclear receptors. *Cell* **85**: 403-414.
- Karmakar S, Jin Y, Nagaich AK. 2013. Interaction of glucocorticoid receptor (GR) with estrogen receptor (ER) alpha and activator protein 1 (AP1) in dexamethasone-mediated interference of ERalpha activity. *The Journal of biological chemistry* **288**: 24020-24034.
- Kent WJ, Zweig AS, Barber G, Hinrichs AS, Karolchik D. 2010. BigWig and BigBed: enabling browsing of large distributed datasets. *Bioinformatics* **26**: 2204-2207.
- Kim SW, Kim HJ, Jung DJ, Lee SK, Kim YS, Kim JH, Kim TS, Lee JW. 2001. Retinoid-dependent antagonism of serum response factor transactivation mediated by transcriptional coactivator proteins. *Oncogene* **20**: 6638-6642.
- Kim TK, Hemberg M, Gray JM, Costa AM, Bear DM, Wu J, Harmin DA, Laptewicz M, Barbara-Haley K, Kuersten S et al. 2010. Widespread transcription at neuronal activity-regulated enhancers. *Nature* **465**: 182-187.
- Kleinjan DA, van Heyningen V. 2005. Long-range control of gene expression: emerging mechanisms and disruption in disease. *American journal of human genetics* **76**: 8-32.
- Kung J, Henry RR. 2012. Thiazolidinedione safety. *Expert Opin Drug Saf* **11**: 565-579.
- Lam MT, Cho H, Lesch HP, Gosselin D, Heinz S, Tanaka-Oishi Y, Benner C, Kaikkonen MU, Kim AS, Kosaka M et al. 2013. Rev-Erbs repress macrophage gene expression by inhibiting enhancer-directed transcription. *Nature* **498**: 511-515.
- Lam MT, Li W, Rosenfeld MG, Glass CK. 2014. Enhancer RNAs and regulated transcriptional programs. *Trends in biochemical sciences* **39**: 170-182.
- Langmead B, Trapnell C, Pop M, Salzberg SL. 2009. Ultrafast and memory-efficient alignment of short DNA sequences to the human genome. *Genome biology* **10**: R25.
- Lee YK, Dell H, Dowhan DH, Hadzopoulou-Cladaras M, Moore DD. 2000. The orphan nuclear receptor SHP inhibits hepatocyte nuclear factor 4 and retinoid X receptor transactivation: two mechanisms for repression. *Molecular and cellular biology* **20**: 187-195.
- Lefterova MI, Zhang Y, Steger DJ, Schupp M, Schug J, Cristancho A, Feng D, Zhuo D, Stoeckert CJ, Jr., Liu XS et al. 2008. PPARgamma and C/EBP factors orchestrate adipocyte biology via adjacent binding on a genome-wide scale. *Genes & development* **22**: 2941-2952.
- Lehmann JM, Moore LB, Smith-Oliver TA, Wilkison WO, Willson TM, Kliewer SA. 1995. An antidiabetic thiazolidinedione is a high affinity ligand for peroxisome proliferator-activated receptor gamma (PPAR gamma). *The Journal of biological chemistry* **270**: 12953-12956.
- Li M, Pascual G, Glass CK. 2000. Peroxisome proliferator-activated receptor gamma-dependent repression of the inducible nitric oxide synthase gene. *Molecular and cellular biology* **20**: 4699-4707.

- Li W, Notani D, Ma Q, Tanasa B, Nunez E, Chen AY, Merkurjev D, Zhang J, Ohgi K, Song X et al. 2013. Functional roles of enhancer RNAs for oestrogen-dependent transcriptional activation. *Nature* **498**: 516-520.
- Li Y, Lazar MA. 2002. Differential gene regulation by PPARgamma agonist and constitutively active PPARgamma2. *Molecular endocrinology* **16**: 1040-1048.
- Lopez GN, Webb P, Shinsako JH, Baxter JD, Greene GL, Kushner PJ. 1999. Titration by estrogen receptor activation function-2 of targets that are downstream from coactivators. *Molecular endocrinology* **13**: 897-909.
- Luecke HF, Yamamoto KR. 2005. The glucocorticoid receptor blocks P-TEFb recruitment by NFkappaB to effect promoter-specific transcriptional repression. *Genes & development* **19**: 1116-1127.
- Maeda N, Takahashi M, Funahashi T, Kihara S, Nishizawa H, Kishida K, Nagaretani H, Matsuda M, Komuro R, Ouchi N et al. 2001. PPARgamma ligands increase expression and plasma concentrations of adiponectin, an adipose-derived protein. *Diabetes* **50**: 2094-2099.
- Mahaffey KW, Hafley G, Dickerson S, Burns S, Tourt-Uhlig S, White J, Newby LK, Komajda M, McMurray J, Bigelow R et al. 2013. Results of a reevaluation of cardiovascular outcomes in the RECORD trial. *American heart journal* **166**: 240-249 e241.
- Mangelsdorf DJ, Thummel C, Beato M, Herrlich P, Schutz G, Umesono K, Blumberg B, Kastner P, Mark M, Chambon P et al. 1995. The nuclear receptor superfamily: the second decade. *Cell* **83**: 835-839.
- Manna PR, Stocco DM. 2007. Crosstalk of CREB and Fos/Jun on a single cis-element: transcriptional repression of the steroidogenic acute regulatory protein gene. *Journal of molecular endocrinology* **39**: 261-277.
- Matusue K, Haluzik M, Lambert G, Yim SH, Gavrilova O, Ward JM, Brewer B, Jr., Reitman ML, Gonzalez FJ. 2003. Liver-specific disruption of PPARgamma in leptin-deficient mice improves fatty liver but aggravates diabetic phenotypes. *The Journal of clinical investigation* **111**: 737-747.
- Melo CA, Drost J, Wijchers PJ, van de Werken H, de Wit E, Oude Vrielink JA, Elkon R, Melo SA, Leveille N, Kalluri R et al. 2013. eRNAs are required for p53-dependent enhancer activity and gene transcription. *Molecular cell* **49**: 524-535.
- Mercer TR, Dinger ME, Mattick JS. 2009. Long non-coding RNAs: insights into functions. *Nature reviews Genetics* **10**: 155-159.
- Millard CJ, Watson PJ, Fairall L, Schwabe JW. 2013. An evolving understanding of nuclear receptor coregulator proteins. *Journal of molecular endocrinology* **51**: T23-36.
- Motani A, Wang Z, Weiszmann J, McGee LR, Lee G, Liu Q, Staunton J, Fang Z, Fuentes H, Lindstrom M et al. 2009. INT131: a selective modulator of PPAR gamma. *Journal of molecular biology* **386**: 1301-1311.
- Mousavi K, Zare H, Dell'orso S, Grontved L, Gutierrez-Cruz G, Derfoul A, Hager GL, Sartorelli V. 2013. eRNAs promote transcription by establishing chromatin accessibility at defined genomic loci. *Molecular cell* **51**: 606-617.

- Moyers JS, Shiyanova TL, Mehrbod F, Dunbar JD, Noblitt TW, Otto KA, Reifel-Miller A, Kharitonov A. 2007. Molecular determinants of FGF-21 activity-synergy and cross-talk with PPARgamma signaling. *Journal of cellular physiology* **210**: 1-6.
- Müllner D. 2011. fastcluster: Fast hierarchical clustering routines for R and Python. Version.
- Natoli G, Andrau JC. 2012. Noncoding transcription at enhancers: general principles and functional models. *Annual review of genetics* **46**: 1-19.
- Neumann A, Weill A, Ricordeau P, Fagot JP, Alla F, Allemand H. 2012. Pioglitazone and risk of bladder cancer among diabetic patients in France: a population-based cohort study. *Diabetologia* **55**: 1953-1962.
- Nielsen R, Pedersen TA, Hagenbeek D, Moulos P, Siersbaek R, Megens E, Denissov S, Borgesen M, Francoijs KJ, Mandrup S et al. 2008. Genome-wide profiling of PPARgamma:RXR and RNA polymerase II occupancy reveals temporal activation of distinct metabolic pathways and changes in RXR dimer composition during adipogenesis. *Genes & development* **22**: 2953-2967.
- Nissen SE, Wolski K. 2007. Effect of rosiglitazone on the risk of myocardial infarction and death from cardiovascular causes. *The New England journal of medicine* **356**: 2457-2471.
- Nolan JJ, Ludvik B, Beerdsen P, Joyce M, Olefsky J. 1994. Improvement in glucose tolerance and insulin resistance in obese subjects treated with troglitazone. *The New England journal of medicine* **331**: 1188-1193.
- Norris AW, Chen L, Fisher SJ, Szanto I, Ristow M, Jozsi AC, Hirshman MF, Rosen ED, Goodyear LJ, Gonzalez FJ et al. 2003. Muscle-specific PPARgamma-deficient mice develop increased adiposity and insulin resistance but respond to thiazolidinediones. *The Journal of clinical investigation* **112**: 608-618.
- Odom DT, Zizlsperger N, Gordon DB, Bell GW, Rinaldi NJ, Murray HL, Volkert TL, Schreiber J, Rolfe PA, Gifford DK et al. 2004. Control of pancreas and liver gene expression by HNF transcription factors. *Science* **303**: 1378-1381.
- Ogawa S, Lozach J, Benner C, Pascual G, Tangirala RK, Westin S, Hoffmann A, Subramaniam S, David M, Rosenfeld MG et al. 2005. Molecular determinants of crosstalk between nuclear receptors and toll-like receptors. *Cell* **122**: 707-721.
- Ohoka N, Kato S, Takahashi Y, Hayashi H, Sato R. 2009. The orphan nuclear receptor RORalpha restrains adipocyte differentiation through a reduction of C/EBPbeta activity and perilipin gene expression. *Molecular endocrinology* **23**: 759-771.
- Pascual-Garcia M, Rue L, Leon T, Julve J, Carbo JM, Matalonga J, Auer H, Celada A, Escola-Gil JC, Steffensen KR et al. 2013. Reciprocal negative cross-talk between liver X receptors (LXRs) and STAT1: effects on IFN-gamma-induced inflammatory responses and LXR-dependent gene expression. *Journal of immunology* **190**: 6520-6532.
- Pascual G, Fong AL, Ogawa S, Gamliel A, Li AC, Perissi V, Rose DW, Willson TM, Rosenfeld MG, Glass CK. 2005. A SUMOylation-dependent pathway mediates transrepression of inflammatory response genes by PPAR-gamma. *Nature* **437**: 759-763.

- Quinlan AR, Hall IM. 2010. BEDTools: a flexible suite of utilities for comparing genomic features. *Bioinformatics* **26**: 841-842.
- Rangwala SM, Lazar MA. 2004. Peroxisome proliferator-activated receptor gamma in diabetes and metabolism. *Trends in pharmacological sciences* **25**: 331-336.
- Rapicavoli NA, Qu K, Zhang J, Mikhail M, Laberge RM, Chang HY. 2013. A mammalian pseudogene lncRNA at the interface of inflammation and anti-inflammatory therapeutics. *eLife* **2**: e00762.
- Rival Y, Stennevin A, Puech L, Rouquette A, Cathala C, Lestienne F, Dupont-Passelaigue E, Patoiseau JF, Wurch T, Junquero D. 2004. Human adipocyte fatty acid-binding protein (aP2) gene promoter-driven reporter assay discriminates nonlipogenic peroxisome proliferator-activated receptor gamma ligands. *The Journal of pharmacology and experimental therapeutics* **311**: 467-475.
- Robinson MD, McCarthy DJ, Smyth GK. 2010. edgeR: a Bioconductor package for differential expression analysis of digital gene expression data. *Bioinformatics* **26**: 139-140.
- Rogatsky I, Luecke HF, Leitman DC, Yamamoto KR. 2002. Alternate surfaces of transcriptional coregulator GRIP1 function in different glucocorticoid receptor activation and repression contexts. *Proceedings of the National Academy of Sciences of the United States of America* **99**: 16701-16706.
- Rong JX, Klein JL, Qiu Y, Xie M, Johnson JH, Waters KM, Zhang V, Kashatus JA, Remlinger KS, Bing N et al. 2011. Rosiglitazone Induces Mitochondrial Biogenesis in Differentiated Murine 3T3-L1 and C3H/10T1/2 Adipocytes. *PPAR research* **2011**: 179454.
- Rosen ED, Sarraf P, Troy AE, Bradwin G, Moore K, Milstone DS, Spiegelman BM, Mortensen RM. 1999. PPAR gamma is required for the differentiation of adipose tissue in vivo and in vitro. *Molecular cell* **4**: 611-617.
- Saijo K, Winner B, Carson CT, Collier JG, Boyer L, Rosenfeld MG, Gage FH, Glass CK. 2009. A Nurr1/CoREST pathway in microglia and astrocytes protects dopaminergic neurons from inflammation-induced death. *Cell* **137**: 47-59.
- Schiltz RL, Mizzen CA, Vassilev A, Cook RG, Allis CD, Nakatani Y. 1999. Overlapping but distinct patterns of histone acetylation by the human coactivators p300 and PCAF within nucleosomal substrates. *The Journal of biological chemistry* **274**: 1189-1192.
- Schimke RT, Doyle D. 1970. Control of enzyme levels in animal tissues. *Annual review of biochemistry* **39**: 929-976.
- Schmidt SF, Jorgensen M, Chen Y, Nielsen R, Sandelin A, Mandrup S. 2011. Cross species comparison of C/EBPalpha and PPARgamma profiles in mouse and human adipocytes reveals interdependent retention of binding sites. *BMC Genomics* **12**: 152.
- Sears DD, Hsiao A, Ofrecio JM, Chapman J, He W, Olefsky JM. 2007. Selective modulation of promoter recruitment and transcriptional activity of PPARgamma. *Biochemical and biophysical research communications* **364**: 515-521.

- Shiau AK, Barstad D, Loria PM, Cheng L, Kushner PJ, Agard DA, Greene GL. 1998. The structural basis of estrogen receptor/coactivator recognition and the antagonism of this interaction by tamoxifen. *Cell* **95**: 927-937.
- Sotomaru Y, Katsuzawa Y, Hatada I, Obata Y, Sasaki H, Kono T. 2002. Unregulated expression of the imprinted genes H19 and Igf2r in mouse uniparental fetuses. *The Journal of biological chemistry* **277**: 12474-12478.
- Soutourina J, Wydau S, Ambroise Y, Boschiero C, Werner M. 2011. Direct interaction of RNA polymerase II and mediator required for transcription in vivo. *Science* **331**: 1451-1454.
- Spiegelman BM, Green H. 1980. Control of specific protein biosynthesis during the adipose conversion of 3T3 cells. *The Journal of biological chemistry* **255**: 8811-8818.
- Steger DJ, Lefterova MI, Ying L, Stonestrom AJ, Schupp M, Zhuo D, Vakoc AL, Kim JE, Chen J, Lazar MA et al. 2008. DOT1L/KMT4 recruitment and H3K79 methylation are ubiquitously coupled with gene transcription in mammalian cells. *Molecular and cellular biology* **28**: 2825-2839.
- Step SE, Lim HW, Marinis JM, Prokesch A, Steger DJ, You SH, Won KJ, Lazar MA. 2014. Anti-diabetic rosiglitazone remodels the adipocyte transcriptome by redistributing transcription to PPARgamma-driven enhancers. *Genes & development* **28**: 1018-1028.
- Steppan CM, Bailey ST, Bhat S, Brown EJ, Banerjee RR, Wright CM, Patel HR, Ahima RS, Lazar MA. 2001. The hormone resistin links obesity to diabetes. *Nature* **409**: 307-312.
- Stromstedt PE, Poellinger L, Gustafsson JA, Carlstedt-Duke J. 1991. The glucocorticoid receptor binds to a sequence overlapping the TATA box of the human osteocalcin promoter: a potential mechanism for negative regulation. *Molecular and cellular biology* **11**: 3379-3383.
- Struhl K. 2007. Transcriptional noise and the fidelity of initiation by RNA polymerase II. *Nature structural & molecular biology* **14**: 103-105.
- Tontonoz P, Hu E, Graves RA, Budavari AI, Spiegelman BM. 1994a. mPPAR gamma 2: tissue-specific regulator of an adipocyte enhancer. *Genes & development* **8**: 1224-1234.
- Tontonoz P, Hu E, Spiegelman BM. 1994b. Stimulation of adipogenesis in fibroblasts by PPAR gamma 2, a lipid-activated transcription factor. *Cell* **79**: 1147-1156.
- Tsai MC, Manor O, Wan Y, Mosammaparast N, Wang JK, Lan F, Shi Y, Segal E, Chang HY. 2010. Long noncoding RNA as modular scaffold of histone modification complexes. *Science* **329**: 689-693.
- Vernochet C, Peres SB, Davis KE, McDonald ME, Qiang L, Wang H, Scherer PE, Farmer SR. 2009. C/EBPalpha and the corepressors CtBP1 and CtBP2 regulate repression of select visceral white adipose genes during induction of the brown phenotype in white adipocytes by peroxisome proliferator-activated receptor gamma agonists. *Molecular and cellular biology* **29**: 4714-4728.

- Wang D, Garcia-Bassets I, Benner C, Li W, Su X, Zhou Y, Qiu J, Liu W, Kaikkonen MU, Ohgi KA et al. 2011. Reprogramming transcription by distinct classes of enhancers functionally defined by eRNA. *Nature* **474**: 390-394.
- Wang F, Mullican SE, DiSpirito JR, Peed LC, Lazar MA. 2013. Lipotrophy and severe metabolic disturbance in mice with fat-specific deletion of PPARgamma. *Proceedings of the National Academy of Sciences of the United States of America* **110**: 18656-18661.
- Westin S, Kurokawa R, Nolte RT, Wisely GB, McInerney EM, Rose DW, Milburn MV, Rosenfeld MG, Glass CK. 1998. Interactions controlling the assembly of nuclear-receptor heterodimers and co-activators. *Nature* **395**: 199-202.
- Xie W, Ren B. 2013. Developmental biology. Enhancing pluripotency and lineage specification. *Science* **341**: 245-247.
- Yang Q, Graham TE, Mody N, Preitner F, Peroni OD, Zabolotny JM, Kotani K, Quadro L, Kahn BB. 2005. Serum retinol binding protein 4 contributes to insulin resistance in obesity and type 2 diabetes. *Nature* **436**: 356-362.
- Yuan W, Condorelli G, Caruso M, Felsani A, Giordano A. 1996. Human p300 protein is a coactivator for the transcription factor MyoD. *The Journal of biological chemistry* **271**: 9009-9013.
- Zhang Z, Teng CT. 2001. Estrogen receptor alpha and estrogen receptor-related receptor alpha1 compete for binding and coactivator. *Molecular and cellular endocrinology* **172**: 223-233.
- Zhao J, Sun BK, Erwin JA, Song JJ, Lee JT. 2008. Polycomb proteins targeted by a short repeat RNA to the mouse X chromosome. *Science* **322**: 750-756.
- Zhu Y, Sun L, Chen Z, Whitaker JW, Wang T, Wang W. 2013. Predicting enhancer transcription and activity from chromatin modifications. *Nucleic acids research* **41**: 10032-10043.